12-2013

Biogeochemical Modeling of the Response of Forest Watersheds in the Northeastern U.S. to Future Climate Change

Afshin Pourmokhtarian

Abstract

In this dissertation I assessed the potential hydrochemical responses of future climate change conditions on forested watersheds in the northeastern U.S. using climate projections from several atmosphere ocean general circulation models (AOGCMs) under different carbon dioxide (CO_2) emissions scenarios. The impacts of changing climate on terrestrial ecosystems have been assessed by observational, gradient, laboratory and field studies; however, state-of-the-art biogeochemical models provide an excellent tool to investigate climatic perturbations to these complex ecosystems. The overarching goal of this dissertation was to apply a fully integrated coupled hydrological and biogeochemical model (PnET-BGC) to evaluate the effects of climate change and increasing concentrations of atmospheric CO_2 at seven diverse, intensively studied, high-elevation watersheds and to evaluate aspects of these applications. I downscaled coarse scale results to local watersheds and applied these values as input to a biogeochemical model, PnET-BGC.

I conducted my research in this dissertation in three phases. In phase one, I used PnET-BGC to evaluate the direct and indirect effects of global change drivers (i.e., temperature, precipitation, solar radiation, CO_2) on biogeochemical processes in a northern hardwood forest ecosystem at the Hubbard Brook Experimental Forest (HBEF) New Hampshire, USA. A sensitivity analysis was conducted to better understand how the model responds to variation in climatic drivers, showing that model results are sensitive to temperature, precipitation and photosynthetically active radiation inputs. Model calculations suggested that future changes in climate that induce water stress (decreases in summer soil moisture due to shifts in hydrology and increases in evapotranspiration), uncouple plant-soil linkages allowing for increases in net

mineralization/nitrification, elevated leaching losses of NO_3^- and soil and water acidification. Anticipated forest fertilization associated with increases in CO_2 appears to mitigate this perturbation somewhat.

In phase two, I compared the use of two different statistical downscaling approaches- Bias Correction-Spatial Disaggregation (BCSD) (Grid-based) and Asynchronous Regional Regression Model (ARRM) (station-based) - on potential hydrochemical projections of future climate at the HBEF. The choice of downscaling approach has important implications for streamflow simulations, which is directly related to the ability of the downscaling approach to mimic observed precipitation patterns. The climate and streamflow change signals indicate that the current flow regime with snowmelt-driven spring-flows in April will likely shift to conditions dominated by larger flows throughout winter. Model results from BCSD downscaling show that warmer future temperatures cause midsummer drought stress which uncouples plant-soil linkages, leading to an increase in net soil nitrogen mineralization and nitrification, and acidification of soil and streamwater. In contrast, the precipitation inputs depicted by ARRM downscaling overcame the risk of drought stress due to greater estimates of precipitation inputs.

In phase three of this research, I conducted a cross-site analysis of seven intensive study sites in the northeastern U.S. with diverse characteristics of climate, soil and vegetation type, and historical land disturbances to assess the range of forest-watershed responses to changing climate. Model results show that evapotranspiration increases across all sites under potential future conditions of warmer temperature and longer growing season. Modeling results indicate that spruce-fir forests will likely experience temperature stress and decline in productivity, while some of the northern hardwood forests are likely to experience water stress due to early loss of snowpack, longer growing season and associated water deficit. This latter response is somewhat

counter-intuitive as most sites are expected to have increases in precipitation. Following increases in temperature, ET and water stress associated with future climate change scenarios, a shifting pattern in carbon allocation in plants was evident causing significant changes in NPP. The soil humus C pool decreased significantly across all sites and showed strong negative relationship with increases in temperature. Cross-site analysis among different watersheds in the Northeast indicated that dominant type of vegetation, and historical land disturbances coupled with climate variability will influence future responses of watersheds to climate change. The variability in hydrochemical response across sites is due to vegetation type, soil and geological characteristics, and historical land disturbances.

Biogeochemical Modeling of the Response of Forest Watersheds in the Northeastern U.S. to Future Climate Change

By

Afshin Pourmokhtarian

B.S., Tehran University, Tehran, Iran, 2002

M.S., Tarbiat Modares University, Tehran, Iran, 2005

DISSERTATION

Submitted in partial fulfillment of the requirements for the degree of Doctor of Philosophy in Civil Engineering in the Graduate School of Syracuse University

December 2013

Acknowledgements

I would like to begin my acknowledgements by expressing my sincere gratitude to my advisor Professor Charles T. Driscoll for giving me the opportunity to pursue my Ph.D. under his guidance while giving me the freedom to pursue my research interests. Dr. Driscoll's insightful and intelligent questions, comments and feedbacks always indirectly pointed me in the right direction. He is not only my advisor but my role model both in life and academia which I strive to follow his footsteps. I cannot express my appreciation for Dr. Driscoll's patience and flexibility during my Ph.D. especially toward the end. I could never ask for a better advisor to pursue my Ph.D. and I will be indebted to him for rest of my life.

My profound gratitude are due to the Syracuse University and the Department of Civil and Environmental Engineering, for giving me the opportunity to pursue my Ph.D. and for the opportunities I have received because of that. I am thankful for assistantship awards to pursue my degree objectives and achieving my goals. I would like to thank the Environmental Protection Agency Science to Achieve Results (EPA-STAR) program, US Forest Service Northeastern States Research Cooperative (FS-NSRC) program, and the National Science Foundation Long Term Ecological Research (NSF-LTER) program for providing the funding to conduct the research for this dissertation and funding for travel expenses which allowed me to present my research at multiple national and international conferences. This dissertation is a contribution of the Hubbard Brook Ecosystem Study.

I would also like to thank my committee members, Dr. John Campbell, Dr. Peter Groffman, Dr. Chris Johnson, Dr. Myron Mitchell, and Dr. Scott Ollinger for providing constructive feedback and improving the quality of my work and Dr. Jane Read for chairing my

Ph.D. defense committee. Your insights and thoughtful questions and comments during the process always made me to think and learn and improve my research skills and prospective.

I would also like to thank the many people who contributed directly to this research by providing the data and feedback; Dr. Scott Bailey, Dr. Douglas Burns, Dr. Kimberley Driscoll, Dr. Ivan Fernandez, Dr. Stephen Sebestyen, Dr. James Shanley, and Mr. Robert Smith. I also greatly appreciate the help that I received from Dr. Wei Wu from The University of Southern Mississippi for helping me with the coding and debugging of PnET-BGC model when I started my research. My gratitude to Dr. Katharine Hayhoe and her lab crew at Texas Tech University for providing the downscaling data which was an essential part for my research. I want to especially thank Dr. Anne Stoner at Texas Tech for helping me with the last part of my research and providing the required data on a timely manner to help me finish my dissertation.

During my seven years at Syracuse University, I was fortunate to get to know great people who changed my life. I would like to thank you my best friends Dr. Makan Fardad and Kambiz Aminishakib who treated me like their brother. I truly cherish every moment of our friendship and truly appreciate your support and encouragement during my Ph.D. program. I like to thank my fellow graduate students and friends Dr. Bradley Blackwell, Joe Denkenberger, Colin Fuss, Sam Fashu Kanu, Amy Sauer, Sam Werner, Dong Zheng and Qingtao Zhou. Special thanks to Dr. Aude Lochet and Colin Fuss for their friendship and great support during my job search and finishing my Ph.D. and putting up with my stress in the office. Although I never worked in the lab but I am thankful to the lab staff, Ed Mason, Jordan Brinkley, Mary Margaret Koppers, Mario Montesdeoca, and Michael Rice, for encouragement and friendship and all the hard time they gave me because of modeling. I would like to thank CIE Department staff, Elizabeth Buchanan, Maureen Hale, Mickey Hunter, and Heather Kirkpatrick for their help and

support. Special thanks to Elizabeth Buchanan and Maureen Hale for helping me with everything that I needed during my studies at Syracuse University and being great listeners, I always appreciate your advice.

I was fortunate to being selected as Teaching Mentor (Fellow) for August TA orientation and the most beneficial part of this opportunity was the interaction with other Teaching Mentors from diverse disciplines and their sophisticated reflections on teaching. I came to know an elite group of intellectual people who frame my thinking and gave me the prospective that I have never had before. Special thanks to Shawn Loner and Dr. Glenn Wright for your friendship and support.

Finally, my deepest appreciation goes to my parents and brother Shervin, for their endless love and providing the moral support and encouragement to pursue and complete this degree. I am sure I was not able to finish my Ph.D. without their love. I would like to dedicate this dissertation to them.

Table of Contents

List of Tables

List of Figures

1. Introduction and Objectives

The 2007 report of the Intergovernmental Panel on Climate Change (IPCC AR4, 2007) [*Intergovernmental Panel on Climate Change (IPCC)*, 2007] provides strong and convincing evidence that human activities, mainly intensive fossil fuel consumption and tropical deforestation, are the main drivers of global climate change [*NECIA*, 2006]. The latest IPCC report (IPCC AR5, 2013) provides even stronger and more convincing evidence that human activities are extremely likely has been the dominant cause of the observed warming since the mid-20th century. These disturbances accelerate the release of carbon dioxide (CO_2) and other heat-trapping gases increasing concentrations of greenhouse gases (GHG) in the atmosphere compared to pre-industrial values. The interaction of global climate change with the unique geographic characteristics of different land areas will result in distinct regional responses to this perturbation. Changes in climate have the potential to alter the structure, function and ecosystems services of forested watersheds and streams that drain them. Moreover, changes in upland terrestrial ecosystems, in turn, will likely influence the water quantity and quality of downstream rivers and estuaries. Projected future changes in climate could pose stress on water resources. Therefore, there is a keen interest in assessing the vulnerability of headwater streams to climate change.

There have been limited assessments of the extent of climate-induced disturbances on forested watersheds. Experimental manipulations and historical observations have provided some insight, but the long-term effects of climate change on hydrological and biogeochemical processes in forested watersheds need to be addressed. To assess the potential impacts of climate change, a multi-faceted approach is required that is capable of resolving multiple climatic drivers (e.g., temperature, precipitation quantity and distribution) and other anthropogenic stressors

likely to simultaneously affect ecosystems over the coming decades. As a result, modeling is the only practical approach to probe how future changes in climate are likely to interact with other drivers of global change such as atmospheric deposition, land disturbance and increasing concentration of CO_2 over broad regions. Hydrochemical watershed models are an important tool to help to understand the long-term effects of climate change on ecosystems.

The consequences of future climate change scenarios are primarily assessed through projections from coupled atmosphere-ocean general circulation models (AOGCMs) from the IPCC AR4, 2007 [*IPCC*, 2007]. AOGCMs are large, complex three dimensional models which incorporate the latest knowledge of physical processes among the lands, oceans and atmosphere of the Earth [*IPCC*, 2007]. They provide geographic grid-based projections of climate variables [*IPCC*, 2007]. In the past, it has been difficult to model future climate change effects at small scales (on the order of kms) since the output from AOGCMs has a comparatively coarse spatial resolution (on the order of 100s of km). The coarse resolution is particularly problematic in linking AOGCM output to hydrochemical models for projections in small watersheds that are located in complex mountainous terrain because these areas are affected by local weather patterns, but are nevertheless critically important for water supplies. Recently, both statistical and dynamical techniques have been applied to downscale coarse resolution AOGCM output to provide finer spatial resolution to improve climate projections at the local scale [*Hayhoe et al.*, 2004, 2007, 2008, *O'Brien et al.*, 2001, *Stoner et al.*, 2012]. Understanding and applying AOGCM output for use with hydrochemical models is an important step to improve quantification of the direct and indirect effects of climate change on watersheds and water resources.

The overarching goal of my dissertation is to improve understanding and assess responses of several forested watersheds with a range of climate conditions, historical land disturbance (e.g., clear cut, fire, ice storm) and biophysical characteristics (e.g., latitude, longitude, elevation, vegetation, soil types, and wetland or lake presence) in the northeastern U.S. to climate change over the 21st century using the hydrochemical model, PnET-BGC. PnET-BGC is a forest-soil-water model that simulates energy, water, and elements fluxes at the watershed scale. This research took advantage of long-term data from intensive watershed study sites that exhibit climatic conditions (temperature, precipitation) spanning the expected range of future climate change. Multiple approaches and tools were used to accomplish the objectives, and three distinct research phases were developed and implemented in this study. Three phases of this dissertation are: 1) an evaluation of the effects of future climate change on soil and surface water chemistry at the Hubbard Brook Experimental Forest, NH; 2) application of the use of two statistical downscaling approaches (BCSD and ARRM) on model (PnET-BGC) output; and 3) conducting an assessment of the variation in responses of forested watersheds in the northeastern U.S. to changing climate through cross-site and spatial analysis of seven intensive study sites.

1.1. Dissertation Objectives and Hypotheses

The following are the specific hypotheses of the dissertation:

Hypothesis 1: The annual average quantity of stream water will decrease and the seasonal pattern will be more evenly distributed due to higher temperatures and associated higher evapotranspiration under future climate conditions. Invoking atmospheric CO_2 effects on vegetation will offset temperature effects to some extent depending on the future climate change scenario causing an increase in the annual average quantity of stream water (Phase one);

Hypothesis 2: Future increases in temperature will cause midsummer droughts and water stress on trees which will impair vegetation uptake of nutrients and increase net mineralization. This uncoupling of soil and plant processes will increase watershed element losses and changes in ecosystem dynamics, changing streamwater and soil chemistry (Phases one and three);

Hypothesis 3: The choice of downscaling technique has a significant impact on projected responses of soil and streamwater chemistry to changing climate. These differences are mainly due to the ability of downscaling technique to capture the changes in precipitation at small scale watersheds and are manifested through changes in hydrology, soil moisture, and hydrochemistry (Phase two); and

Hypothesis 4: Stream water responses, changes in biogeochemical cycling and fluxes of ecologically relevant chemical elements to climate change will vary across different watersheds due to site characteristics, hydro-meteorological, chemical and biological gradients (Phase three).

There are three main research phases in this dissertation. Following a literature review (Chapter 2) and an overview of the sites, data and methods used (Chapter 3), in Phase 1 (Chapter 4) the hydrochemical model, PnET-BGC, is applied to evaluate direct and indirect effects of global change on biogeochemical processes, pools and fluxes of different elements in a northern hardwood forest ecosystem at the Hubbard Brook Experimental Forest (HBEF) New Hampshire, USA. Model performance was evaluated using long-term data collected from the biogeochemical reference watershed (W6) at the HBEF over the last half century. A sensitivity analysis was conducted to better understand how the model responds to variations in climatic drivers, including air temperature, precipitation, and PAR. The PnET-BGC model was modified to consider the two confounding effects of increasing atmospheric CO_2 on vegetation, changes in stomatal conductance and CO_2 fertilization effect on biomass, by using a multilayered sub-model

of photosynthesis and phenology based on Free-Air Concentration Enrichment (FACE). This analysis should improve the understanding of the potential consequences of changing climate in high elevation forest watersheds, and the strengths and limitations of using AOGCM-derived climate projections as input to hydrochemical watershed models. Availability of comprehensive measured data from the HBEF provided an opportunity to evaluate and test the model output.

In Phase 2 (Chapter 5), I compared and contrasted the use of two different statistical downscaling techniques on model-projected responses to future climate change at the HBEF. Bias Correction-Spatial Disaggregation (BCSD) uses an empirical statistical technique broadly referred to as "quantile mapping" (grid-based). I employed this method for model application and analysis described in Chapter 4. The second technique, Asynchronous Regional Regression Model (ARRM), uses piecewise regression to quantify the relationship between measured and modeled quantiles (station-based). In this phase, I did not run the model with CO_2 effects on vegetation. Based on results from Phase 2, I used the ARRM technique for downscaling of climate input for Phase 3.

Phase 3 (Chapter 6) is a cross-site analysis for seven headwater watersheds in the northeastern U.S. The study sites cover different forest ecosystem types; northern hardwood, spruce-fir, and central hardwood. They have a range of climate conditions, historical land disturbance (e.g., clear cut, fire, ice storm) and biophysical characteristics (e.g., climate, latitude, longitude, elevation, different vegetation, soil types). The geographic extent of these watersheds creates spatial variation in climatic patterns (temperature, precipitation, solar radiation), atmospheric deposition, site characteristics, and a host of other variables. In this phase, I used the ARRM approach for downscaling future global climate model output. Also I used output from four new AOGCMs from the latest report of the Intergovernmental Panel on Climate Change

(IPCC AR5) along with Representative Concentration Pathway scenarios (RCP) instead of Special Report on Emissions Scenarios (SRES) which was used in Phases 1 and 2.

The final chapter of this dissertation provides a synthesis of the findings of three phases of my research and their applications and is followed by a list of conclusions and suggestions for future work.

2. Literature Review

2.1. Climate Change in the Northeast

Human activities after the Industrial Revolution have accelerated emissions of greenhouse gases (GHG). Increasing concentrations of GHG are affecting climate and ecosystems. This perturbation raises challenges to important choices and decisions that we face in this century. These anthropogenic emissions of heat-trapping gases are the main cause for most of the averaged global warming since 1950 [*Committee on Stabilization Targets for Atmospheric Greenhouse Gas Concentrations; National Research Council*, 2011; *Intergovernmental Panel on Climate Change (IPCC)*, 2007]. The major heat-trapping gases that make significant contributions to global warming are CO_2, methane (CH_4), nitrous oxide (N_2O), and ozone (O_3), with CO_2 providing the major driver (55%) (greenhouse effect). Future projections show the contribution of CO_2 will increase to between 75 and 85% of the total greenhouse effect by the end of this century depending on emission scenarios [*Committee on Stabilization Targets for Atmospheric Greenhouse Gas Concentrations; National Research Council*, 2011]. The current pool of CO_2 in the atmosphere is larger than for any time in the last 800,000 years and based on future emission scenarios this pool could double or triple by end of this century, amplifying effects on climate [*Luthi et al.*, 2008]. The average global surface air temperature has increased by about $0.75^{o}C$ in response to the increase in atmospheric GHG over the last century, and approximately 2/3 of the increase has occurred since 1980 [*IPCC*, 2007]. Therefore, GHG emission control policies that we make today define potential climate change impacts decades and centuries into the future.

Global climate change is manifested through several atmospheric and ecosystem effects: increasing atmospheric concentrations of CO_2; increasing air temperature and warming of the Earth's surface, especially in winter; more frequent extreme hot days [*DeGaetano and Allen*, 2002]; less precipitation as snow and more as rain [*Wolfe et al.*, 2005; *Huntington et al.*, 2004]; decreases in snow cover [*NECIA*, 2006]; earlier arrival of spring and spring snowmelt, and earlier high spring river flows [*Hodgkins et al.*, 2003]; a longer growing season [*Wake and Markham*, 2005]; more severe drought; changes in storms and extreme events; alterations in soil and surface water chemistry; and sea-level rise [*Huybrechts* et al., 2001]. Across the Northeast U.S., climate is changing. The region has been warming at a rate of nearly 0.27°C per decade since 1970 [*NECIA*, 2006]. Winter air temperatures show a higher rate of increase; 0.72°C per decade from 1970 to 2000 [*NECIA*, 2006]. Total precipitation has increased 100 mm and is characterized by increased temporal variability [*Hayhoe et al.*, 2007].

Climate projections from coupled AOGCMs suggest that across the Northeast U.S. annual average air temperature and precipitation will continue to increase over the 21st Century. The extent of these increases depends on future GHG emissions; a lower emissions scenario (B1) is projected to increase air temperature by 2.1°C and annual precipitation by 7%, while an upper emissions scenario (A1fi) would increase air temperature by 5.3°C and precipitation by 14%, with larger changes in winter and spring as compared to summer and fall [*Hayhoe et al.*, 2007, 2008]. Increases in winter temperature and precipitation mean more available water for runoff and evaporation. Warmer temperatures would cause snow to melt faster and the peak of the snowmelt hydrograph to shift toward early spring (four to five days over 2010–2039) which will cause increases in soil moisture and runoff in late winter and early spring [*NECIA*, 2006]. Projections show that by the end of the 21st century the peak of streamflow, compared to the

historical period (1961-1990), would move 10 days and more than 14 days earlier under lower-emissions and higher-emissions scenarios, respectively [*NECIA*, 2006]. Soil moisture will decrease in late summer and early fall due to higher temperature and higher evaporation. It is anticipated that increases in precipitation will not be able to compensate for this decrease, causing short-term drought [*Campbell et al.*, 2009; *NECIA*, 2006]. These effects are more pronounced under higher emissions scenarios compared to lower-emissions scenarios, which highlights the significant effects of temperature on the hydrological cycle in the Northeast [*NECIA*, 2006]. As warming is projected to continue across the Northeast [*NECIA*, 2006], changes in climate have the potential to alter the region's economy, ecosystems and services they provide, and quality of life. Although the impacts of climate change on U.S. ecosystems are already evident, the degree and direction of these changes are highly variable in time and space [*IPCC*, 2007].

The dynamic nature of climate change, both temporally and spatially, makes it challenging to generalize long-term climatic shifts for any given region. The pattern of warming is more consistent than the pattern for changes in precipitation quantity and timing [NECIA, 2006]. The US Global Change Research Program (USGCRP) Assessment on the Coupled Model Intercomparison Project Three (CMIP3) projected changes in extreme events (heaviest 1% of precipitation events) in addition to seasonal changes to precipitation [*Karl et al.*, 2009]. This report projected that extreme rainfall events would increase the most in the Northeast by 67% [*Karl et al.*, 2009]. Changes in the frequency of extreme events have significant impacts on flood frequency and return period and associated damages to ecosystems. Increased risk of flooding has important implications for climate change adaptation policies.

2.2. Climate Change Impacts on Forest Ecosystems

Forests are one of the most important ecosystems on Earth in terms of biodiversity, biogeochemistry, and ecosystem services. A wide array of human-induced disturbances can alter the structure and function of forests, including climate change. Climate is an important regulator of the structure and function of ecosystems [*Campbell et al.*, 2011]. Therefore changes in climate are anticipated to impact ecosystems and the services they provide. Forested watersheds have an essential role in regulating carbon and nitrogen storage, and water for downstream aquatic ecosystems. Headwater streams drain into larger watersheds and rivers, and ultimately supply downstream estuaries. Climate change likely affects the quantity, distribution and quality of water resources across the U.S. [*Stewart et al.*, 2005; *Hayhoe et al.*, 2007]. Water quantity and its distribution and water quality are affected by year-to-year and long-term variations in climate [*Mitchell et al.*, 1996; *Murdoch et al.*, 1998]. Therefore, hydrology and water quality could be used as effective indicators of global climate change. In this century, climate change could emerge as an important stressor of water resources, challenging water resource management.

There is a keen interest in better understanding the responses of small watersheds to climate change. The direct and indirect effects of climate changes on terrestrial and aquatic ecosystems are likely to be complex and highly variable in time and space [*Campbell et al.*, 2009]. Watershed responses to climate change vary depending on their characteristics. Although climatic effects are substantial, they should not be studied in isolation from other aspects of global change, such as atmospheric deposition, land disturbance (e.g., clear cut, fire, ice storm) and increases in atmospheric concentrations of CO_2. For instance, the structure and function of high elevation terrestrial and aquatic ecosystems have been altered by air pollution and ongoing

air pollution emission controls are driving ecosystem recovery from these effects [*Driscoll et al.*, 2001]. Higher atmospheric CO_2 concentrations appear to affect forest productivity, water use efficiency (WUE) and therefore influence hydrochemistry [*Keenan et al.*, 2013; *Ollinger et al.*, 2009]. The combined influence of multiple factors contributes to the complexity of the response of forest ecosystems to global change. As a result, assessing the effects of global climate is a grand research challenge. Research is needed to evaluate the long-term consequences of climate change on ecosystem structure and function.

2.3. Assessment of Climate Change Impacts

Ecological responses to climate change have been assessed to some extent by observational, gradient, laboratory and field studies; however, hydrochemical models are the only practical approach to comprehensively investigate how future changes in climate are likely to interact with other drivers of global change such as atmospheric deposition, increasing atmospheric CO_2 concentrations, and land disturbance in forest watersheds over broad regions. In order to assess the potential effects of climate change in the Northeast, climate projections from coupled AOGCMs have been used (e.g., [*IPCC*, 2007; *Hayhoe et al.*, 2007; *Ollinger et al.*, 2009; *Campbell et al.*, 2009]).

There are very few comprehensive long-term assessment of whole ecosystem responses to climate change. Past research has focused on individual processes or organisms. However there is interest and need to better understand the linkages among climate, hydrology and biogeochemistry in watershed ecosystems. There are multiple drivers of climate change, including changes in precipitation, solar radiation, temperature and atmospheric concentrations of CO_2 which vary with time and space. Past studies have generally not considered the

interactions of these multiple drivers. Therefore, there is a need to study the consequences of climate change considering multiple climatic drivers on a whole ecosystem basis. The fully integrated hydrochemical model, PnET-BGC, could be an effective tool to assess the effects of climate change on hydrology and the cycles and fluxes of elements across multiple watershed sites over the century.

2.4. Downscaling of Atmosphere-Ocean General Circulation Models (AOGCMs)

Application of hydrochemical models for assessment of climate change impacts on forest ecosystems necessitates the use of climatic variables simulated by atmosphere-ocean general circulation models (AOGCMs) to determine inputs to drive model projections. AOGCMs are an important tool in climate change impact assessments and researchers primarily rely on projections from these models to forecast the plausible range of ecosystem responses to changing climate. AOGCMs have a considerable potential for use in climate change studies due to their ability to incorporate various and complex processes which represent the Earth's climate dynamics including atmosphere, oceans, land surface, land cover, and sea ice and their interactions (e.g., water and energy fluxes) [*IPCC*, 2007]. Although AOGCMs are the only tool which can provide detailed and sophisticated regional projections of climate change, their coarse resolution (~1-2 degrees in latitude or longitude) is unable to resolve sub-grid scale characteristics (topography, land use, clouds, etc.). For instance, the HadCM3 model resolution is 2.5° latitude by 3.75° longitude [*Pope et al.*, 2000] while hydrological models such as Variable Infiltration Capacity (VIC) [*Liang et al.*, 1994] requires 1/8° resolution. Therefore, AOGCM projections due to their coarse resolution are inadequate for assessment of climate change

impacts on small, high elevation watersheds which are affected by local weather patterns due to complex mountainous terrain and are critically important for water supplies.

The gap between AOGCMs coarse resolution output and fine resolution required by local scale models, is a significant problem for climate change impact assessment studies that hampers the application of hydrological/hydrochemical models. Linking coarse AOGCM outputs to resolve important hydroclimatological processes at a finer scales has been problematic in the past. Therefore, there is a need to bridge the gap between coarse spatial resolution and the higher resolution required for hydrochemical models. In order to bridge this gap, considerable effort has been focused on techniques known as "downscaling" [*IPCC*, 2007]. There are two general downscaling techniques: (1) the first is dynamical downscaling, in which a high resolution regional climate model is incorporated within the AOGCM, and (2) the second method involves the use of statistical techniques to develop empirical relationships between AOGCMs coarse resolution and fine local scale climate [*IPCC*, 2007]. Recent statistical techniques have been applied to downscale coarse resolution AOGCM output to a finer spatial resolution, matching long-term observations [*Hayhoe et al.*, 2004, 2007, 2008; *O'Brien et al.*, 2001; *Stoner et al.*, 2012].

2.5. Uncertainties in Modeling Approach

Dynamic hydrochemical models are useful tools to understand and predict the interactive effects of climate change, atmospheric CO_2, and atmospheric deposition on the hydrology and water quality of watersheds. Models have the ability to simulate the dynamics of energy, water and element cycles in terrestrial ecosystems over spatial and temporal scales that are difficult to achieve through observation and experimentation. Model projections have inherent uncertainties

which stem from simplifications and assumptions of hydrological, biological, and biogeochemical processes depicted in the model and inaccurate parameterization of the model (model uncertainty due to lack of data). When models are used to assess the potential impacts of climate change on a terrestrial ecosystem, new additional sources of uncertainty become embedded in the analysis. These include uncertainties in estimates of future emissions due to human activities (scenario uncertainty), the ability of the AOGCMs to simulate the response of the climate system to human forcing (AOGCM uncertainty), and the assumption of downscaling approaches (downscaling uncertainty).

One of the most challenging issues in climate change modeling of forest ecosystems is scaling up leaf-level responses of an individual tree species to changes in atmospheric concentrations of CO_2 to the stand level. There are two confounding effects of atmospheric CO_2 on vegetation: changes in stomatal conductance, leading to increased intrinsic water use efficiency (WUE), and a CO_2 fertilization effect on biomass as increased efficiency of photosynthesis [*Beerling*, 1996; *Drake et al.*, 1997; *Ellsworth*, 1999; *Lewis et al.*, 1996; *Nowak et al.*, 2004; *Ollinger et al.*, 2009; *Saxe et al.*, 1998]. As a result of extrapolation and scaling of these leaf-level mechanisms to the terrestrial ecosystem scale, scientists expect that carbon sequestration should increase under water stress due to increased WUE while in the absence of water stress, carbon storage will weaken and growth might be limited by nutrient deficiency [*Strain and Bazzaz*, 1983; *Luo et al.*, 2004].

Unfortunately, CO_2 enrichment experiments and observations often contradict these projections [*Farrior et al.*, 2013]. *Nowak et al.*, [2004] and *McCarthy et al.*, [2010], compared years of several different CO_2 enrichment experiments and did not find any correlation between

soil moisture in drier years and greater carbon sequestration. Moreover, *Peñuelas et al.*, [2011] synthesized CO_2 enrichment studies and reported significant increases in WUE without associated increases in woody biomass allocation. *Norby and Zak*, [2011] reported strong CO_2 fertilization effects despite nitrogen limitation in several experiments. Finally, *Keenan et al.*, [2013] in a synthesis of forests in the Northern Hemisphere showed a substantial increase in WUE in both temperate and boreal forests over the past two decades. They also observed that the increase in WUE is a result of a CO_2 fertilization effect. This increase is larger than projections by existing theory and terrestrial biosphere model (TBM). They concluded that the increase in WUE is the result of an increase in leaf-level photosynthesis and net carbon sequestration, and a decrease in evapotranspiration [*Keenan et al.*, 2013]. Therefore, there is a keen interest to incorporate current knowledge of CO_2 effects on vegetation into biogeochemical and terrestrial models in a way that can capture and mimic responses of terrestrial ecosystems on the whole stand level.

Models can only depict processes to the extent that they are understood and quantified. Different models can have different responses for the same site and model predictions may not match measured values [*Melillo et al.*, 1995; *Cramer et al.*, 2001; *Friedlingstein et al.*, 2006]. Models are often criticized for being unrealistic, overly complex or simplistic, or producing the right output for the wrong reasons. Nevertheless, they provide the only practical means for evaluating whole ecosystem responses to multiple climatic drivers and stressors over very long periods under changing environmental conditions [*Keenan et al.*, 2012]. Even if modeling results are imperfect, they help constrain the range of potential responses, and when combined with results from field studies, serve as a useful guide to establish guidelines for climate mitigation and adaptation, and a powerful tool for water resource and forest management.

Modeling and use of available data from field and laboratory studies are interconnected approaches which are crucial to enable future projections and help inform decision making on watershed and water resources management. The application of models to environmental problems inevitably brings up new questions that need to be addressed through field and laboratory experiments; this feedback loop is an essential component of the process of science and engineering research which pushes forward the boundaries of knowledge on ecosystems dynamics and processes. Therefore, modeling and long term monitoring should be used hand-in-hand to quantify and project the potential long-term effects of climate change.

3. Methods

3.1. Study Sites

In order to achieve the study objectives and to test hypotheses, seven intensively-monitored forest watersheds in the northeastern U.S., with relatively long records (14 to 45 years) of vegetation, soils, meteorological, hydrological and biogeochemical data have been selected for this study (Table 3.1). The study watersheds include the Hubbard Brook Experimental Forest (HBEF) and Cone Pond Watershed (CPW) in the White Mountains, New Hampshire; East Bear Brook (EBB) in Maine; Sleepers River Watershed (SRW) in Vermont; Biscuit Brook (BSB) in the Catskill Mountains; and Huntington Wildlife Forest (HWF) in the Adirondack Mountains, New York, and the Fernow Experimental Forest (FEF) in the Allegheny Mountains, West Virginia (Figure 3.1). These sites encompass a range of climate, atmospheric deposition, soil conditions, and historical land disturbances.

The selected study sites are all small, relatively high-elevation watersheds which represent different forest ecosystem types (northern hardwood, spruce-fir, central hardwood). These watersheds are relatively undisturbed with the exception of air pollution and changing climate. The study sites include headwater streams that drain these watersheds, which are likely important indicators of changing climate. Using small, undisturbed watershed as the unit of study provides an opportunity to accurately quantify hydrologic and chemical fluxes. High-elevation watersheds generally have shallow soils with poor buffering capacity, which makes them sensitive to small, but measurable changes in land disturbance, atmospheric deposition and CO_2, energy, water and chemical inputs. Therefore these watersheds are sensitive to global climate changes, relatively easy to study, and may act as a “canary in a coal mine” for more complex,

larger watersheds. All of these watersheds are remote, relatively small and generally isolated from urban influences and land cover change. Therefore I used these sites to tease out the effects of climate change, while minimizing the effects of other confounding factors.

The range of drainage areas for the study watersheds varies from almost 10 to greater than 1000 hectares, and the precipitation is relatively high due to their high elevation and location in the Northeast U.S. The scale of all the study sites are much smaller compared to the AOGCM coarse resolution grids which are on the order of hundreds of kilometers. All sites include detailed long term monitoring and are able to meet the data requirements of this study and PnET-BGC specifically. Long-term datasets in order to run and test the model such as meteorology, atmospheric deposition, hydrology, stream and soil chemistry, and historical land disturbances, and data to establish model parameters such as soil and vegetation, were obtained from site researchers. Measured values enabled me to evaluate the model output and performance and gain confidence to project future changes associated with changing climate. The thorough characterization of these intensive long-term sites helped me examine complex processes such as the effects of snowmelt, rainfall events or drought on hydrology, soil and stream water chemistry, and in-lake processes that are associated with changing climate and other disturbances (e.g., atmospheric deposition, land disturbance).

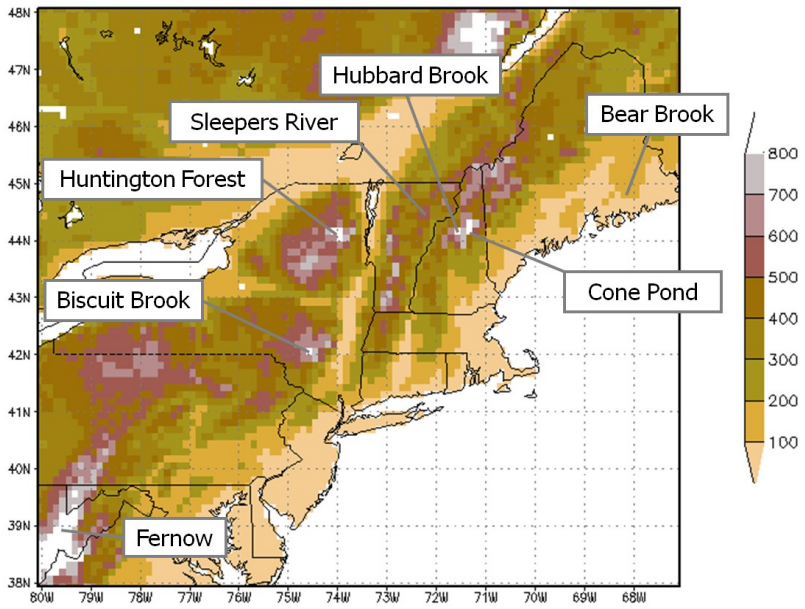

Figure 3.1. Location of seven intensive study sites for this study and their elevation in meters.

Table 3.1. Location and characteristics of study watershed sites.

Site (Id., Region)	Stream	Lat., Long.	State	Record Length (yrs)	Elevation (m)	Forest Cover	Size (ha)	Annual Precipitation (mm)	Annual Discharge (mm)	Literature
Bear Brook (EBB; NE)	East Bear	44°52'N, 68°06'W	ME	20	265-475	Northern Hardwood	11	1250	920	Norton et al., 1999
Hubbard Brook (HBR; NE)	WS6	43°57'N, 71°44'W	NH	45	550-790	Northern Hardwood	13	1400	880	Likens and Bormann, 1995
Cone Pond (CPW; NE)	Inlet	43°54'N, 71°36'W	NH	19	485-650	Spruce-Fir	33	1280	670	Bailey et al., 1995
Sleepers River (SRW; NE)	W-9	44°29'N, 72°10'W	VT	18	520-680	Northern Hardwood	41	1320	740	Shanley et al., 2002
Huntington Forest (HWF; NE)	Archer Creek	44°00'N, 74°13'W	NY	14	460-825	Northern Hardwood	135	1210	830	Mitchell et al., 2001
Biscuit Brook (BSB; NE)	Biscuit Brook	41°59'N, 74°30'W	NY	25	620-1125	Northern Hardwood	990	1520	970	Murdoch et al., 1998
Fernow (FEF; SE)	WS4	39°03'N, 79°41'W	WV	37	750-870	Central Hardwood	39	1460	710	Adams et al., 1994

3.2. PnET-BGC

PnET-BGC is a biogeochemical model that has been used to evaluate the effects of climate change, atmospheric deposition and land disturbance on soil and surface waters in northern forest ecosystems [*Chen and Driscoll*, 2005]. PnET-BGC was created by linking the forest-soil-water model PnET-CN [*Aber and Driscoll*, 1997; *Aber et al.*, 1997], with a biogeochemical (BGC) submodel [*Gbondo-Tugbawa et al.*, 2001], thereby enabling the simultaneous simulation of major element cycles (Ca^{2+}, Mg^{2+}, K^{+}, Na^{+}, C, N, P, S, Si, Al^{3+}, Cl^{-}, and F^{-}). PnET-BGC has been used extensively to evaluate fluxes of water and elements in forest ecosystems by depicting ecosystem processes, including atmospheric deposition, CO_2 effects on vegetation, canopy interactions, plant uptake, litterfall, soil organic matter dynamics, nitrification, mineral weathering, chemical reactions involving gas, solid and solution phases, and surface water processes [*Gbondo-Tugbawa et al.*, 2001]. These processes determine the hydrochemical characteristics of the ecosystem because water and solutes interact with forest vegetation and soil before emerging as surface runoff.

Model inputs include meteorological data (photosynthetically active radiation (PAR), precipitation, maximum and minimum temperature), atmospheric CO_2 concentration and atmospheric deposition (wet and dry), vegetation type (northern hardwoods, spruce-fir), and elemental stoichiometry, soil characteristics (soil mass, soil cation exchange capacity, element weathering rates, soil cation exchange and anion adsorption coefficients, water holding capacity), and historical land disturbance (e.g., forest harvesting, hurricane, ice storm, fire) [*Chen and Driscoll*, 2005; *Gbondo-Tugbawa et al.*, 2001; *Zhai et al.*, 2008]. A detailed description of

PnET-BGC is provided by *Aber and Driscoll*, [1997]; *Aber et al.*, [1997]; and *Gbondo-Tugbawa et al.*, [2001], including a sensitivity analysis of parameters.

In my dissertation, the model was run on a monthly time-step from the year 1000 to 2100. This time frame includes a "spin-up" period (1000 to 1850), which allows the model to reach steady state under "background" conditions of climate and atmospheric deposition. Hindcast simulations from 1850 to 2009 (phase 1) or to 2012 (phases two and three) were based on estimates of historical climate, atmospheric deposition and land-disturbance. Early values for these inputs were recreated from historical records [*Aber and Federer*, 1992; *Driscoll et al.*, 2001] by matching them with measured values later in the record (e.g., for the HBEF meteorology and hydrology since 1955; bulk deposition since 1963; wet deposition since 1978). The model was run from 2009 (or 2012) through 2100 using future global change scenarios that are based on projected changes in climate, atmospheric CO_2, and business as usual scenarios for atmospheric deposition.

3.2.1. Algorithm for CO_2 Effects on Vegetation

Although there have been numerous CO_2 enrichment experiments (e.g., *Ainsworth and Long*, 2005; *Ainsworth and Rogers*, 2007; *Ainsworth et al.*, 2002; *Norby et al.*, 1999, 2010), few have occurred in forests [*Ainsworth and Long*, 2005; *Curtis and Wang*, 1998; *Curtis et al.*, 1995; *Ellsworth*, 1999; *Ellsworth et al.*, 1995; *Lewis et al.*, 1996; *Saxe et al.*, 1998], and those have been short duration experiments that have utilized relatively young stands [*Drake et al.*, 1997; *Ellsworth*, 1999; *Nowak et al.*, 2004; *Ollinger et al.*, 2009; *Saxe et al.*, 1998]. Nevertheless, the effects of increasing atmospheric CO_2 were depicted in PnET-BGC using a multilayered sub-model of photosynthesis and phenology developed by *Aber et al.*, [1995, 1996], and modified by

Ollinger et al., [1997, 2002]. There are two confounding effects of atmospheric CO_2 on vegetation: changes in stomatal conductance, and a CO_2 fertilization effect on biomass. In order to simulate these effects, stomatal conductance and photosynthesis are coupled [*Jarvis and Davies*, 1998] such that stomatal conductance varies in proportion to changes in ambient atmospheric CO_2 (C_a) across the boundary of stomata [*Ollinger et al.*, 2002, 2009; *Saxe et al.*, 1998]. Water use efficiency (WUE) is a function of CO_2 assimilation and is inversely related to vapor pressure deficit (VPD) [*Ollinger et al.*, 2002, 2009]. The internal concentration of CO_2 (C_i) is estimated from C_i/C_a which is relatively constant in response to changes in ambient atmospheric CO_2 (C_a) [*Beerling*, 1996; *Drake et al.*, 1997; *Ellsworth*, 1999; *Lewis et al.*, 1996; *Nowak et al.*, 2004; *Ollinger et al.*, 2009; *Saxe et al.*, 1998] and varies with changes in foliar N concentration [*Farquhar and Wong*, 1984]. Therefore, the model depicts higher assimilation of CO_2 along with depletion of C_i in foliage with higher N concentrations [*Ollinger et al.*, 2002, 2009]. A detailed description of the processes and parameters related to photosynthesis in the algorithm are described by *Ollinger et al.*, [2009].

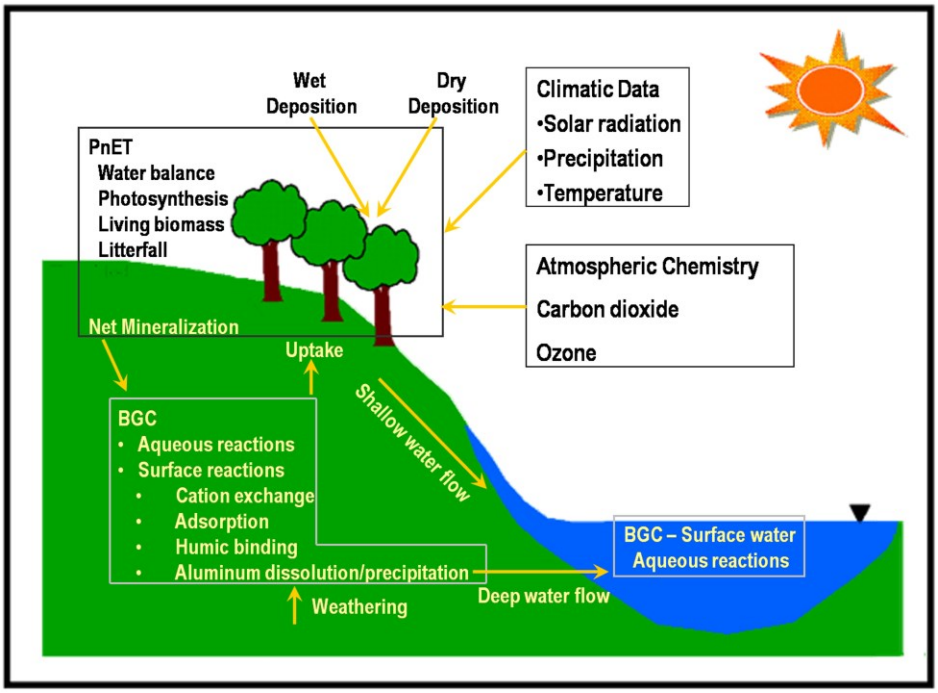

Figure 3.2. Schematic illustration of inputs, processes, interactions and outputs of PnET-BGC.

3.3. Model Application and Validation

To evaluate model performance, I used two statistical indicators: normalized mean error (NME) and normalized mean absolute error (NMAE) [*Janssen and Heuberger*, 1995]:

$$NME = \frac{\overline{P} - \overline{O}}{\overline{O}} \qquad (1)$$

$$NMAE = \frac{\sum_{i=1}^{n} \left(\left| P_i - O_i \right| \right)}{n\overline{O}} \qquad (2)$$

Where P_i is the predicted value and O_i is the observed value at time i. $\overline{P}$ and $\overline{O}$ are means of the individual observations of P_i and O_i, respectively, and n is the number of observations. NME provides a comparison of the means of predicted and observed values and is

an index of relative bias, indicating overestimation (NME > 0) or underestimation (NME < 0) of simulations. The NMAE indicates any discrepancy between model simulations and observed values which is scaled relative to mean observations. The smaller the absolute value, the closer model simulations are to observed values.

3.4. AOGCMs and Future Scenarios

Emissions scenarios [*Moss et al.*, 2008, 2010; *Nakićenović et al.*, 2000] have been used as inputs to AOGCMs [*Committee on Stabilization Targets for Atmospheric Greenhouse Gas Concentrations; National Research Council*, 2011; *IPCC*, 2007]. A wide range of projections based on future demography, technology, and energy consumption have been used to drive a range of plausible emissions scenarios in the future [*IPCC*, 2007]. As output, AOGCMs produce geographic grid-based projections of precipitation, temperature, pressure, cloud cover, humidity, and a host of other climate variables at daily, monthly, and annual scales [*IPCC*, 2007]. In order to estimate potential changes in climate during the next century, for phases 1 and 2 of the dissertation, I used the Special Report on Emissions Scenarios (SRES) [*Nakićenović et al.*, 2000] from the Intergovernmental Panel on Climate Change (IPCC) analysis AR4. I used Representative Concentration Pathway scenarios (RCP) [*Moss et al.*, 2008, 2010] from the IPCC AR5 for phase 3. The World Climate Research Programme's Fifth Coupled Model Intercomparison Project (CMIP5) also used RCPs to drive climate model simulations [*Taylor et al.*, 2009].

In phases 1 and 2 of this research, I rely on calculations from three AOGCMs, the U.S. National Oceanographic and Atmospheric Administration/Geophysical Fluid Dynamics

Laboratory model CM2.1 [*Delworth et al.*, 2006], the United Kingdom Meteorological Office model HadCM3 [*Pope et al.*, 2000], and the U.S. Department of Energy/National Center for Atmospheric Research Parallel Climate Model (PCM) [*Washington et al.*, 2000]. These three models represent different climate sensitivities in terms of temperature change resulting from a doubling of atmospheric CO_2 concentrations relative to pre-industrial conditions. Climate sensitivity for these models range from 1.3ºC to 3.3ºC, covering the lower part of the IPCC 1.5ºC-4.5ºC uncertainty range [*Solomon et al.*, 2007]. GFDL and HadCM3 have medium to medium-high climate sensitivities, while PCM has low climate sensitivity [*Hayhoe et al.*, 2008; *NECIA*, 2006]. I used the SRES A1fi (fossil fuel-intensive) and B1 scenarios to represent possible higher- and lower-emission futures, respectively (2008-2099). At the end of the current century (2099) atmospheric CO_2 concentrations are estimated to reach 970 (ppm) under the higher emissions scenario (A1fi) and 550 ppm in the lower emissions scenario (B1). These concentrations are about triple and double pre-industrial concentrations, respectively.

In phase 3, I employed results from four more recent AOGCMs, the Community Climate System Model version 4 (CCSM4) from NCAR [*Gent et al.*, 2011], the Hadley Centre Global Environmental Model version 2 (HadGEM2) of Met Office Hadley Centre, UK [*Collins et al.*, 2011], the Model for Interdisciplinary Research on Climate version 5 (MIROC5) of Center for Climate System Research, Japan [*Watanabe et al.*, 2010], and The Meteorological Research Institute Coupled GCM version 3 (MRI-CGCM3) of Meteorological Research Institute, Tsukuba, Japan [*Yukimoto et al.*, 2012]. I used the RCP8.5 [*Thomson et al.*, 2011] and RCP4.5 [*Riahi et al.*, 2011] scenarios to represent possible higher- and lower-emission futures, respectively. At the end of the current century (2099) atmospheric CO_2 concentrations are

estimated to reach approximately 936 ppm CO_2-equivalent under the RCP8.5 and approximately 538 ppm CO_2-equivalent in RCP4.5.

The Representative Concentration Pathways (RCPs) approach was designed to depict emissions pathways and concentrations of GHGs in order to support climate change impact assessments as well as providing a framework for potential policy makers and managers to address climate mitigation [*Moss et al.*, 2010; *Vuuren et al.*, 2011]. The representation of climate policy is included in the socioeconomic scenarios that drive the RCPs, in order to enable the scenario to achieve the target radiative forcing by 2100 [*Jones et al.*, 2013]. SRES scenarios, which were reported in the IPCC [Nakićenović *et al.*, 2000], were developed to assess possible future changes in socioeconomic and associated emissions of GHGs without considering any possible action and policy to limit climate change. RCPs are stabilization scenarios that invoke future climate policies and steps toward mitigation. The detailed characteristics of these scenarios are provided by *Moss et al.*, [2008, 2010], *Riahi et al.*, [2011], and *Thomson et al.*, [2011].

Representative Concentration Pathway (RCP) 4.5 considers global emissions of GHGs, short-lived species (aerosols, black carbon on snow or ice, and methane), and changes in land-use and land-cover that stabilizes radiative forcing at 4.5 W m^{-2} (approximately 538 ppm CO_2-equivalent) [*Thomson et al.*, 2011]. It assumes that policy makers will take steps to limit emissions and associated radiative forcing [*Thomson et al.*, 2011]. These steps include, but are not limited to: introducing global GHG emissions markets, assigning emission prices for land use change, advancement in lower emissions technology, changes in energy systems and improving energy efficiency, and carbon capture and geologic storage technology [*Thomson et al.*, 2011].

The Representative Concentration Pathway (RCP) 8.5 represents a high GHG emissions pathway. The RCP8.5 assumes high population growth along with low income growth, modest advancement in technology and energy efficiency which lead to high energy demand and associated GHG emissions over the long term (21st century). It does not include any policies on emissions control or mitigation target [*Riahi et al.*, 2011]. The GHG emissions under this scenario increase over the 21st century, causing radiative forcing at 8.5 W m^{-2} by 2100 [*Riahi et al.*, 2011].

3.5. Downscaling

Atmosphere-Ocean General Circulation Models (AOGCMs) provide a "coarse-scale" resolution, with geographic grid cells ranging in size from 80 to 400 kilometers [*IPCC*, 2007]. In general, this type of resolution is too coarse to capture the type of "fine-scale" changes experienced by small watersheds, which are in the range of km^2, across the northeast and eastern U.S. Therefore, outputs from global climate models were downscaled to transform simulation results into higher-resolution projections for the Earth's surface and watershed model applications. There are two main types of downscaling approaches: dynamical and statistical. All of the downscaling of AOGCM outputs for this dissertation was statistical and done by Katharine Hayhoe and her research group at Texas Tech University.

3.5.1. Dynamical Downscaling

Dynamical downscaling uses high-resolution (~30 kilometers) regional-scale models. These models take small-scale processes and detailed topography. Therefore, their output is

usually closer to observed climatic patterns especially over the Northeast compared to output from global models [*Hayhoe et al.*, 2008; *Liang et al.*, 2004, 2004b; *Zhu and Liang*, 2005]. Another reason for the closer match is that observations are "local" since they are from specific weather stations. Also, dynamical downscaling has the ability to account for important changes in smaller-scale processes which in turn affect regional climate [*Hayhoe et al.*, 2008b; *Tryhorn and DeGaetano*, 2011]. Furthermore, dynamical downscaling is based on physical rather than statistical relationships and hence in theory it should be a preferable approach. Although, in order to obtain the meteorological output, a regional climate model (RCM) needs to be nested within an AOGCM in order to create high-resolution output. In practice this approach has a high computational burden which significantly limits the number of RCM runs [*Committee on Stabilization Targets for Atmospheric Greenhouse Gas Concentrations; National Research Council*, 2011]. Another practical limitation is that AOGCM output, which supplies essential variables at the domain boundaries of RCMs, often is not archived, or at least not archived at vertical levels in the atmosphere and at a temporal resolution required to meet RCM needs [*Committee on Stabilization Targets for Atmospheric Greenhouse Gas Concentrations; National Research Council*, 2011]. Lastly, *Wood et al.*, [2004] showed that RCM output has a bias which needs to be removed through statistical post-processing similar to those used in statistical downscaling methods.

3.5.2. Statistical Downscaling

Statistical downscaling utilizes historical measured data for model calibration and application at the local scale. This involves interpolation onto a regular grid or for individual weather stations. This method "trains" relationships between measured climate and model output

in such a way as to correct for biases in the AOGCM, and in temporal and spatial patterns [*Hayhoe et al.*, 2008]. First, a statistical relationship is established between AOGCM output and measured data. In order to remove year-to-year variation, the relationship is averaged over a relatively long period (at least 20 years) [*Hayhoe et al.*, 2008; *NECIA*, 2006]. The relationship between AOGCM output and measured climate variables (monthly or daily) is then used to downscale future AOGCM outputs to the same scale (grid or weather station). The statistical downscaling method is based on the assumption that the relationships between large and small scale processes remains constant over time, which can be problematic for precipitation [*Committee on Stabilization Targets for Atmospheric Greenhouse Gas Concentrations; National Research Council*, 2011]. However, this technique has a substantial time and cost benefit over dynamical downscaling and is therefore practical and cost-effective [*Hayhoe et al.*, 2008]. I used two different statistical downscaling approaches for this dissertation: Bias Correction-Spatial Disaggregation (BCSD) (Grid-based) and Station-based Daily Asynchronous Regression (SDAR) (station-based).

3.5.2.1. Bias Correction-Spatial Disaggregation (BCSD)

BCSD is the most commonly used method for downscaling monthly AOGCM data [NECIA, 2006]. It uses an empirical statistical technique known as quantile mapping, whereby probability density functions (PDFs) for modeled monthly and daily precipitation and temperature for a period (in this case, 1961–1990) are mapped onto gridded historical observations [*Maurer et al.*, 2002; *Maurer and Hidalgo*, 2008]. In this approach, the mean and variability of both monthly and daily observations were reproduced by climate model output. The BCSD technique was originally developed to adjust AOGCM output for long-range

streamflow forecasting [*Wood et al.*, 2002], and later adapted for studies examining the hydrologic impacts of climate change [*VanRheenen et al.*, 2004]. BCSD originated from the requirement to downscale ensemble climate model forecasts as input to a macro-scale hydrologic model, the Variable Infiltration Capacity (VIC) model, to simulate runoff and streamflow at spatial and temporal scales appropriate for water management [*Wood et al.*, 2002]. I used these high resolution climate projections and removed any bias through comparison with local weather records for phases 1 and 2 of this dissertation.

Hydrologists have considerable interest in understanding and forecasting surface water and energy balance responses to changing climate. For water management, most studies have focused on basins at the scale of 10^2–10^3 km^2. The VIC macroscale hydrology model is well-suited for these applications [*Liang et al.*, 1994; *VanRheenen et al.*, 2004 *Wood et al.*, 2002], and requires climate projections with a 1/8º resolution grid cell as input to project runoff for each grid within the basin [*Liang et al.*, 1994]. Following successful applications of the VIC model to forecast hydrological responses to climate change (e.g., [*Hamlet and Lettenmaier*, 1999; *Liang et al.*, 1994; *VanRheenen et al.*, 2004; *Wood et al.*, 2002]), the 1/8º grid cell, known as VIC grid, has become popular among hydrologists and climate scientists.

In phases 1 and 2, the monthly coarse spatial resolution output of temperature, precipitation, and solar radiation from the two AOGCMs under the two future emission scenarios were statistically downscaled to 1/8º resolution for the period 1950 to 2100 using a standard downscaling routine [*Liang et al.*, 1994]. The latest generation of AOGCM outputs represents observed climate change at the global scale over the last century based on model analyses and inter-comparisons [*Solomon et al.*, 2007]. A detailed description, comparison, and validation of

the BCSD downscaling method is provided by *Hayhoe et al.*, [2004, 2007, 2008]; *NECIA*, [2006]; and *Campbell et al.*, [2011].

3.5.2.2. Station-based Daily Asynchronous Regression (SDAR)

SDAR is a more complex statistical method that uses quantile regression to determine relationships between two quantities that do not have temporal correspondence, but that are expected to have similar statistical properties such as mean and variance [*O'Brien et al.*, 2001]. A regression relationship is assigned by only using probability distribution functions (PDFs) between two independent time series. This method addresses the issue of relating two measurements made at different times to each other [*O'Brien et al.*, 2001], which occurs when measured values are related to historical climate model simulations. Although these two time-series do not have temporal correspondence, over timescales of about 30 years they are expected to have similar probability distributions [*O'Brien et al.*, 2001].

For daily asynchronous regression, each historical time series is reordered by rank and a relationship between observed and modeled temperature or precipitation is determined using piecewise linear regression [*O'Brien et al.*, 2001]. This relationship is then used to correct global climate model output to site-specific conditions over the future period. The relationship between measured values and AOGCM simulations can be improved further by additional steps such as pre-filtering the AOGCM output by principal component analyses (PCA) to remove low-level noise, spatial interpolation of the global model to the scale of the observations, and including information generated by the climate models for convective and large-scale precipitation [*O'Brien et al.*, 2001].

The Asynchronous Regional Regression Model (ARRM) builds on the same statistical technique used by SDAR [*Dettinger et al.*, 2004]. It assigns a quantitative relationship between a daily measured and simulated variable that has a symmetric distribution. ARRM, similar to SDAR, makes historical measurements and simulations independent of time by ranking them before matching their quantiles [*Stoner et al.*, 2012]. Time-independence is an important aspect of this approach since AOGCMs have inherent variability patterns that do not correspond with day-to-day or even year-to-year variability patterns of measured values [*Stoner et al.*, 2012]. *Dettinger et al.*, [2004] first applied this AOGCM downscaling approach in order to study simulated hydrologic responses under changing climate.

In this dissertation, the time series of measured observations from the HBEF (meteorological station#1 for maximum and minimum temperature, and watershed 6 for precipitation) were compared with results from historical AOGCM simulations. Future model simulations were downscaled based on the regression model derived from these two distributions [*Stoner et al.*, 2012]. I used the ARRM method in phases 2 and 3 of my dissertation.

4. Modeling Potential Hydrochemical Responses to Climate Change and Increasing CO_2 at the Hubbard Brook Experimental Forest Using a Dynamic Biogeochemical Model (PnET-BGC)

The objective of this phase of the dissertation was to use the hydrochemical model, PnET-BGC, to evaluate the direct and indirect effects of global change drivers (i.e., temperature, precipitation, solar radiation, CO_2) on biogeochemical processes in a northern hardwood forest ecosystem at the Hubbard Brook Experimental Forest (HBEF) New Hampshire, USA.

4.1. Site Description

The HBEF is located in the southern White Mountains of New Hampshire, USA (43°56'N, 71°45'W) [*Likens and Bormann*, 1995]. The site was established by the U.S. Forest Service in 1955 as a center for hydrological research, and in 1987 was designated as a National Science Foundation Long-Term Ecological Research (LTER) site. The climate is humid continental, with short, cool summers and long, cold winters. Soils are well-drained Spodosols with an average depth of 1-2 m. Vegetation is mostly northern hardwoods, dominated by sugar maple (*Acer saccharum*), American beech (*Fagus grandifolia*), and yellow birch (*Betula alleghaniensis*). Conifer species are more prevalent at higher elevations, largely balsam fir (*Abies balsamea*) and red spruce (*Picea rubens*) [*Johnson et al.*, 2000].

The model was run for Watershed 6 (W6), which has one of the longest continuous records of meteorology, hydrology and biogeochemistry in the U.S. [*Likens and Bormann*, 1995; *Likens et al.*, 1994] (http://www.hubbardbrook.org/). The watershed area is 13.2 ha, with an

elevation range of 549-792 m. Watershed 6 was logged intensively from 1910 to 1917, and has experienced some subsequent disturbances including a hurricane in 1938, which prompted some salvage logging, and an ice-storm in 1998.

4.2. Results

4.2.1. Validation of Climate Projections

I calculated the average of all six different AOGCM scenarios on a monthly basis (model time step) and compared these values with measured climatic data using NME, NMAE, and regression analysis over the period of 1960 to 2008. The three AOGCMs have different values in the hindcast period (1960-2008) and each has its own climate variability. Note that there is no temporal correspondence between AOGCM simulations and observations on a year-to-year basis [*Maurer and Hidalgo*, 2008; *Maurer et al.*, 2002]; therefore I used monthly values to evaluate climate projections based on ranking. There is a good match between measured and statistically downscaled air temperature, with a slight over-prediction for the maximum air temperature (NME = 0.14, NMAE = 0.14; see Table 4.1 and Figure 4.1a) and under-prediction for the minimum temperature (NME = -1.82, NMAE = 1.85; see Table 4.1 and Figure 4.1b). A single linear regression analysis for maximum and minimum temperatures ($r^2 = 0.997$; $\beta = 1.04$; s.e. = 0.002; $P < 0.001$ and $r^2 = 0.997$; $\beta = 0.96$; s.e. = 0.002; $P < 0.001$, respectively) indicates that the slopes of downscaled and measured data are similar. The analyses shows that the downscaled PAR values slightly over-predict the measured values, although they match closely (NME = 0.13, NMAE = 0.13; see Table 4.1 and Figure 4.1c) and the regression slopes are similar ($r^2 = 0.98$; $\beta = 1.05$; s.e. = 0.006; $P < 0.001$). The statistically downscaled precipitation data under-

predict the measured values by greater than 20 cm leading to an overall under-prediction of 32.9% (NME = -0.25, NMAE = 0.27; see Table 4.1 and Figure 4.1d). A regression analysis showed a discrepancy between observed and downscaled data based on the deviation in slope from the one-to-one line ($r^2 = 0.97$; $\beta = 0.38$; s.e. = 0.003; $P < 0.001$). Consequently the precipitation data are scaled upward by 32.9% to match the measured data for model forecasts which resulted in better performance criteria for downscaled precipitation values (NME = -0.003, NMAE = 0.16; see Table 4.1 and Figure 4.1e; $\beta = 0.51$; s.e. = 0.004; $P < 0.001$).

Table 4.1. Summary of statistically downscaled AOGCM output validation for the period of measurement (1964-2008) as indicated by normalized mean error (NME) and normalized mean absolute error (NMAE).

Simulated Constituent	**Model Performance**	
	NME	**NMAE**
Max. Temperature (°C)	0.14	0.14
Min. Temperature (°C)	-1.82	1.85
PAR (mmol m^{-2} s^{-1})	0.13	0.13
Precipitation (cm) - Original	-0.25	0.27
Precipitation (cm) - Scaled Upward by 32.9%	-0.003	0.16

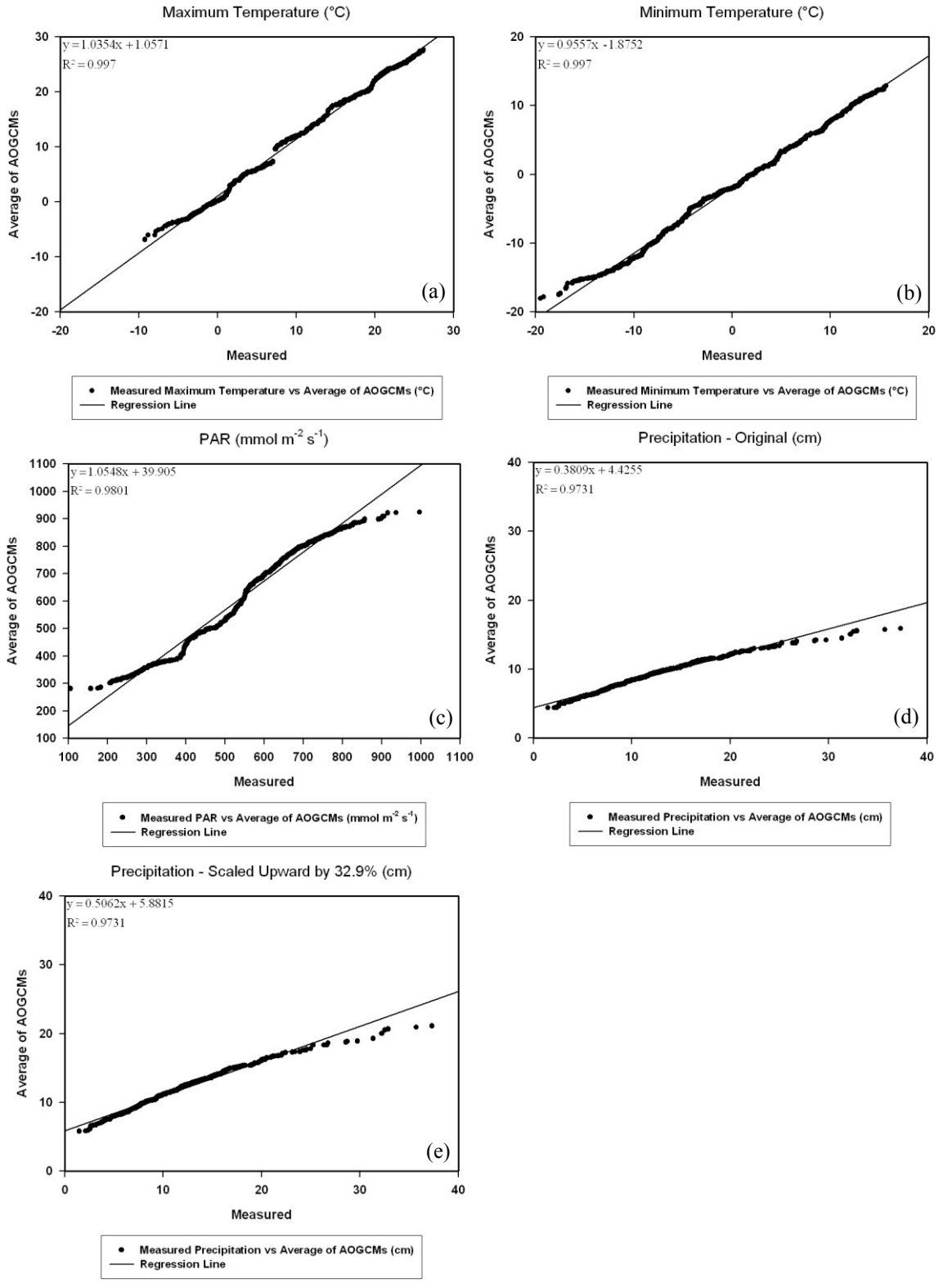
Maximum Temperature (°C)
y = 1.0354x + 1.0571
R² = 0.997
Average of AOGCMs
Measured
(a)
Measured Maximum Temperature vs Average of AOGCMs (°C)
Regression Line
Minimum Temperature (°C)
y = 0.9557x - 1.8752
R² = 0.997
Average of AOGCMs
Measured
(b)
Measured Minimum Temperature vs Average of AOGCMs (°C)
Regression Line
PAR (mmol m-2 s-1)
y = 1.0548x + 39.905
R² = 0.9801
Average of AOGCMs
Measured
(c)
Measured PAR vs Average of AOGCMs (mmol m-2 s-1)
Regression Line
Precipitation - Original (cm)
y = 0.3809x + 4.4255
R² = 0.9731
Average of AOGCMs
Measured
(d)
Measured Precipitation vs Average of AOGCMs (cm)
Regression Line
Precipitation - Scaled Upward by 32.9% (cm)
y = 0.5062x + 5.8815
R² = 0.9731
Average of AOGCMs
Measured
(e)
Measured Precipitation vs Average of AOGCMs (cm)
Regression Line

Figure 4.1. Regression analysis between measured (a) maximum temperature (°C), (b) minimum temperature (°C), (c) photosynthesis active radiation (PAR) (mmol m^{-2} s^{-1}), (d) precipitation (cm), and the average of all AOGCM scenarios over the period of 1960-2008. Graph (e) shows regression analysis between measured precipitation and the average of all AOGCM scenarios (cm) after being scaling up by 32.9% over the same period.

4.2.2. Sensitivity Analysis

Building on previous sensitivity analyses for PnET-BGC [*Aber et al.*, 1997; *Gbondo-Tugbawa et al.*, 2001; *Schecher and Driscoll*, 1995], I evaluated the sensitivity of model calculations to climatic inputs: temperature, precipitation and PAR. The state variables used to assess model sensitivity to these inputs were discharge, stream NO_3^-, DOC, and acid neutralizing capacity (ANC), and soil base saturation (BS%). These state variables were selected because of their role in the acid-base status of soil and water and importance in the response of water supplies to climate change. The sensitivity analysis was conducted by testing the relative change in each state variable *X* values divided by the relative change in the value of the input (Input) tested [*Gbondo-Tugbawa et al.*, 2001]. Thus the sensitivity of an input $S_{Input,\,X}$ was as follows [*Jørgensen*, 1988]:

$$S_{Input,X} = \frac{\partial X / X}{\partial Input / Input} \qquad (3)$$

Higher $S_{Input,\,X}$ values indicated that the model is more sensitive to that climate driver [*Jørgensen*, 1988]. A positive number indicated a positive correlation between the parameter and the state variable while a negative number is an indication of negative correlation [*Gbondo-*

Tugbawa et al., 2001; *Jørgensen*, 1988]. The range of maximum and minimum temperature, precipitation and PAR used for this analysis was determined from long-term measurements at the HBEF. Climatic input values included: the warmest and coolest year, wettest and driest year, and maximum and minimum long-term annual PAR values. In each model run, all other inputs and parameters were held constant, while varying only one maximum or minimum value for the input of interest (total of 6 runs).

4.2.3. Model Performance

The predicted annual streamflow over the measurement period of 1964-2008 generally matched observed values, with the exception of 1973, 1990 and 1996, which are the three highest annual discharge years on record and were under-predicted by the model (NME = -0.02, NMAE = 0.07; see Table 4.2 and Figure 4.2a). A long-term increase in discharge at the HBEF is consistent with a pattern of increasing precipitation [*Campbell et al.*, 2011]. The seasonal variation in streamflow matched observed values reasonably well (Table 4.3). Although there is variability in model performance metrics over different seasons with minimum (NMAE = 0.19) and maximum (NMAE = 0.31) discrepancies over spring (April-June) and winter (January-March), respectively. The model slightly under-predicts spring (NME = -0.08) and winter (NME = -0.07) stream discharge while slightly over-predicting summer (July-September) (NME = 0.07) and fall (October-December) (NME = 0.06) streamflow (Table 4.3).

The model generally captured the long-term trend of decreasing SO_4^{2-} concentrations and shows little over-prediction (NME = 0.03, NMAE = 0.06; see Table 4.2 and Figure 4.2b). The model reproduces the long-term pattern of stream NO_3^- concentrations until about 1990 (1964-1990; NME = 0.12, NMAE = 0.36; see Table 4.2 and Figure 4.2c), after which the model over-

predicts measured NO_3^- concentrations, resulting in poorer model performance compared to predictions of SO_4^{2-} concentrations over the record (NME = 1.17, NMAE = 1.38; see Table 4.2).

Stream Ca^{2+} concentrations were somewhat under-predicted by the model during the beginning of the record (Figure 4.2d), especially the peak in 1970, and over-predicted during the latter part of the record. However, overall, the model sufficiently captured the declining trend of observed Ca^{2+} values (NME < 0.01, NMAE = 0.19; see Table 4.2). The model also simulated stream concentrations of Mg^{2+} (NME = 0.05, NMAE = 0.12; see Table 4.2), K^+ (NME < 0.01, NMAE = 0.16; see Table 4.2) and Na^+ (NME = 0.03, NMAE = 0.09; see Table 4.2) well.

Measured streamwater concentrations of DOC are available since 1982 (Figure 4.2e). The simulated annual volume-weighted average concentration of DOC in stream water depicts the measured values reasonably well (NME = 0.03, NMAE = 0.14; see Table 4.2). The long-term average DOC concentration produced by the model was 167 μmol C L^{-1}, which is similar to the measured value of 162 μmol C L^{-1}.

The model also captured the trend in stream water pH, although slightly under-predicting pH values (NME < -0.01, NMAE = 0.02; see Table 4.2 and Figure 4.2f). The model also under-predicted ANC values (NME = 4.24, NMAE = -4.24; see Table 4.2). The average of the simulated and measured stream water ANC was -12.7 and -2.4 μeq L^{-1}, respectively. The under-predictions in stream pH and ANC are consistent with the over-prediction of NO_3^- in recent years. Simulated soil base saturation was 10%, which is similar to a field value of 9.5% measured in 1983 by *Johnson et al.*, [1991].

Table 4.2. Summary of annual model performance metrics normalized mean error (NME) and normalized mean absolute error (NMAE) over the period of 1964-2008.

Simulated Constituent	Model Performance	
	NME	NMAE
Stream Flow	-0.02	0.07
SO_4^{2-}	0.03	0.06
NO_3^- (1964-90)	1.17 (0.12)	1.38 (0.36)
Ca^{2+}	<0.01	0.19
Mg^{2+}	0.05	0.12
K^+	<0.01	0.16
Na^+	0.03	0.09
DOC	0.03	0.14
pH	<-0.01	0.02
ANC	4.24	-4.24

Table 4.3. Summary of annual and seasonal streamflow model performance metrics normalized mean error (NME) and normalized mean absolute error (NMAE) over the period of 1964-2008.

Period	Model Performance	
	NME	NMAE
Annual	-0.02	0.07
Spring	-0.08	0.19
Summer	0.07	0.29
Fall	0.06	0.20
Winter	-0.07	0.31

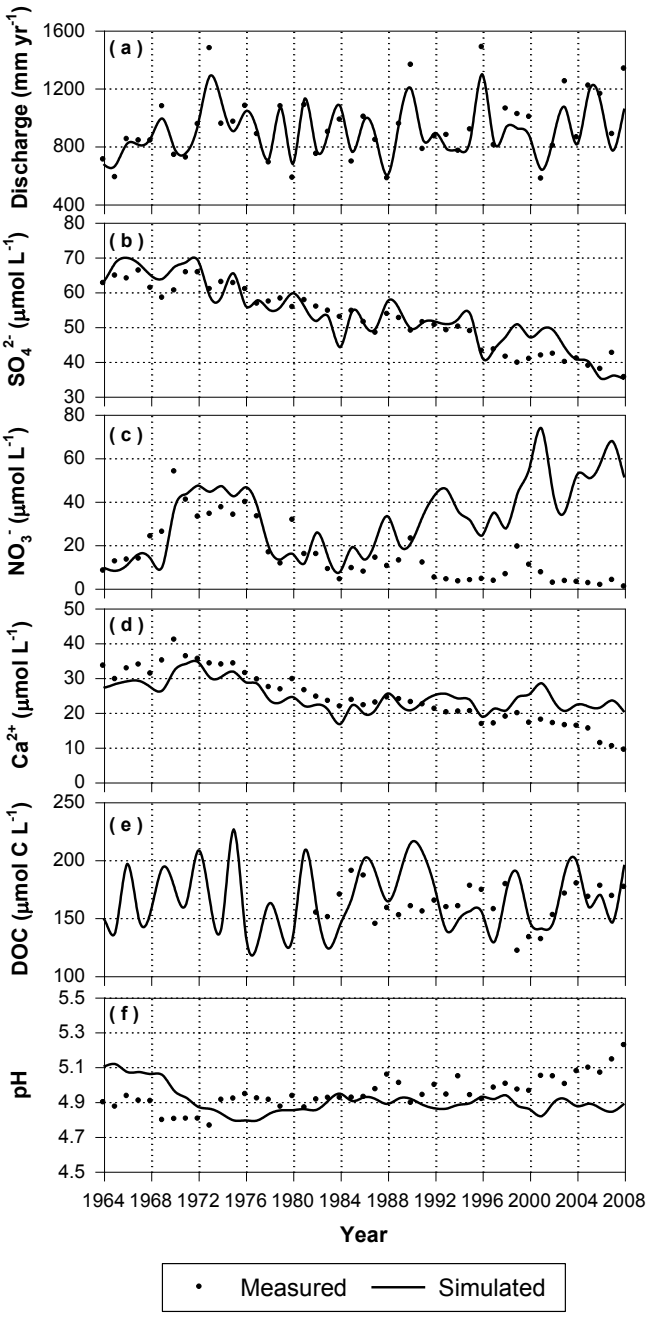

Figure 4.2. A comparison of measured and simulated values of (a) annual discharge and annual volume-weighted concentrations of (b) SO_4^{2-}, (c) NO_3^-, (d) Ca^{2+}, (e) DOC, and (f) streamwater pH over the period of 1964-2008 at watershed 6 of the Hubbard Brook Experimental Forest, NH.

4.2.4. Sensitivity Analysis

The selected state variables show the greatest response to variations in temperature and PAR (Table 4.4). Higher temperatures increase model predictions of NO_3^- and DOC concentrations and decrease discharge, ANC and soil BS%. The sensitivity analysis also suggests that higher annual precipitation decreases NO_3^- and DOC concentrations and soil BS%, while increasing ANC. Higher PAR values result in a decrease in discharge and NO_3^- concentrations and increased DOC, ANC and soil BS%. Precipitation has the greatest effect on discharge. The most sensitive state variable in this analysis is NO_3^- which strongly influences ANC and soil BS%. The least sensitive state variable is DOC, which is mostly dependent on temperature.

Table 4.4. Summary of model sensitivity analysis to changes in temperature, precipitation and photosynthetically active radiation (PAR).

Parameter	**Range**	$S^{Discharge}$	S^{NO3-}	S^{DOC}	S^{ANC}	$S^{\%BS}$
Temperature (°C)	4.46-7.22	-0.03	1.44	0.05	-1.29	-0.09
Precipitation (cm)	104.26-182.45	1.01	-0.51	-0.02	0.59	-0.02
PAR (mmol m^{-2} s^{-1})	456.15-629.99	-0.05	-1.43	0.04	1.25	0.24

4.2.5. Future Climatic Projections

The average measured temperature for the HBEF is 5.7°C (station #1: 1955-2008). Statistically downscaled AOGCM climate projections for the HBEF indicate increases in average air temperature of 1.7 to 6.5°C by the end of the century, depending on the AOGCM and greenhouse gas emission trajectory selected (Table 4.5). The greatest temperature increase is projected by HadCM3-A1fi, while PCM-B1 shows the most modest increase. Precipitation

projections are highly variable, ranging from 4 to 32 cm above the long-term annual measured average of 144 cm. Long-term annual average PAR at the HBEF is 566 mmol m^{-2} s^{-1}, and the climate projections indicate changes ranging from -26.7 to 143.1 mmol m^{-2} s^{-1} by 2100 depending on the scenario and model considered.

Table 4.5. Summary of climate projections from statistically downscaled AOGCM output. The value shown for each scenario is the difference between the mean of measured values for the reference period (1970-2000) and the period 2070-2100.

	1970-2000	2070-2100					
	Observed	HadCM3		PCM		GFDL	
		A1fi	B1	A1fi	B1	A1fi	B1
Temperature (°C)	5.7	6.5	3.1	3.5	1.7	4.4	2.0
Annual Precipitation (cm)	144	31.7	21.5	3.9	12.7	20.2	15.4
PAR (mmol m^{-2} s^{-1})	566	-4.6	41.2	104.7	143.1	17.2	-26.7

4.2.6. Hydrology

Based on PnET-BGC model results, climate change is projected to cause substantial temporal shifts in hydrologic patterns at the HBEF (Figure 4.3). Modeling results indicate that Spring (April-June) snowmelt will occur earlier and will be less extreme in the future. Low flows associated with enhanced evapotranspiration during the summer months (July-Setpember), will extend earlier into the spring and later into the fall (October-December). Future streamflow in late fall and early winter (January-March) will increase because of less snowpack accumulation due to warmer air temperatures and concurrent declines in the ratio of snow to rain.

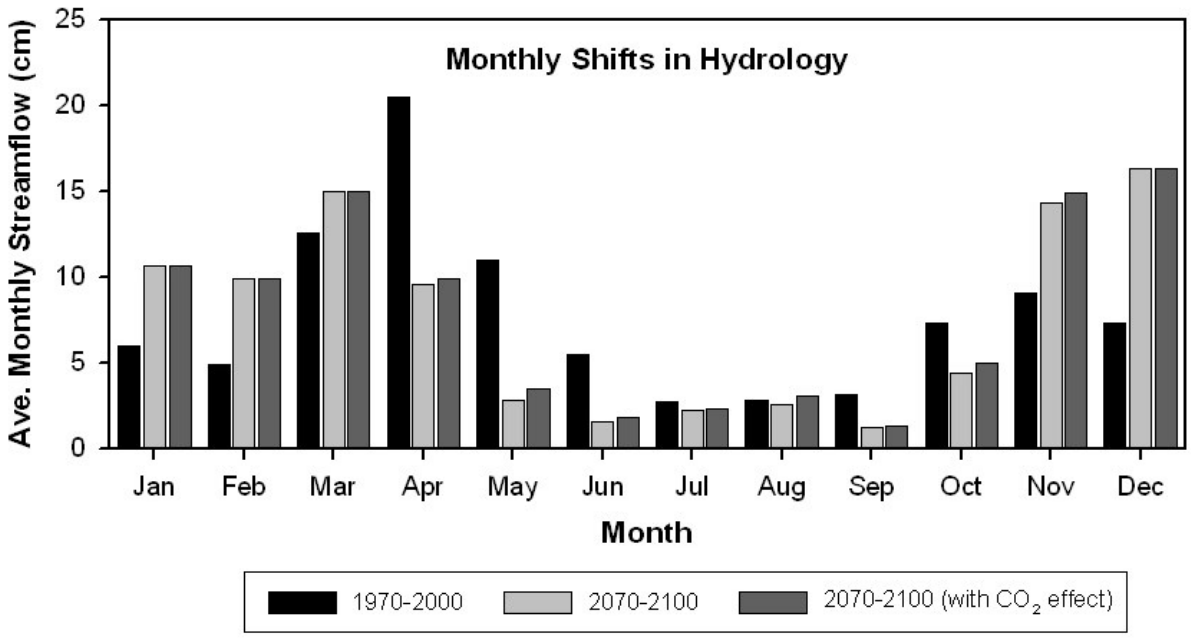

Figure 4.3. Comparison between measured monthly discharge for 1970-2000 and simulated mean monthly discharge for 2070-2100 with and without considering CO_2 effects on vegetation. Note the future climate change scenario depicted in these results is from HadCM3-A1fi (the most aggressive scenario).

4.2.7. Soil and Stream Water Chemistry

Model simulations show that annual volume-weighted NO_3^- concentrations are projected to increase substantially over the next century under all six climate change scenarios considered (Figure 4.4a and Figure 4.5a, Table 4.6). Under HadCM3-A1fi, B1 and GFDL-A1fi, B1 scenarios, predicted annual volume weighted NO_3^- concentration peaks around mid century (2042, 2049, 2059, 2037, respectively) and then declines toward 2100 (Figure 4.6 and Figure 4.7). In comparison, peaks in annual volume-weighted stream NO_3^- concentration under PCM-

A1fi and B1 scenarios are delayed until later in the century. Average annual volume-weighted NO_3^- concentrations for the last 30 years of the 21st century are projected to range from 77 to 132 μmol L^{-1}, compared to an average annual observed value of 18 μmol L^{-1} for 30 recent years (1970-2000).

The model projections for stream SO_4^{2-} show a decline in concentration until around 2025, and level off after that as the watershed approaches steady-state with respect to the business-as-usual scenario for atmospheric S deposition (Figure 4.4b and Figure 4.5b). The average annual volume-weighted SO_4^{2-} concentration projected for 2070-2100 ranges from 23 to 27 μmol L^{-1}, which is lower than the average annual measured value of 53 μmol L^{-1} for the past 30 years.

The model simulations of DOC show that under all scenarios concentrations will decrease over the next century (Figure 4.4c and Figure 4.5c, Table 4.6). The average DOC concentrations projected for 2070-2100 range from 92 to 138 μmol C L^{-1}, which is somewhat lower than the mean annual measured value of 160 μmol C L^{-1} for 1982-2000.

The model simulations for stream Ca^{2+} exhibit patterns that are correlated with changes in NO_3^- (Figure 4.4d and Figure 4.5d). For the HadCM3 and GFDL simulations, annual volume-weighted Ca^{2+} concentrations increase until mid-century, followed by a decline to the end of the century. Under the PCM simulations, stream Ca^{2+} remains constant until mid-century and then increases in response to the later increase in NO_3^-. The average annual volume-weighted concentrations of Ca^{2+} for 2070-2100 range from 17 to 24 μmol L^{-1} (HadCM3-B1 and PCM-A1fi, respectively), which is comparable to the measured value of 25 μmol L^{-1} for 1970-2000. The soil BS% simulation reflects the stream NO_3^- and Ca^{2+} response, decreasing by almost 50% under the high temperature scenarios, while increasing slightly under lower temperature

scenarios. The projected soil %BS for 2070-2100 ranged from 5.1 to 9.0%, in contrast to an average measured value of 9.5% [*Johnson et al.*, 1991].

Future model projections of pH show decreases under all scenarios (Figure 4.4e and Figure 4.5e). The average annual volume-weighted pH projected for 2070-2100 ranges from 4.4 to 5.0, which encompasses the measured volume-weighted mean of 4.9 for 1970-2000. Depending on the scenario used, the acid-base response of the ecosystem to historic acidic deposition ranges from some recovery to no recovery. Acid neutralizing capacity (ANC) projections follow a similar pattern as pH. For the mean of 2070-2100, simulated ANC ranges from -9.5 to -42.2 $\mu eq\ L^{-1}$, which is lower than the measured mean annual volume-weighted ANC of -3.4 $\mu eq\ L^{-1}$ for 1988-2000.

Annual element mass balances for each future climate change scenario were calculated to assess patterns in the fluxes and pools of major elements (NH_4^+-N, NO_3^--N, C, Ca^{2+}, Al) and associated processes depicted in PnET-BGC (Table 4.6). I summarized PnET-BGC model results by calculating average output values using all six future climate change scenarios. These average values were then used to examine the retention and loss of elements in the watershed over the period of 2070-2100, and were compared with the average of simulated values for 1970-2000. The mass balances show that increases in streamwater NO_3^- associated with higher temperature is mainly due to higher rates of N mineralization and nitrification. While NH_4^+ uptake by vegetation declines slightly, NO_3^- uptake greatly increases, resulting in an increase in total N assimilated by plants and a decrease in the pool of N in humus. Mobilization of Al from soil is enhanced due to acidification caused by high NO_3^- concentrations. Mineralization of carbon (C), without considering CO_2 effects on vegetation, decreases compared to the reference period, causing decreases in the humus C pool while the amount of C sequestrated in vegetation

increases substantially. Uptake of Ca by vegetation declines, as do the humus and soil exchangeable pools; however, the total pool of Ca in plants increases.

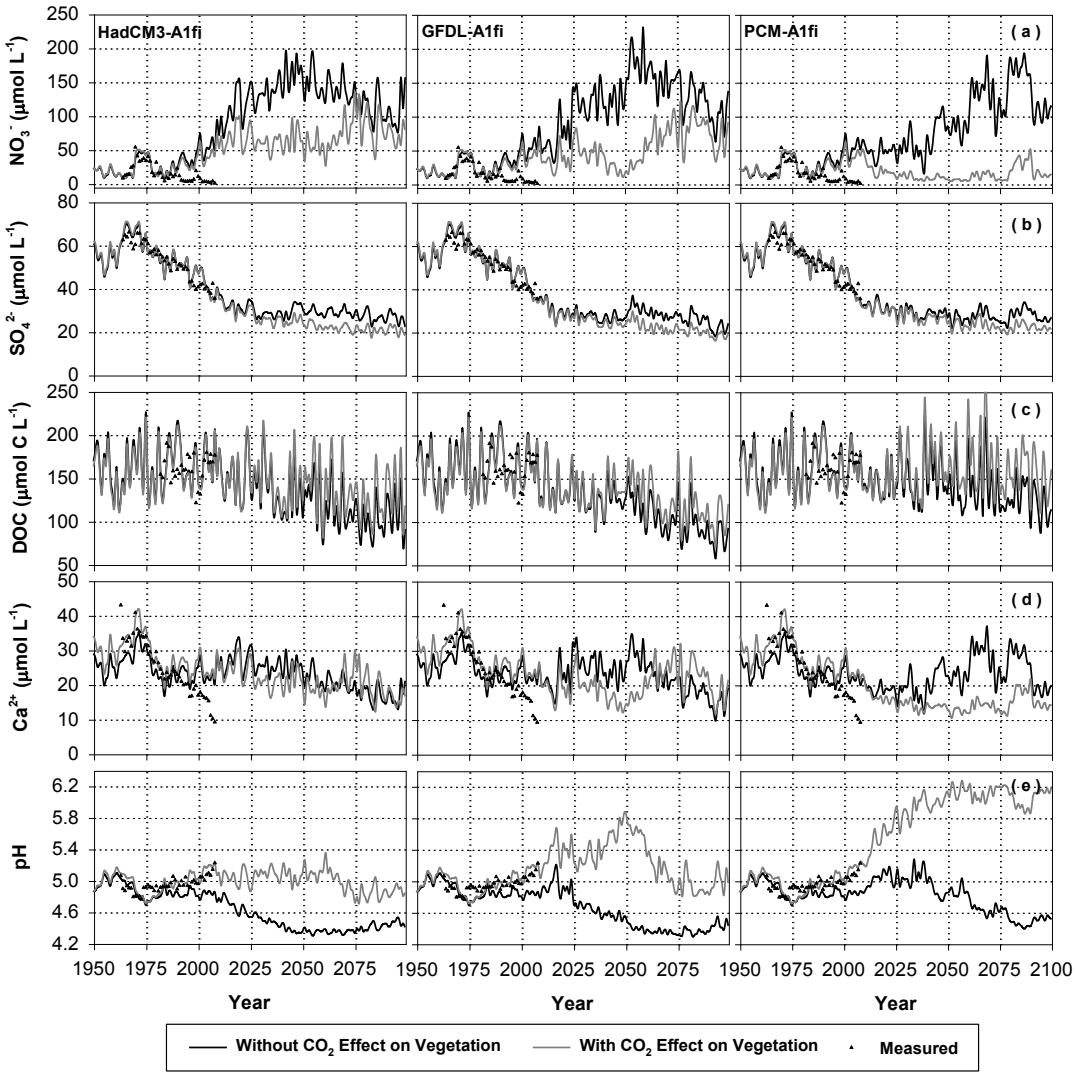

Figure 4.4. Past and future projections of annual volume-weighted concentrations of (a) NO_3^-, (b) SO_4^{2-}, (c) DOC, (d) Ca^{2+}, and (e) pH in streamwater under A1fi scenarios with and without considering CO_2 effects on vegetation. Shown are measured data and simulations using input from three AOGCMs under high emission scenarios (A1fi).

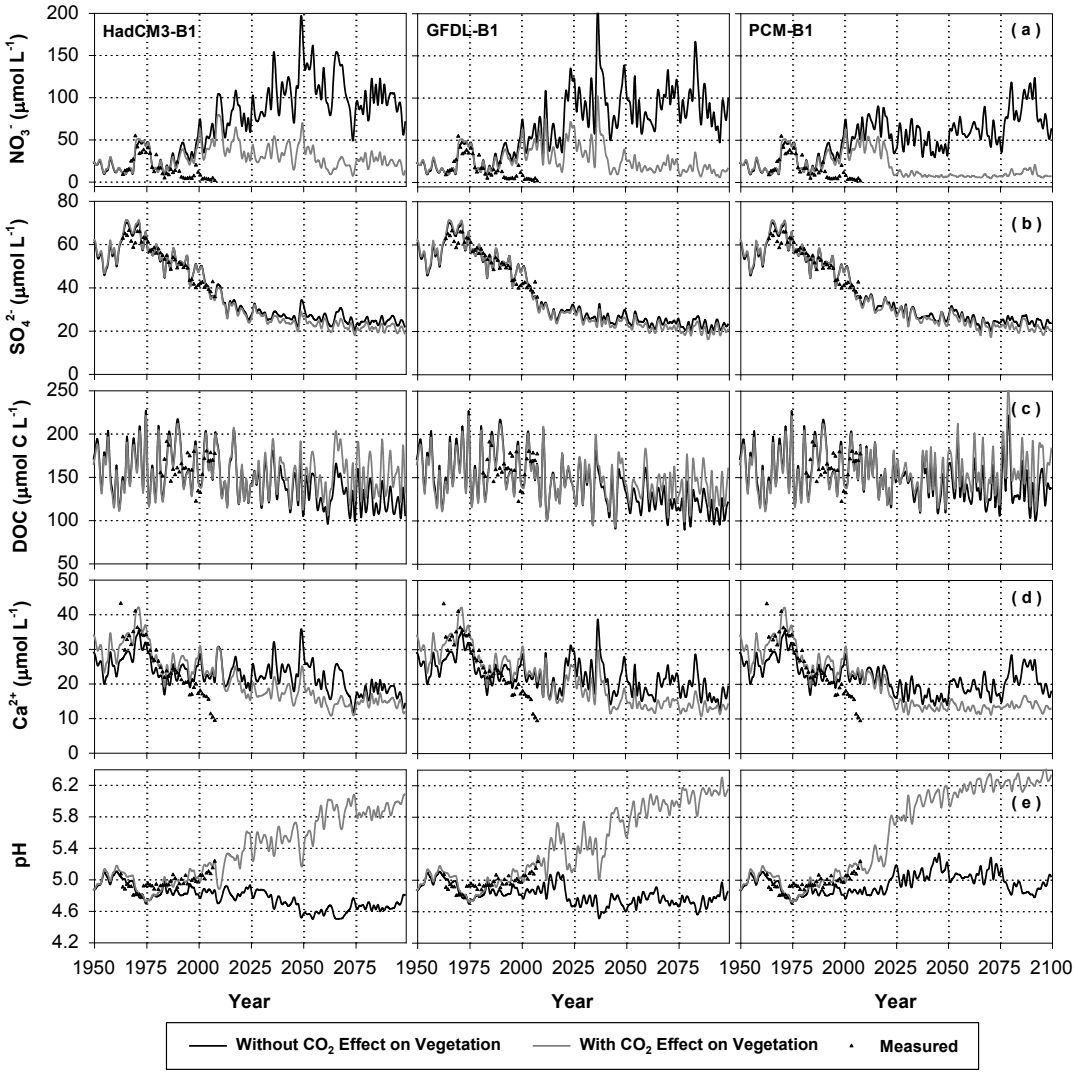

Figure 4.5. Past and future projections of annual volume-weighted concentrations of (a) NO_3^-, (b) SO_4^{2-}, (c) DOC, (d) Ca^{2+}, and (e) pH in streamwater under B1 scenarios with and without considering CO_2 effects on vegetation. Shown are measured data and simulations using input from three AOGCMs under low emission scenarios (B1).

Table 4.6. Projected average changes in biogeochemical fluxes (kg ha^{-1} $year^{-1}$) and pools (kg ha^{-1}) of major elements for the Hubbard Brook Experimental Forest. Values are calculated as the difference between the mean for the period of 2070-2100 and the reference period of 1970-2000.

Fluxes/Pools	NH_4-N			NO_3-N			C/DOC			Ca			Al		
Period	1970-2000	2070-2100[a]	2070-2100[b]	1970-2000	2070-2100[a]	2070-2100[b]	1970-2000	2070-2100[a]	2070-2100[b]	1970-2000	2070-2100[a]	2070-2100[b]	1970-2000	2070-2100[a]	2070-2100[b]
Deposition	2.4	2.0	2.0	5.6	2.5	2.5	17.2	20.0	20.0	1.6	1.8	1.8	0.2	0.3	0.3
Throughfall	2.0	1.6	1.6	5.6	2.5	2.5	17.2	20.0	20.0	3.5	2.0	2.0	0.2	0.3	0.3
Litterfall	93.6	86.8	95.1	0.0	0.0	0.0	6861	5543	6856	23.3	21.4	22.4	0.0	0.0	0.0
Weathering	0.0	0.0	0.0	0.0	0.0	0.0	0.0	0.0	0.0	3.8	3.8	4.8	4.5	4.5	4.5
Uptake	-82.5	-22.2	-71.9	-15.5	-69.0	-30.9	0.0	0.0	0.0	-39.5	-32.9	-34.3	0.0	0.0	0.0
Mineralization	94.2	99.9	103.5	13.7	79.3	33.2	5976	5109	6117	38.6	33.7	34.1	0.0	0.0	0.0
Nitrification	-13.7	-79.3	-33.2	13.7	79.3	33.2	0.0	0.0	0.0	0.0	0.0	0.0	0.0	0.0	0.0
Drainage Losses	0.0	0.0	0.0	-3.8	-12.8	-4.8	-18.1	-11.9	-15.2	-9.7	-6.6	-5.9	-2.5	-3.9	-1.2
Plant total*	682	1036	1310	0.0	0.0	0.0	228778	296835	460706	164	237	310	0.0	0.0	0.0
Humus*	3372	2388	2620	0.0	0.0	0.0	119713	79138	91332	666	443	432	0.0	0.0	0.0
Soil Exchangeable*	0.0	0.0	0.0	0.0	0.0	0.0	0.0	0.0	0.0	282	189	308	1663	1647	1679

Note: Values for reference period (1970-2000) are simulated values from PnET-BGC. Future values are the average output of all six climate scenarios over the period of 2070-2100.

[a] Without CO_2 effects on vegetation

[b] With CO_2 effects on vegetation

* Indicates pool

4.2.8. Modeled CO_2 Effect

Modeling results show that the effect of increasing atmospheric CO_2 on vegetation has little impact on the seasonal distribution of stream discharge, causing only a slight increase in the quantity of streamflow during the growing season (Figure 4.3). A more detailed analysis of hydrologic responses to changes in climate and atmospheric CO_2 using PnET-BGC is given in *Campbell et al.*, [2011].

Compared to hydrology, including CO_2 effects on vegetation in the model has a more pronounced influence on stream NO_3^- concentrations, with substantially lower concentrations when CO_2 effects are considered (Figure 4.4a and Figure 4.5a, Table 4.6). The results for model runs with CO_2 effects on vegetation included, using the four lower and moderate scenarios of climate change (HadCM3-B1, GFDL-B1, PCM-A1fi, PCM-B1), indicate that the average annual volume-weighted NO_3^- concentration for the last 30 years of the 21st century is predicted to range from 9 to 22 μmol L^{-1}, whereas NO_3^- concentrations for the two warmest scenarios (HadCM3-A1fi and GFDL-A1fi) would be substantially higher (85 and 79 μmol L^{-1}, respectively). This differential response is due to a plateau in CO_2 fertilization that occurs at CO_2 concentrations above 600 ppm, such that increased plant demand for N uptake is not able keep the pace with increased available N pools from higher N mineralization associated with increasing temperature. In contrast to simulations of climate change, stream NO_3^- concentrations are lower under scenarios with the CO_2 effect on vegetation included. A condition of ecosystem N saturation is not as prominent, as elevated tree growth associated with CO_2 fertilization largely mitigating any elevated NO_3^- losses.

The model projections for stream Ca^{2+} concentrations were lower when CO_2 effects were included in the model (Figure 4.4d and Figure 4.5d, Table 4.6). Under the four lower and

moderate climate scenarios (HadCM3-B1, GFDL-B1, PCM-A1fi, PCM-B1), the decline in the stream water Ca^{2+} concentration was due to enhanced uptake of Ca^{2+} by vegetation associated with CO_2 fertilization. Under the two warmest climate scenarios (HadCM3-A1fi and GFDL-A1fi), the peak in Ca^{2+} occurred later in response to elevated NO_3^-. The average annual volume-weighted concentration of Ca^{2+} for 2070-2100 for the four lower and moderate scenarios with CO_2 effects varied between 13 and 15 μmol L^{-1} compared to a measured mean value of 25 μmol L^{-1} for 1970-2000. The average annual volume-weighted Ca^{2+} concentrations for 2070-2100 for the warmest model simulations (HadCM3-A1fi and GFDL-A1fi) with CO_2 effects were 20 and 22 μmol L^{-1}, respectively.

Invoking CO_2 effects under climate change results in a change in the simulation of DOC loss (Figure 4.4c and Figure 4.5c, Table 4.6). The simulated mean DOC concentrations for 2070-2100 were higher in comparison to values from model simulations without CO_2 effects on vegetation and exhibit increased variation. This change is due higher inputs of litterfall and fine roots to decomposition pool. The average DOC concentrations for the four lower and moderate scenarios with CO_2 effects on vegetation for 2070-2100 varied from 137 to 163 μmol C L^{-1}, while for the two warmest scenarios (HadCM3-A1fi and GFDL-A1fi) mean DOC concentrations were 126 and 112 μmol C L^{-1}, respectively.

Future model projections of pH under the four lower and moderate scenarios of climate change with CO_2 effects showed recovery from current conditions by up to 1 pH unit (steady-state value around 6). The annual volume-weighted pH for the four low and moderate scenarios including CO_2 effects for 2070-2100 varies between 5.90 and 6.24, while pH values for the two warmest scenarios (HadCM3-A1fi and GFDL-A1fi) are considerably lower (4.84 and 4.95, respectively). Acid neutralizing capacity projections follow similar patterns as pH. The mean

annual volume-weighted ANC for the four low and moderate scenarios of climate change with CO_2 fertilization for 2070-2100 ranges from 6.9 to 15.5 μeq L^{-1}, in comparison with -3.4 μeq L^{-1} for mean annual measured values (for 1988-2000). Model simulations suggest that the mean annual volume-weighted ANC values for HadCM3-A1fi and GFDL-A1fi (the two warmest) were -13.6 and -10.5 μeq L^{-1}, respectively. Model outputs for soil %BS follow a similar pattern as NO_3^-, pH, and ANC. There is some increase in soil %BS under four moderate and low temperature scenarios which range from 10.0 to 13.3% for the period of 2070-2100. The average BS% for last 30 years of the 21st century produced by HadCM3-A1fi and GFDL-A1fi however, are comparatively low (4.3 and 5.6, respectively). These results suggest when CO_2 fertilization stimulates tree growth without elevated NO_3^- leaching, some recovery from acidic deposition occurs, resulting in an increase in stream pH and ANC, and soil %BS. However under the highest temperature scenarios (HadCM3-A1fi and GFDL-A1fi) enhanced mineralization of soil N and NO_3^- leaching re-acidify soil and streamwater.

The model simulations indicate that climate change may alter the hydrologic cycle and the seasonality of stream discharge. Since drainage quantity strongly influences solute transport [*Likens and Bormann*, 1995] seasonal changes in discharge may also alter the seasonal patterns of chemical constituents. I assessed changes in seasonal patterns of concentrations of NO_3^-, Ca^{2+}, pH, and ANC under all climate change scenarios with and without CO_2 effects on vegetation over the period of 2070-2100 and compared these with the seasonal patterns of measured values from 1970-2000. The timing, patterns and magnitude of streamwater NO_3^- concentrations are highly variable depending on the climate scenarios used (Figure 4.6 and Figure 4.7). Since NO_3^- is the largest contributor of strong acids and therefore the main driver of the acid-base status of the ecosystem, Ca^{2+}, pH, and ANC follow similar patterns. These results

suggest that as climate change will likely alter the overall element concentrations and fluxes, these changes will be manifested in the seasonal patterns of solutes concentrations and fluxes and the timing of these changes.

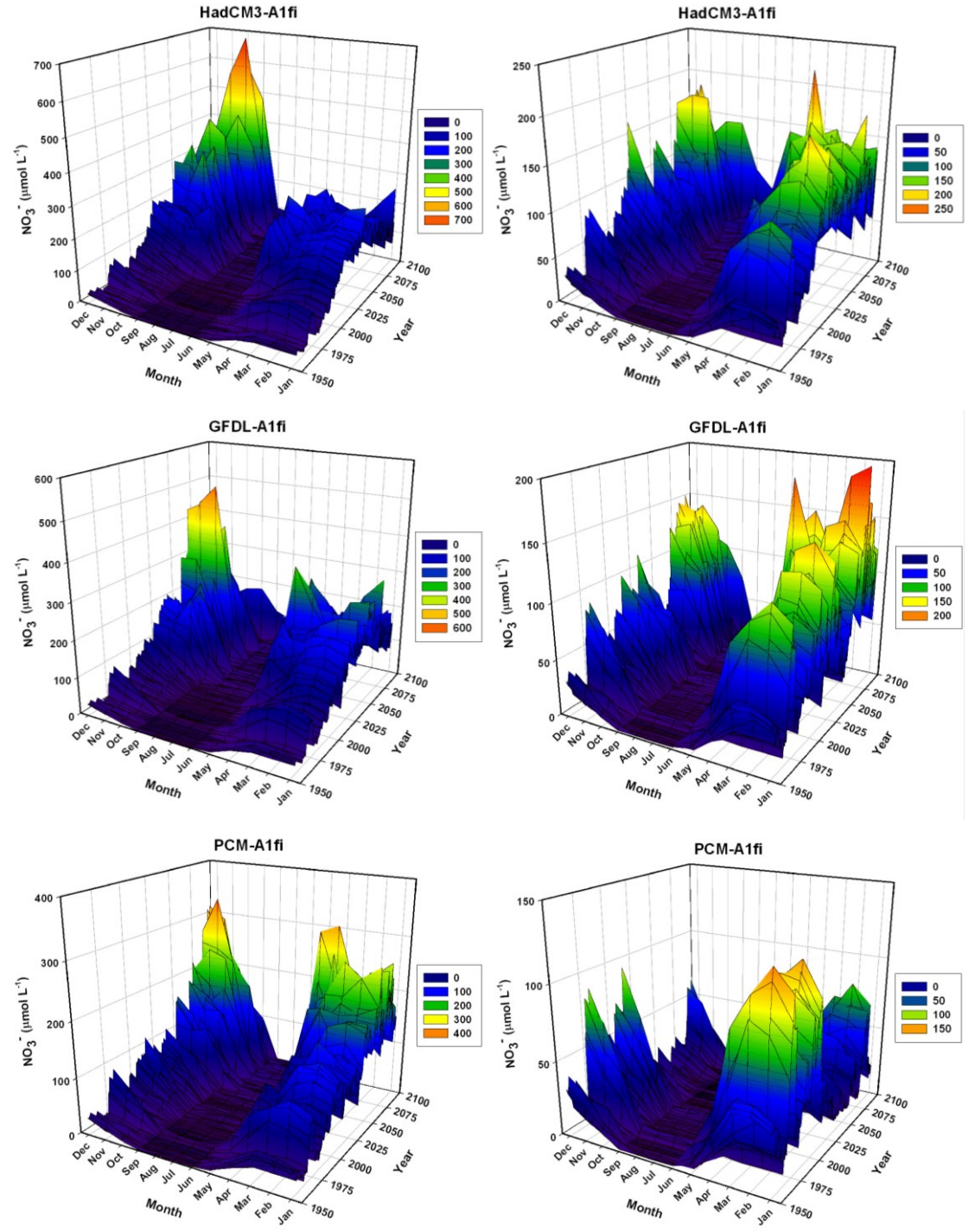

Figure 4.6. Past and future projections of monthly volume-weighted concentrations of NO_3^- in streamwater under the A1fi scenarios without (left panel) and with (right panel) consideration of CO_2 effects on vegetation.

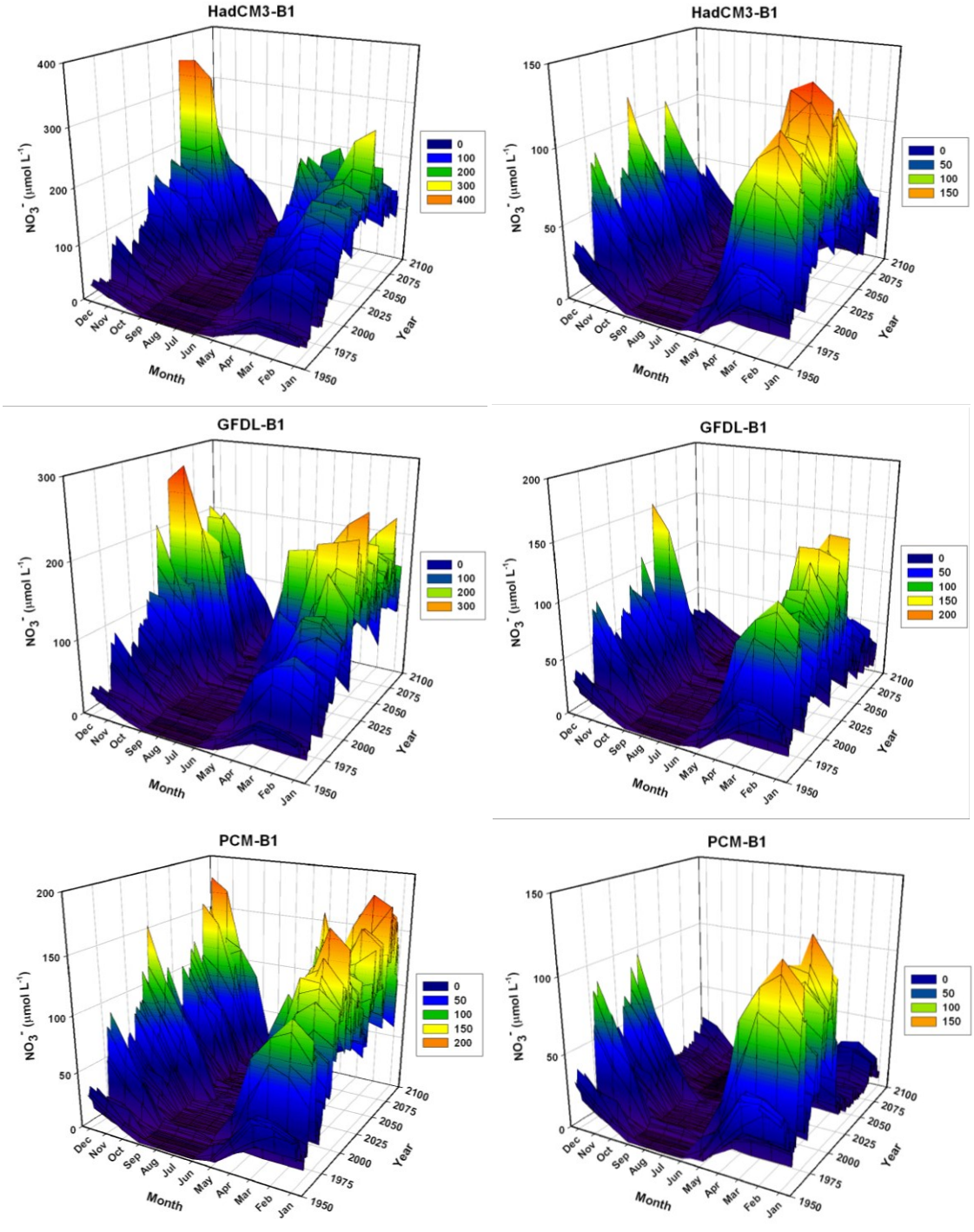

Figure 4.7. Past and future projections of monthly volume-weighted concentrations of NO_3^- in streamwater under the B1 scenarios without (left panel) and with (right panel) consideration of CO_2 effects on vegetation.

Element mass balances show that when CO_2 effects were included, uptake of NH_4^+ by vegetation increased and exceeded uptake of NO_3^-. Also, the amount of total N sequestered in plants increase, which was followed by an increase in N in litterfall and the humus pool. Nitrification rates decrease compared with values without considering CO_2 effects, causing less NO_3^- leaching. Carbon sequestration by plants increases which is followed by an increase in litterfall, the humus pool and mineralization of organic C, ultimately resulting in increases in streamwater DOC. The amount of Ca^{2+} sequestered in plants increases, which is followed by an increase in litterfall and mineralization of Ca^{2+}. Pools of exchangeable Ca^{2+} in soil also increase due to lower concentrations of NO_3^-.

4.3. Discussion

4.3.1. Validation of Climate Projections

There is relatively good agreement between the statistically downscaled climate and observed values of maximum and minimum temperature and PAR. In contrast, the statistical downscaling method under-predicts measured precipitation. This underestimation of precipitation is likely related to the high variability of precipitation encountered at the HBEF due to the mountainous terrain and heterogeneous topography. Additionally, even though the output from the various AOGCMs is downscaled to a finer spatial resolution, the grid size is still large

(~10 km^2) relative to the size of the watershed (0.13 km^2). Note that since precipitation is more spatially variable compared to temperature, it is expected that the average of precipitation over 100 km^2 or more would be smaller than they would be at an individual location. Although, temperature, which tends to be more evenly distributed, would be expected to be close to the gridded average. Recently a statistical-based downscaling method has been developed [*Dettinger et al.*, 2004; *O'Brien et al.*, 2001] which provides much closer agreement with observations especially for precipitation. Incorporating station-based projections into future research will decrease bias and uncertainty. Additional research, experience, and tools are needed to improve the linkages between AOGCM output and hydrochemical models to better capture the effects of changing climate at ecologically and management-relevant spatial scales [*Dettinger et al.*, 2004; *O'Brien et al.*, 2001].

4.3.2. Model Performance

Overall, the model performs well and adequately simulates the observed values. The model satisfactorily captures seasonal variation in streamflow patterns, with slight over-prediction during summer and fall, and slight under-prediction during spring and winter. These over- and under-predictions are manifested in a slight under-prediction of annual discharge. Therefore the model captures the general annual hydrologic pattern over the period of 1964-2008 without any tendency in over- or under-prediction.

Although there is a slight over-prediction of stream SO_4^{2-}, the model captures the long-term trend of decreasing SO_4^{2-} concentration. This long-term decline in stream SO_4^{2-} is due to emission controls of SO_2 associated with the 1970 and 1990 Amendments to the Clean Air Act [*Driscoll et al.*, 2001]. In general, the model over-predicts NH_4^+ concentrations. Due to the low

selectivity coefficient for soil NH_4^+ exchange (Log K = -0.107) and the low potential for NH_4^+ exchange [*Gbondo-Tugbawa et al.*, 2001], the exchangeable pool of NH_4^+ is very small. The higher simulated concentration of NH_4^+ and subsequent increase in soil pools triggers higher rates of nitrification and soil N mineralization which contributes to the over prediction of NO_3^- in stream water. There has been an unexplained decline in measured stream NO_3^- concentrations at the HBEF and in the surrounding region despite high chronic atmospheric deposition of N and the increasing age of the forest [*Goodale et al.*, 2003, 2005] which is consistent with over-prediction of simulated stream NO_3^- concentrations. Modeling the N cycle in forest ecosystems is a challenge due to complexity, confounding factors, and limitations in knowledge about the N cycle in forest ecosystems, hampering development of algorithms in the model that enable adequate depiction of streamwater N losses. PnET-BGC incorporates current thinking of the nitrogen cycle of forest ecosystems to the extent that we understand it, but until a mechanism for the decrease in N loss can be identified and quantified it seems inappropriate to modify an input or parameter of the model or invoke a poorly understood process to fit the measured data. Nevertheless PnET-BGC is effective in simulating the response of the N to vegetation disturbance [*Aber et al.*, 2002] and so likely captures the plant-soil perturbation associated with changing climate.

The model calculates pH from a charge balance of all ions in streamwater and mass law expressions of dissolved inorganic carbon, Al and natural occurring organic acids [*Gbondo-Tugbawa et al.*, 2001]. Accurate modeling of pH is a key component in most watershed models which simulate acid-base chemistry because many biological processes and effects are closely linked with pH [*Gbondo-Tugbawa et al.*, 2001]. Simulation of pH is especially challenging in systems with ANC values close to 0 μeq L^{-1}, like the HBEF (pH 4.7-5.7) due to low buffering

capacity [*Davis et al.*, 1987]. Since pH values are affected by all biogeochemical processes which influence the concentrations of ionic solutes, slight errors in the simulation of major elements can result in high variation and possible errors in pH predictions. Based on model performance criteria for pH, slight over-prediction of SO_4^{2-} and over-prediction of NO_3^- are compensated for, to some extent, by slight over-prediction of base cations. The under-prediction of ANC values are mainly due to over prediction of NO_3^- and naturally occurring organic acids (i.e., DOC).

4.3.3. Sensitivity Analysis

Higher temperatures result in higher rates of mineralization and nitrification, causing higher NO_3^- concentration and lower ANC in streamwater and lower soil %BS. Higher PAR results in higher rates of photosynthesis and greater plant uptake of nutrients, especially N, causing lower surface water NO_3^- and higher values of ANC and soil %BS. Also, higher photosynthesis and the associated increase in vegetation growth and litterfall leads to the projected increase in DOC. DOC is most sensitive to temperature since it is a by-product of organic carbon mineralization. The results of this sensitivity analysis coupled with the previous sensitivity analysis of PnET-BGC inputs and parameters [*Gbondo-Tugbawa et al.*, 2001] show that model predictions are sensitive to changes in climate, indicating that future climate change will likely elicit a marked hydrochemical response in temperate forest watersheds.

4.3.4. Modeling Results for Hydrology, Soil and Stream Water Chemistry

Under PnET-BGC model runs without CO_2 effects, warmer temperatures in the future cause a decrease in soil moisture and an increase in vapor pressure deficit, despite the increase in precipitation. These factors increase evapotranspiration and cause midsummer drought stress, the

extent of which is dependent on the climate change scenario considered. Although wood NPP increases due to warmer temperatures and a longer growing season, repeated midsummer drought is projected to decrease maximum leaf area index, foliar NPP and litterfall and fine root NPP [*Aber and Federer*, 1992; *Campbell et al.*, 2009, 2011] (Table 4.6). Overall, these changes translate into less C sequestration in foliage and fine roots, and more in wood. Because of slower decomposition rates associated with woody litter, the model simulates a decrease in C transfer to humus. The increase in wood NPP does not offset the decline in the litter inputs (sum of leaf litterfall and fine roots) to the soil organic matter (SOM) pool.

The assimilation of N, Ca and other nutrients in plant tissues is similar to the pattern for C. The result of the shift in NPP is a decrease in litterfall elements, causing declines in the humus pool (Table 4.6). Due to water stress, the plant demand for N decreases and the available N pool for plants increases, resulting in a 6.6% decrease in the C:N ratio of the humus pool (Table 4.6). Although both model simulations and observed values show that the HBEF is currently a sink for atmospheric N deposition, future model simulations suggest that climate change may cause the site to shift to a N source for downstream aquatic ecosystems. Note that previous experiments and measurements at the HBEF have demonstrated that the N cycle is very sensitive to ecosystem disturbances that affect forest vegetation [*Likens et al.*, 1970; *Houlton et al.*, 2003].

Elevated export of NO_3^- from forest soils to surface waters is an environmental concern in the northeastern US and elsewhere [*Aber et al.*, 2003; *Driscoll et al.*, 2003]. Elevated leaching losses of NO_3^- facilitate the depletion of cations from soil, and contribute to soil and surface water acidification [*Driscoll et al.*, 2003]. High NO_3^- can lead to water quality impairments and can contribute to the eutrophication of coastal waters. It is challenging to model N losses from forest ecosystems, due to a poor understanding of processes that control N cycling, particularly

those associated with immobilization and denitrification (e.g., [*Dail et al.*, 2001; *Venterea et al.*, 2004]). Nitrogen retention is sensitive to a variety of factors, including legacy effects of historical land use and disturbance which are often poorly characterized [*Aber et al.*, 2002]. Despite these uncertainties, PnET-BGC is a useful tool for assessing the effects of climate change on the N cycle since it accounts for other disturbances including climate change, N deposition and atmospheric CO_2 simultaneously [*Ollinger et al.*, 2009].

For model runs that include CO_2 effects, plant WUE increases and midsummer drought does not occur appreciably except under the two warmest scenarios (HadCM3-A1fi and GFDL-A1fi). The effect of elevated CO_2 on stomatal conductance and increase in WUE offset the effect of higher temperatures by enhanced tree growth and higher nutrient uptake. Over the second half of the century under the two warmest scenarios (HadCM3-A1fi and GFDL-A1fi), the CO_2 effect on vegetation is not able to offset the effect of temperature; midsummer droughts and water stress cause less uptake of N and elevated availability of N followed by nitrification and elevated leachate of NO_3^-. Increases in atmospheric CO_2 result in increased tree growth and limited NO_3^- leaching over the first half of the 21st century, while tree growth remains constant or decreases over the second half of the century because of water stress. This pattern is due to the nonlinear response of photosynthesis to increasing atmospheric CO_2. Over time, and especially under higher CO_2 emission scenarios and warmer temperatures, the CO_2 fertilization effect declines and N saturation occurs, as temperature becomes the dominant driver of N cycling. This work suggests that the legacy of accumulation of elevated N deposition in forest watersheds downwind of emission sources could have delayed deleterious effects on soil and surface water. If stores of N are mineralized under changing climate, the consequences of elevated NO_3^- leaching could be realized. In my study, I assumed that N emissions remained at current levels and did not consider

future land disturbances in our simulations. If atmospheric N deposition decreases or land disturbance occurs in the future, N saturation would be delayed.

Studies suggest that surface water DOC is increasing in Europe and the northeastern US. The alternative mechanisms explaining this phenomenon are declines in acidic deposition or climate change [*Clark et al.*, 2010; *Evans et al.*, 2006; *Findlay*, 2005; *Freeman et al.*, 2001, 2004; *Garnett et al.*, 2000; *Monteith et al.*, 2007; *Worrall et al.*, 2003]. PnET-BGC simulations suggest that DOC will decrease over the 21st century under all climate change scenarios. This modeled decline in DOC is associated with a decline in litterfall and a decrease soil C mineralization rates (Table 4.6). The trends in streamwater DOC are modified under climate change in the presence of CO_2 fertilization. The higher productivity of the forest (NPP and NEP) due to CO_2 fertilization increases litterfall in comparison to values from model simulations without CO_2 effects on vegetation (Table 4.6). An increase in the decomposition of the organic matter pool triggered by higher temperatures led to higher DOC concentrations in streamwater. Note that when CO_2 effects on vegetation are included in the simulations, large increases in stream DOC are not evident, although on average DOC concentrations are higher compared to simulations without CO_2 effects on vegetation due to higher litter production. Model simulations would seem to be inconsistent with the hypothesis that climate change is driving increases in surface water DOC.

While hydrochemical models such as PnET-BGC provide useful information about how ecosystems may respond to global change, they are somewhat limited by sources of uncertainty. First, there are only a few studies that have evaluated the effects of CO_2 fertilization on NPP, especially in northern hardwood forest ecosystems [*Ainsworth and Long*, 2005; *Curtis and Wang*, 1998; *Curtis et al.*, 1995; *Ellsworth*, 1999; *Ellsworth et al.*, 1995; *Lewis et al.*, 1996; *Saxe*

et al., 1998]. Experimental manipulations show that increased atmospheric CO_2 enhances plant productivity, but the extent of this response over the long-term in conjunction with other global change drivers is not well-established. Second, it is unclear how atmospheric N deposition will change in the future, which could substantially influence the element responses. Moreover, we did not consider scenarios of future land disturbance, which could further affect hydrologic and biogeochemical dynamics. Third, changes in climate and other factors (e.g., pests, pathogens) may alter the composition of vegetation at the HBEF, which could also influence hydrologic (e.g., transpiration) and biogeochemical (e.g., uptake, litterfall, decomposition) fluxes. While changes in established tree species would occur slowly in response to climate change, the effects might be more pronounced at locations such as the HBEF, which are located in a transition forest zone (between northern hardwoods and red spruce-balsam fir forests). In this application, PnET-BGC model simulations assumed that the watershed consisted of a homogeneous distribution of northern hardwood forest. In the future it would be useful to evaluate the influence of shifts in species composition or to link PnET-BGC with a forest community model that projects changes species assemblages. The temperature conditions considered in some of the climate scenarios are beyond the conditions under which parameter values were developed for PnET-BGC. We are currently evaluating model performance for watersheds of lower latitude to assess this limitation. Finally, it is important to reduce the uncertainty of climate change projections, particularly for precipitation, by continuing to improve climate models, downscaling techniques (e.g., station-based instead of gridded), and linkages with hydrochemical models.

5. A comparison of Gridded Quantile Mapping vs. Station Based Downscaling Approaches on Potential Hydrochemical Responses of Forested Watersheds to Climate Change Using a Dynamic Biogeochemical Model (PnET-BGC)

The objective of this chapter was to compare and contrast projections of temperature and precipitation developed by two statistical downscaling techniques: Bias Correction-Spatial Disaggregation (BCSD) (Grid-based) and Asynchronous Regional Regression Model (ARRM) (station-based), and using two different sets of observations; a VIC grid and the HBEF station measurements. I evaluated how their differences manifest through potential biogeochemical responses of forested watersheds using the PnET-BGC model. I evaluated the effects of these different downscaling techniques on simulations of hydrology and water quality under potential future changing climate. This analysis improves understanding of the strengths and limitations of two common statistical downscaling techniques and selection of the appropriate technique for use in hydrochemical watershed models.

5.1. Future Scenarios

Two sets of four future climate scenarios (HadCM3-A1fi, HadCM3-B1, PCM-A1fi, and PCM-B1) were downscaled and developed as input for the PnET-BGC simulations and my analysis; the first set was developed by the BCSD downscaling technique and VIC grid measurements for training the downscaling model (Chapter 4), and the second set was developed by employing the ARRM downscaling approach and using the HBEF station measurements for

training (Chapter 5). Note that measured solar radiation used for both downscaling techniques is from the VIC grid.

The atmospheric deposition from 2012 through 2100 was assumed not to change from current conditions. The dry-to-wet deposition ratios were assumed to be constant during the entire simulation period [*Yanai et al.*, 2013] and wet deposition inputs are from the National Atmospheric Deposition Program (NADP) station (NH02) at the HBEF. Note that for these simulations I did not consider the effects of potential CO_2 fertilization on forest productivity.

5.2. Results

5.2.1. Future Climate Projections

The average daily measured temperature for the HBEF is 5.9°C (station #1: 1955-2011). Both statistically downscaled AOGCM climate projections for the HBEF indicate increases in annual average air temperature ranging from 1.7 to 7.0°C by the end of the century, depending on the AOGCM, emission trajectory, and downscaling technique (Table 5.1). The highest and lowest projected increases in air temperature occurred under the HadCM3-A1fi and PCM-B1 scenarios, respectively. The ARRM projections generally showed higher temperature increases than BCSD except for the PCM-A1fi scenario. Under all scenarios precipitation was projected to increase with high variability, ranging from 4 to 45 cm above the long-term annual measured average of 144 cm (Table 5.1). The ARRM projections of annual precipitation for all scenarios were significantly greater than BCSD projections. Projections of photosynthetically active radiation (PAR) were highly variable and indicated both increases and decreases ranging from -14.0 to 143.1 mmol m^{-2} s^{-1}. Compared to the long-term annual average PAR of 566 mmol m^{-2}

s^{-1}, the ARRM projections showed a decrease in PAR under all scenarios, while BCSD showed increases except for HadCM3-A1fi (Table 5.1).

Table 5.1. Summary of AOGCM climate projections from two statistical downscaling techniques: BCSD and ARRM. The value shown for each scenario is the difference between the mean of measured values for the reference period (1970-2000) and the period 2070-2100.

	1970-2000	2070-2100							
	Observed	HadCM3				PCM			
		A1fi		B1		A1fi		B1	
		BCSD	ARRM	BCSD	ARRM	BCSD	ARRM	BCSD	ARRM
Temperature (°C)	5.7	6.5	7.0	3.1	3.7	3.5	3.3	1.7	1.8
Annual Precipitation (cm)	144	31.7	45.3	21.5	23.4	3.9	16.3	12.7	20.8
PAR (mmol m^{-2} s^{-1})	566	-4.6	-13.0	41.2	-11.5	104.7	-14.0	143.1	-6.8

5.2.2. Comparison between HBEF and VIC Observations

The regression analysis between observations from VIC grid (X axis) and the HBEF (Y axis) for maximum temperature (°C), minimum temperature (°C), and precipitation (mm) are shown in Figure 5.1. There should be a one-to-one correspondence between daily observations. Indeed, there was a strong relationship for air temperature, with slightly higher VIC observations for the both maximum and minimum air temperature (Figure 5.1a and Figure **5.1**b). A single linear regression analysis for maximum and minimum temperatures ($r^2 = 0.91$; $\beta = 0.94$; s.e. = 0.003; $P < 0.001$ and $r^2 = 0.90$; $\beta = 0.96$; s.e. = 0.003; $P < 0.001$, respectively) indicated that the slopes of both observations are similar. In contrast, the relationship for precipitation was not as strong, and precipitation amounts from the HBEF were generally greater than VIC observations

especially for extreme events (Figure 5.1c). A regression analysis showed a discrepancy between these datasets based on the deviation in slope from the one-to-one line ($r^2 = 0.68$; $\beta = 1.33$; s.e. = 0.008; $P < 0.001$). Although a comparison of precipitation time series for the HBEF and VIC grid also showed a similar pattern, measured HBEF precipitation is higher, especially for extreme events (Figure 5.2).

Future projections of monthly precipitation (2012-2100) downscaled with ARRM were higher than with BCSD for the all scenarios (Figure 5.3 and Figure 5.4). Also under all scenarios the ARRM projections showed higher average precipitation, and extreme rainfall events during summer and fall compared to BCSD.

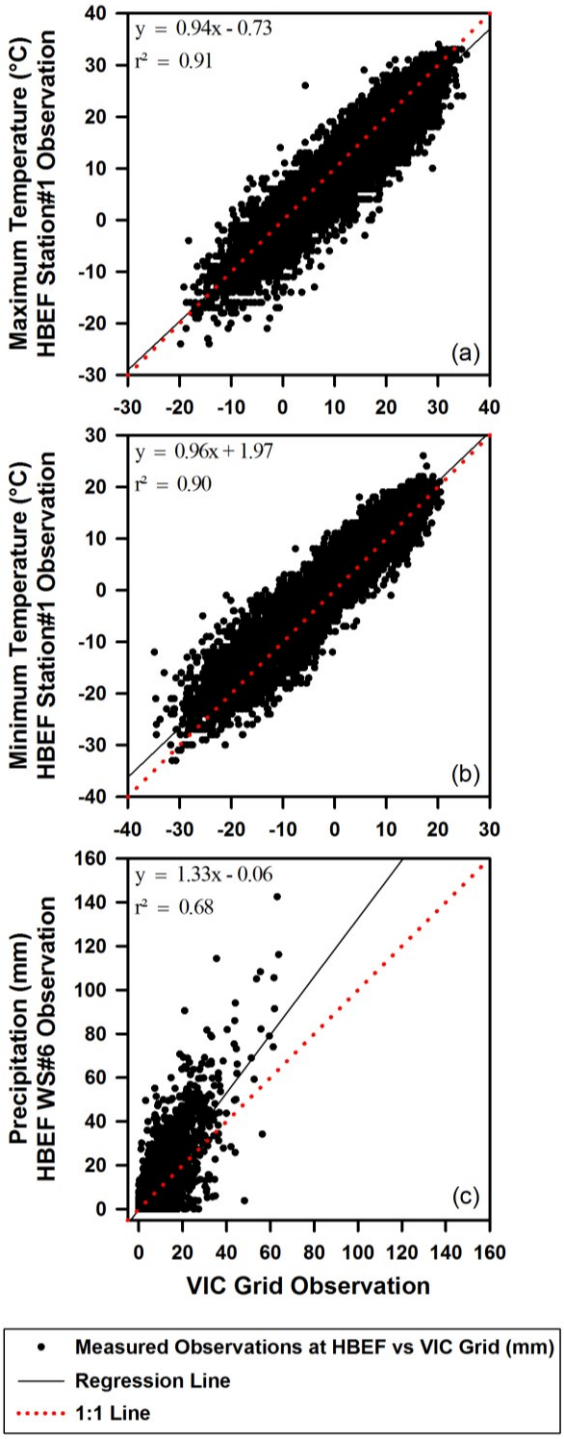

Figure 5.1. Regression analysis between measured (a) maximum temperature (°C), (b) minimum temperature (°C) at HBEF station#1, and (c) measured precipitation (mm) at the HBEF WS#6 and values for the VIC grid over the period of 1964-2000.

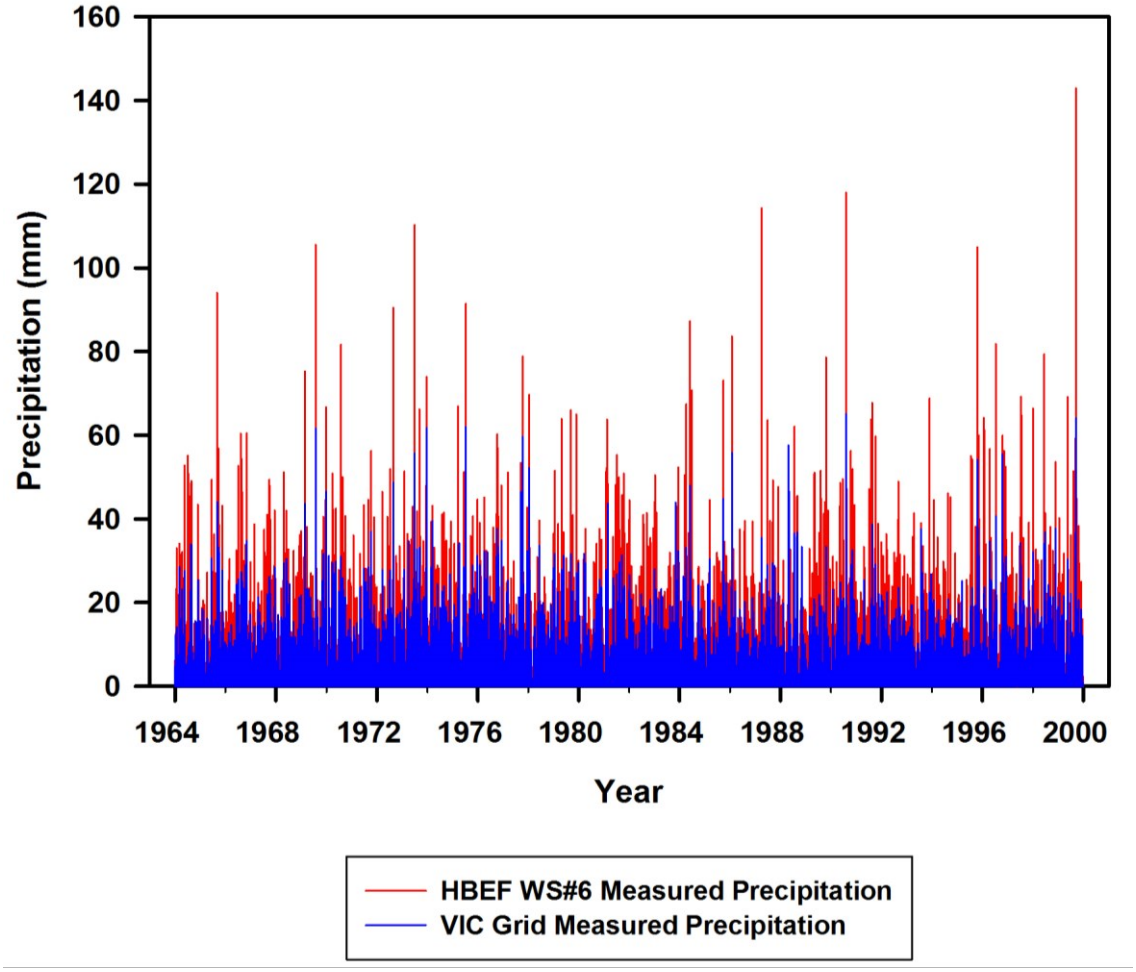

Figure 5.2. Comparison of time series for measured monthly precipitation at the HBEF WS#6 and VIC grid (mm) over the period of 1964-2000.

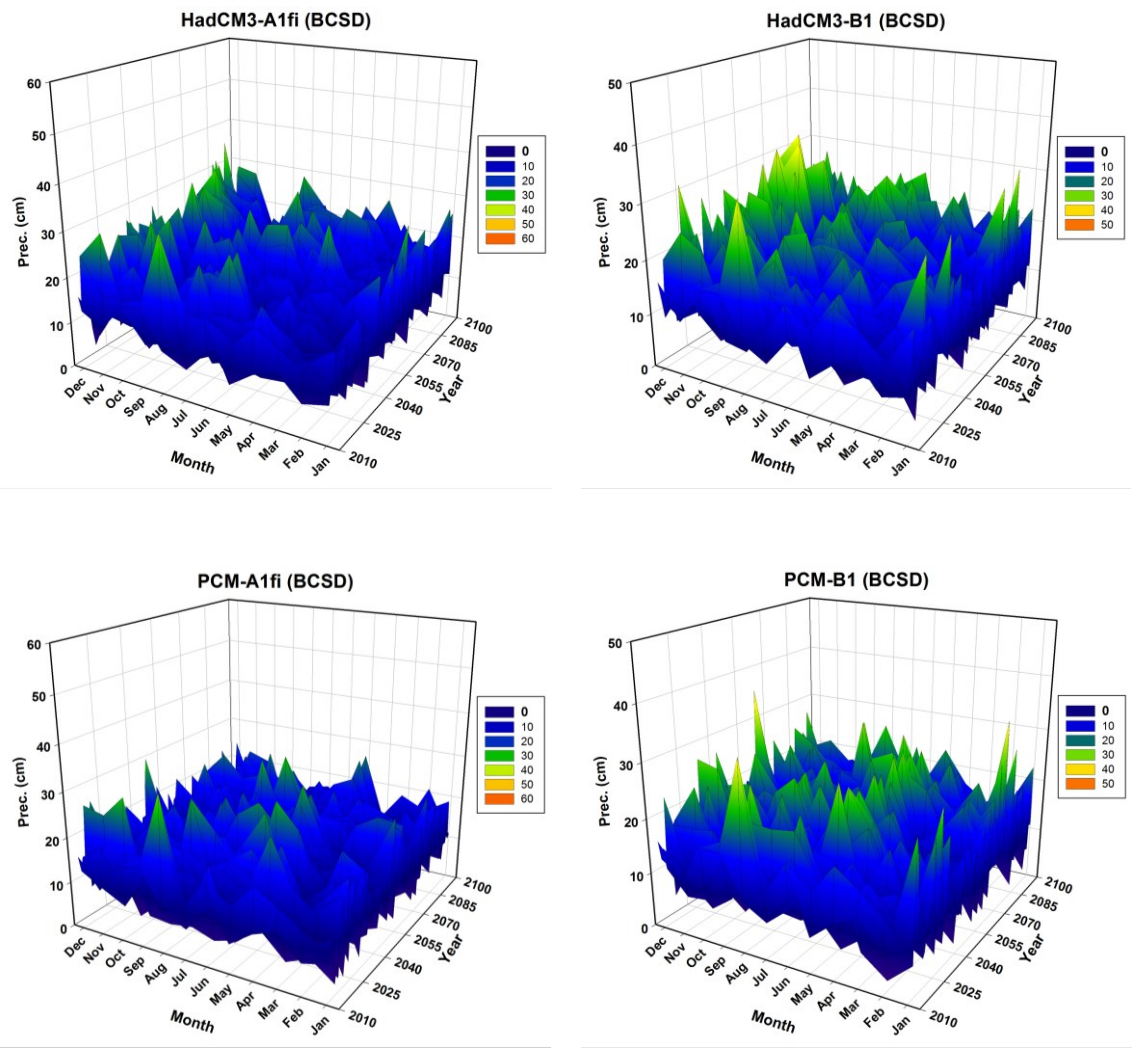

Figure 5.3. Future projections of monthly precipitation under A1fi scenarios (left panel) and B1 scenarios (right panel) downscaled with the BCSD technique.

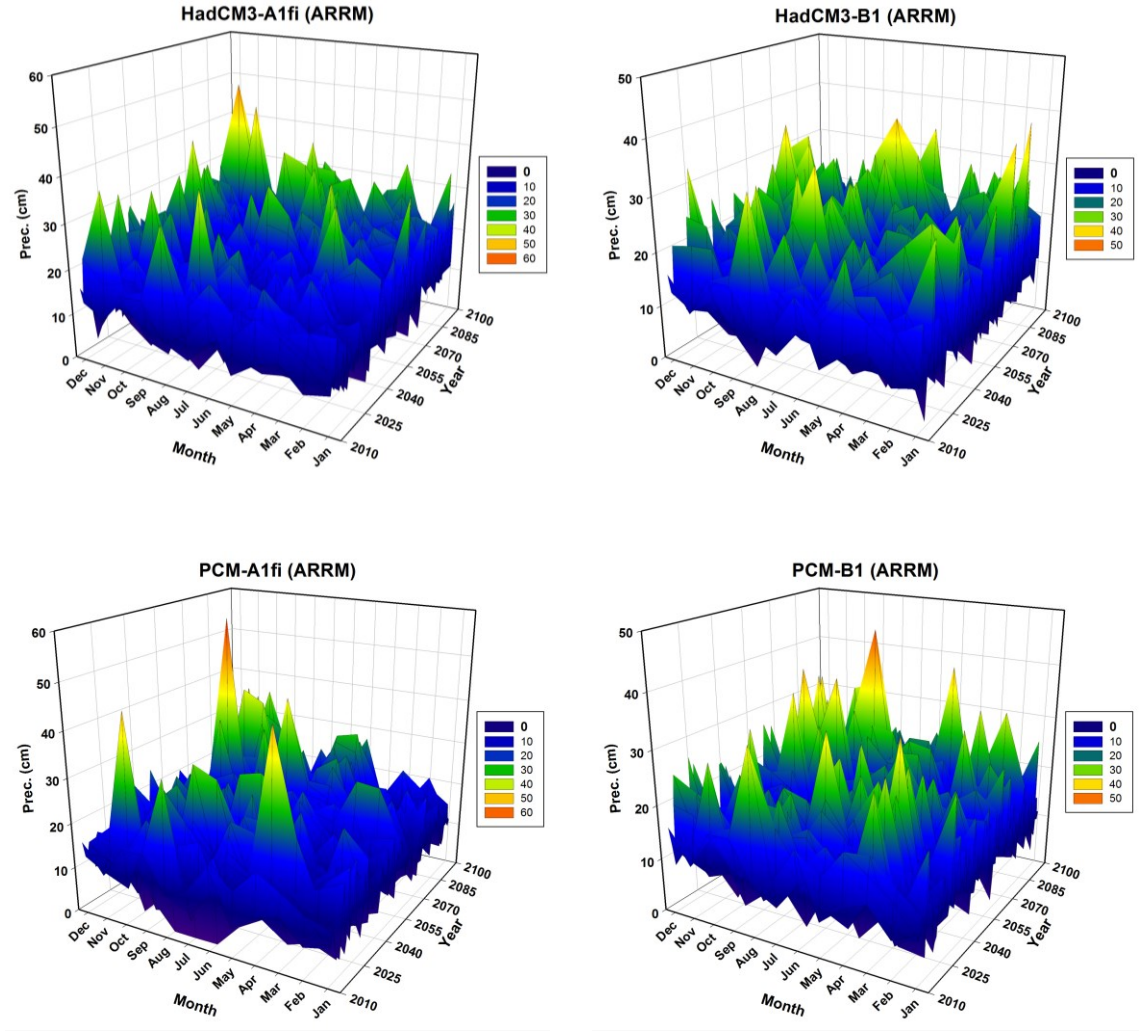

Figure 5.4. Future projections of monthly precipitation under A1fi scenarios (left panel) and B1 scenarios (right panel) downscaled with the ARRM technique.

5.2.3. Hydrology

Model simulations of streamflow change indicated that the current flow regime, of snowmelt-driven spring-flows in April, will likely shift to a flow regime of larger fall/winter

streamflows under changing climate (Figure 5.5 to Figure 5.8). Model projections for both downscaling techniques suggest a shift in the timing of streamwater discharge compared to the historical period (1970-2000), although the downscaling technique had a profound effect on annual discharge. The average annual discharge projected under BCSD simulations was lower for 2070-2100 compared to 1970-2000 values by an average of 8.9%, with a maximum and minimum of 17.3% and 2.4% for PCM-A1fi and HadCM3-A1fi scenarios, respectively (Figure 5.9a and Figure 5.10a). These simulations projected lower flows during the summer (July-September) and higher flows in winter (January-March) compared to the historical period. In contrast, the ARRM downscaled simulations showed an increase in annual stream discharge under HadCM3-A1fi and PCM-B1 of 12.1% and 5.1%, respectively and decrease of 0.4% and 3.3% under HadCM3-B1 and PCM-A1fi, respectively. For each scenario, ARRM projections of annual water yield were higher compared to BCSD for 2070-2100, on average by 13.5% with the maximum and minimum difference of 16.9% and 6.1% under PCM-A1fi and HadCM3-B1 scenarios, respectively (Figure 5.9a and Figure 5.10a).

The ARRM simulations projected higher flows compared to BCSD during the early winter and spring snowmelt, as well as summer. Model projections under both downscaling approaches showed an increase in future streamflow in late fall (October-December) and early winter due to warmer air temperature, resulting from less snow pack accumulation and a decrease in the ratio of snow to rain (Figure 5.11a). Results indicated that under the ARRM downscaled simulations for each scenario, there was a deeper snowpack and associated higher snowmelt flow (Figure 5.11b). Future model projections of soil moisture showed changes in temporal pattern as well as magnitude (Figure 5.11d). Both downscaling techniques indicated a decline in average monthly soil moisture for 2070-2100 compared to 1970-2000 values. Soil

moisture projections for PCM scenarios under the ARRM technique were significantly higher compared to BCSD. In contrast, soil moisture simulated using the HadCM3 scenarios downscaled with ARRM was similar to that simulated with BCSD projections except during late summer and early fall when values were lower. Model projections showed that under all scenarios for both downscaling techniques, decreases in soil moisture start earlier in the spring (April-June) due to earlier loss of snowpack and wet up later into the fall. This phenomenon was more pronounced under the HadCM3 scenarios (Figure 5.11d).

5.2.4. Net Primary Productivity (NPP)

Future model projections of net primary productivity (NPP) using ARRM downscaling were greater than for BCSD for all climate change scenarios. Model simulations showed a decline in annual NPP for all four climate change scenarios downscaled with BCSD (Figure 5.9 b and Figure 5.10b). The average percentage decline in projections of NPP under BCSD simulations for 2070-2100 ranged from 1 to 12% for PCM-B1 and HadCM3-A1fi, respectively, compared to the mean annual simulated value of 1300 g m^{-2} $year^{-1}$ for 1970-2000. In contrast, NPP projections for ARRM downscaled simulations showed an increase under all scenarios. The average percentage increase in annual NPP projected for 2070-2100 ranged from 2 to 17% (HadCM3-A1fi and HadCM3-B1, respectively) compared to the 1970-2000 period. The effects of downscaling technique on NPP projections were more pronounced under the HadCM3 scenarios (average of 15.3%) compared to PCM scenarios (average of 13%). Model projections of water use efficiency (WUE) indicated a significant decline under all four climate change scenarios and for both downscaling techniques (Figure 5.11c). On average, the ARRM

downscaled simulations showed higher WUE compared to BCSD projections for all scenarios. This difference is more pronounced for the PCM scenarios compared to HadCM3 scenarios.

5.2.5. Stream Nitrate

Model simulations of all four climate change scenarios under both downscaling techniques projected statistically significant increases in annual volume-weighted NO_3^- concentrations over the next century, although the magnitude and variability depend on the scenario and downscaling technique (Figure 5.9c and Figure 5.10c). The BCSD projections of average annual volume-weighted NO_3^- concentrations were higher than those of the ARRM downscaled simulations for all four scenarios, with the difference between the two downscaling methods more pronounced under the HadCM3 scenarios. Under the HadCM3 scenarios, the peak in average annual volume-weighted NO_3^- concentrations occurred in mid-century, while under the PCM scenarios the peak was delayed until the end of the century (Figure 5.9c and Figure 5.10c). Under BCSD downscaled simulations, projected annual volume weighted NO_3^- concentration for the last 30 years of the 21st century ranges from 79 to 133 μmol L^{-1} (PCM-B1 and PCM-A1fi, respectively), compared to an average annual observed value of 18 μmol L^{-1} for 1970-2000. The range for the same period under the ARRM scenarios is from 45 to 105 μmol L^{-1} (PCM-B1 and HadCM3-A1fi, respectively). Model projections indicated that timing and magnitude of monthly volume-weighted concentrations of NO_3^- in streamwater differs for the same scenario downscaled with two different techniques (Figure 5.12 and Figure 5.13).

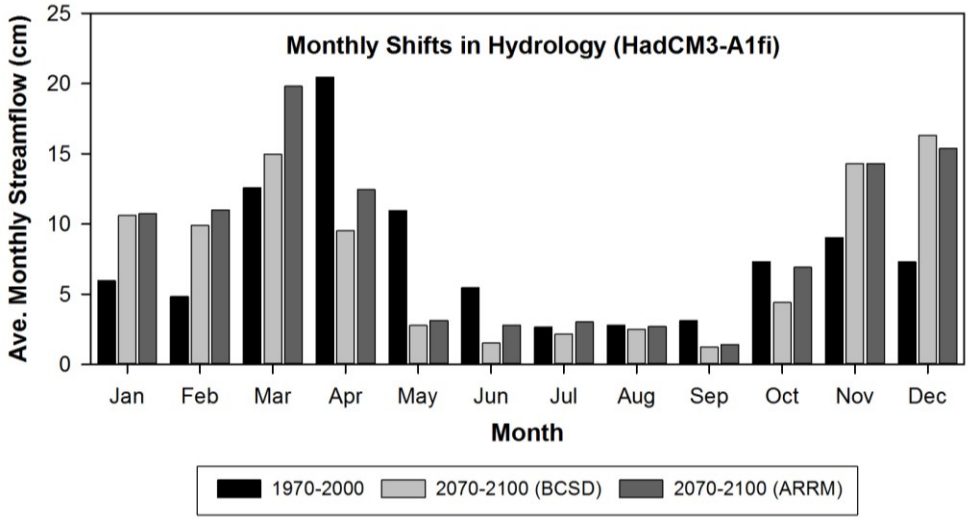

Figure 5.5. Comparison between measured monthly discharge for 1970–2000 and simulated mean monthly discharge for 2070–2100 under the HadCM3-A1fi scenario downscaled with the BCSD and the ARRM techniques.

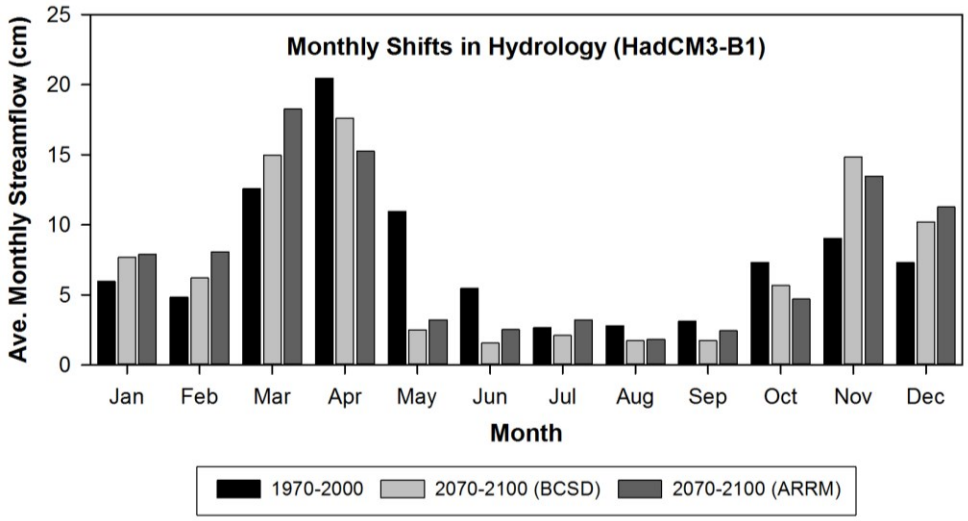

Figure 5.6. Comparison between measured monthly discharge for 1970–2000 and simulated mean monthly discharge for 2070–2100 under the HadCM3-B1 scenario downscaled with the BCSD and the ARRM techniques.

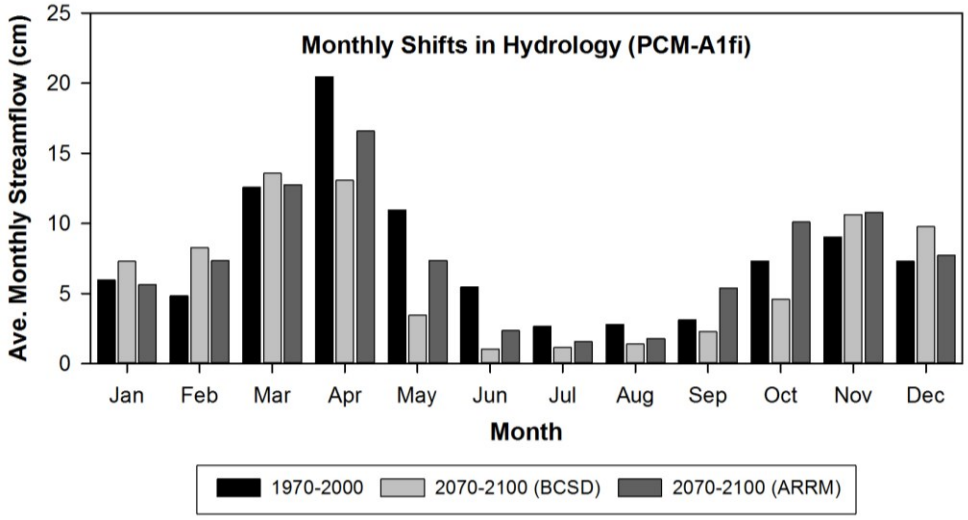

Figure 5.7. Comparison between measured monthly discharge for 1970–2000 and simulated mean monthly discharge for 2070–2100 under the PCM-A1fi scenario downscaled with the BCSD and the ARRM techniques.

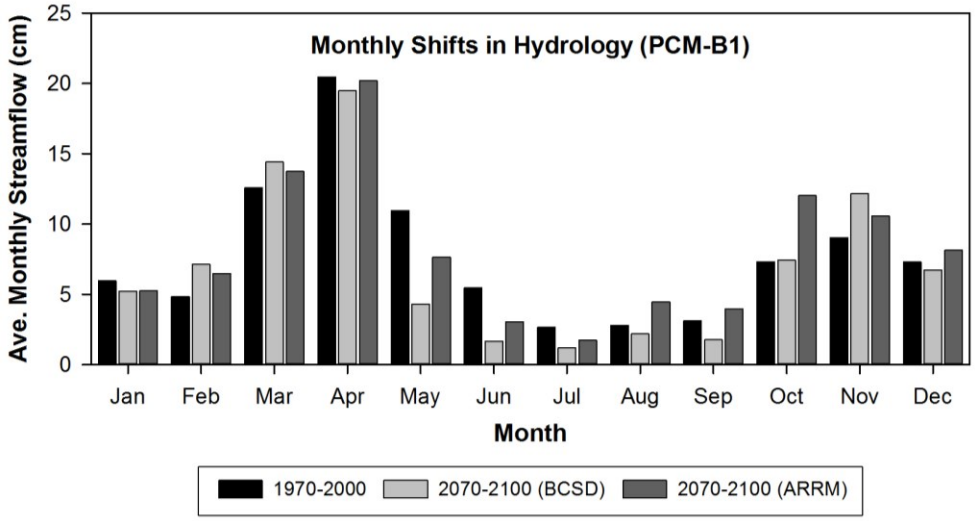

Figure 5.8. Comparison between measured monthly discharge for 1970–2000 and simulated mean monthly discharge for 2070–2100 under the PCM-B1 scenario downscaled with the BCSD and the ARRM techniques.

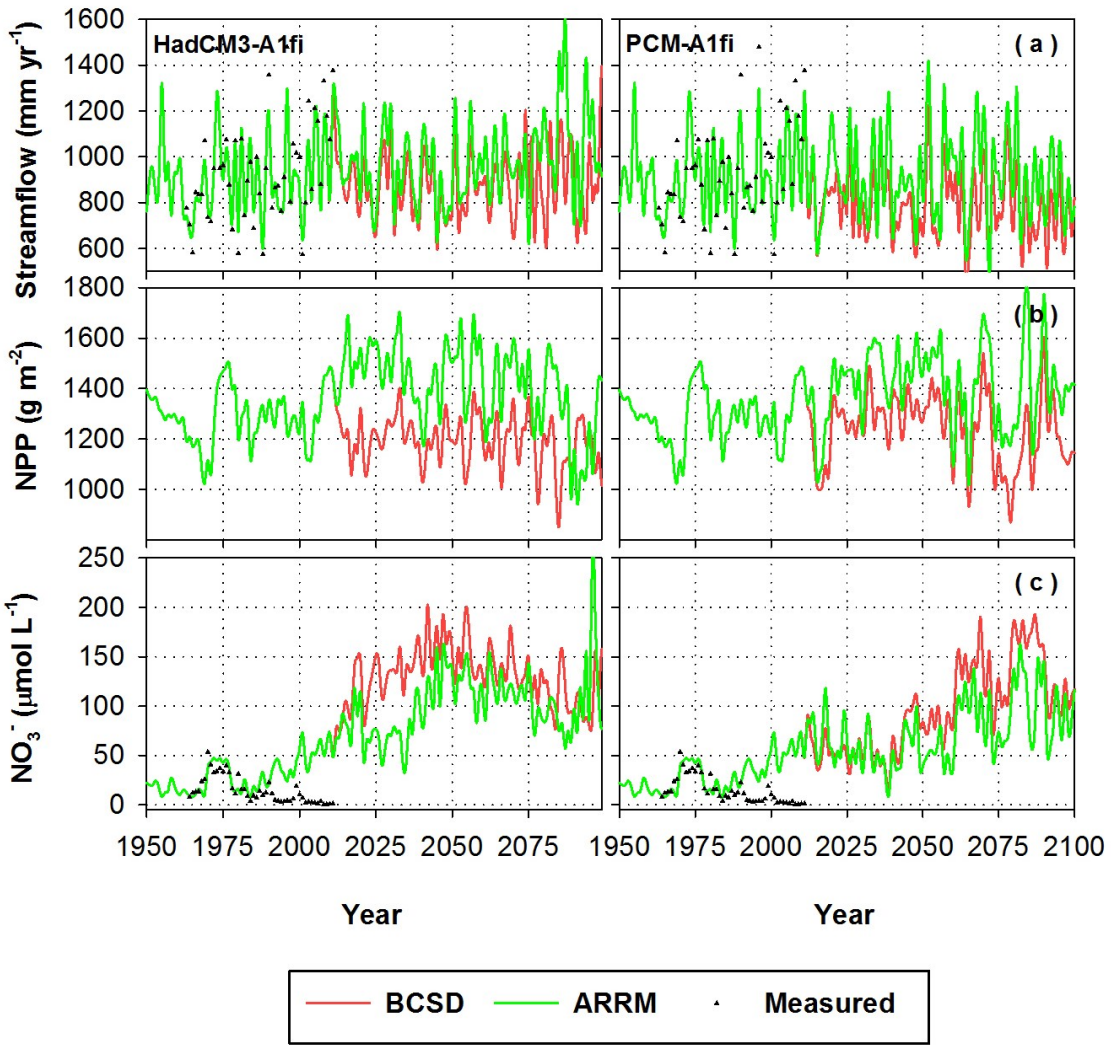

Figure 5.9. Past and future projections of annual: (a) stream discharge, (b) NPP, and (c) volume-weighted concentrations of streamwater NO_3^- modeled using climate input data downscaled with the BCSD (red) and ARRM (green) approaches. Shown are measured data and simulations using input from two AOGCMs under high emission scenarios (A1fi).

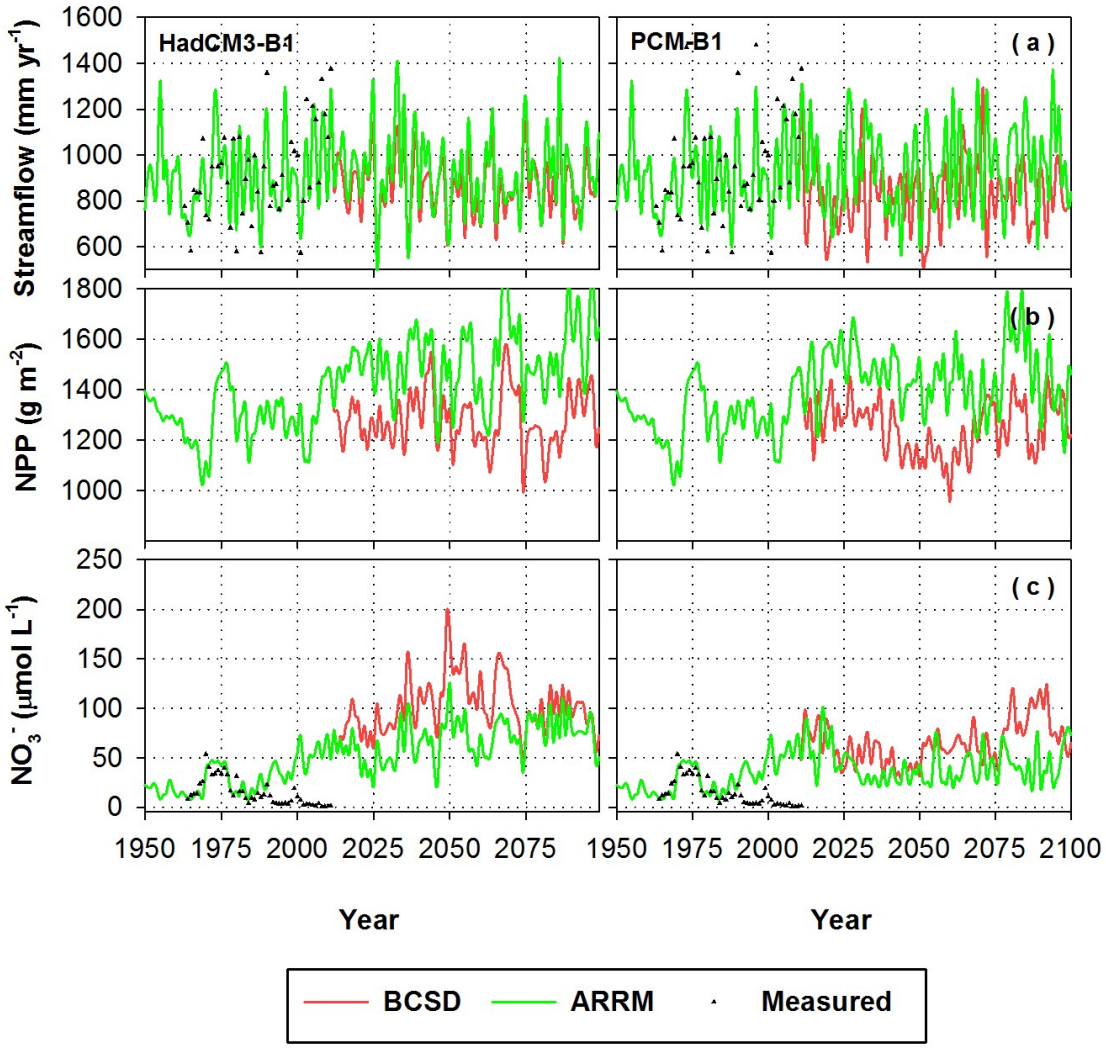

Figure 5.10. Past and future projections of annual (a) stream discharge, (b) NPP, and (c) volume-weighted concentrations of streamwater NO_3^- modeled using climate input data downscaled with BCSD (red) and ARRM (green) approaches. Shown are measured data and simulations using input from two AOGCMs under low emission scenarios (B1).

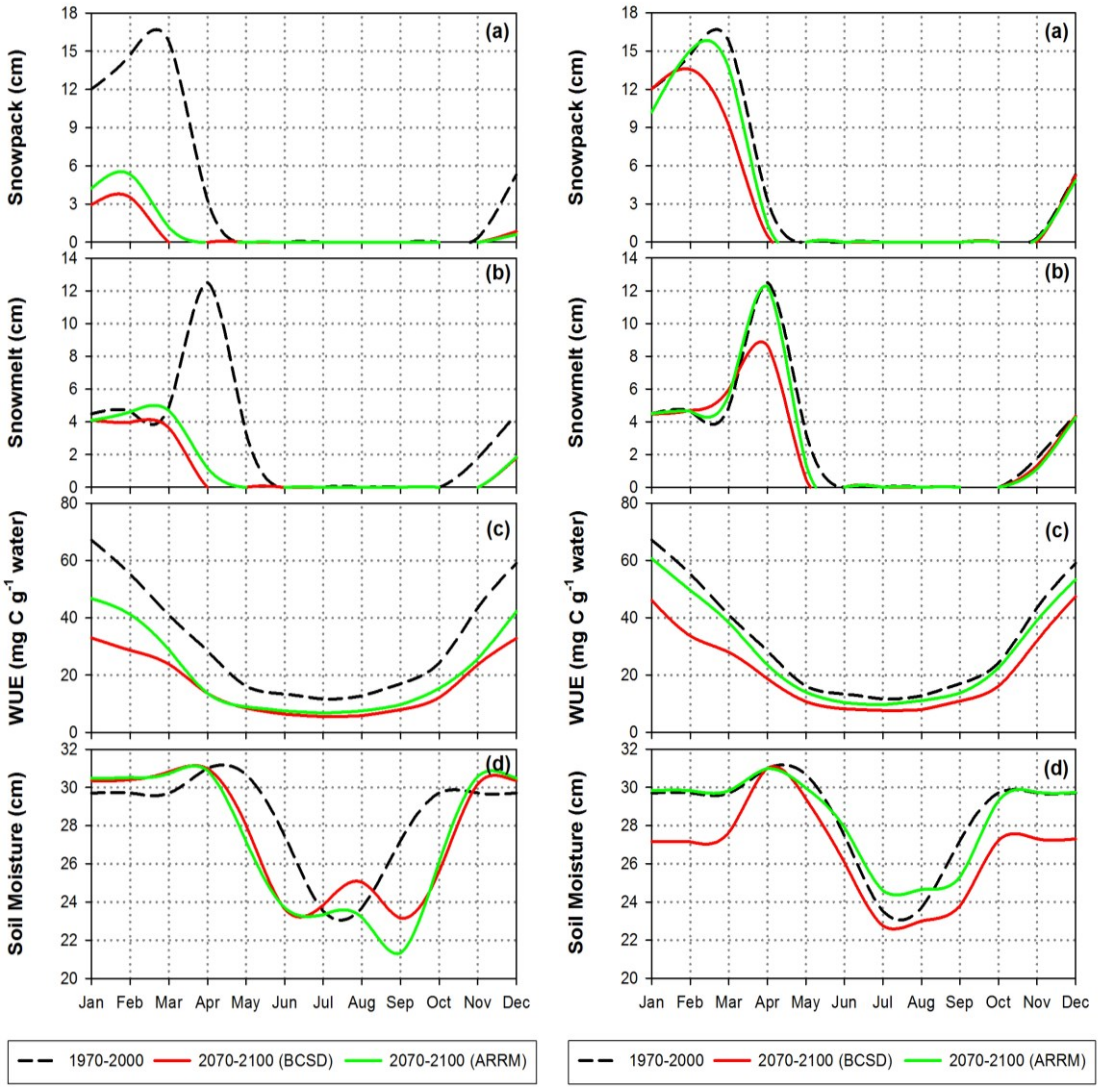

Figure 5.11. Comparison between simulated historical (1970-2000) (a) mean monthly snowpack, (b) snowmelt, (c) water use efficiency (WUE), and (d) soil moisture and future projections for 2070-2100 under the HadCM3-A1fi scenario (left panel) and the PCM-B1 scenario (right panel) downscaled with BCSD (red) and ARRM (green) approaches.

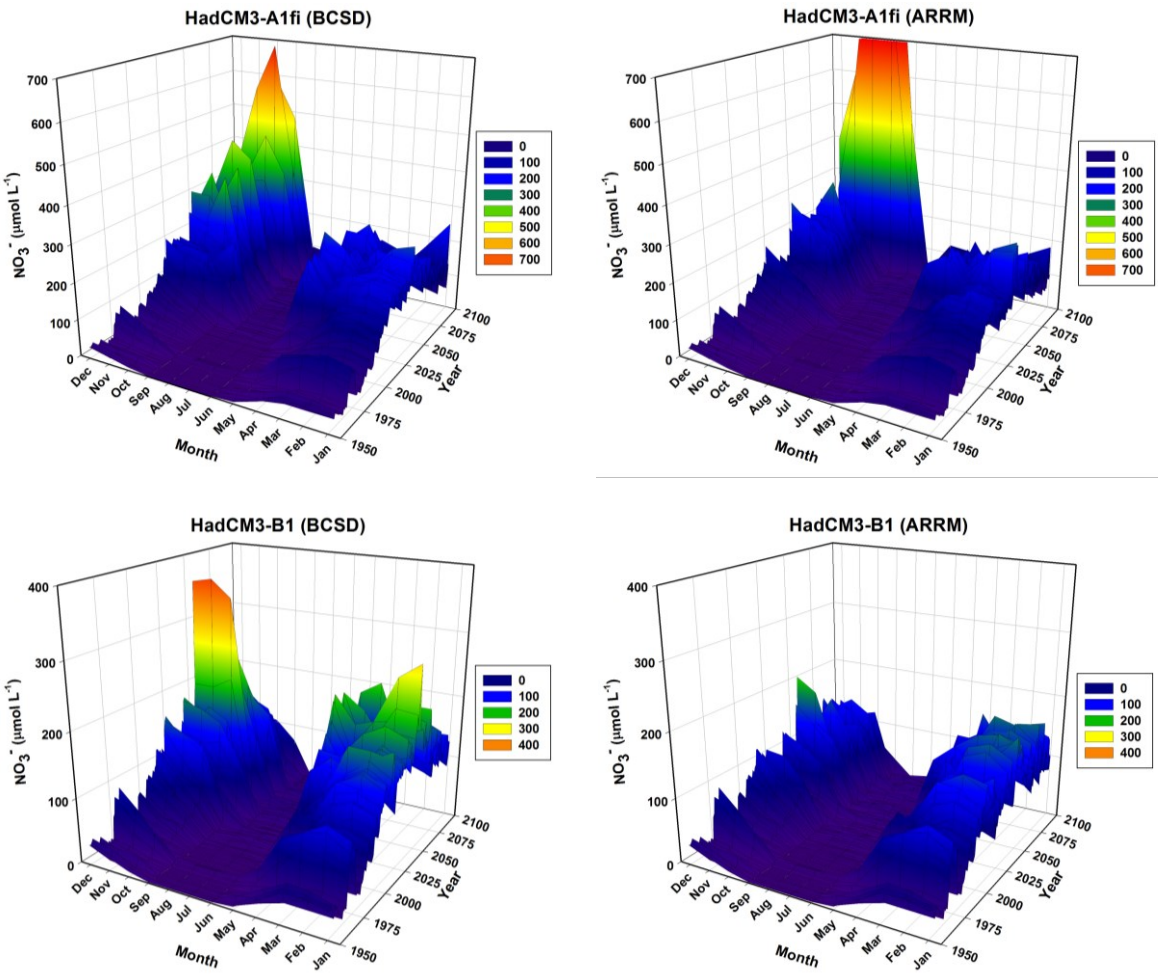

Figure 5.12. Past and future projections of monthly volume-weighted concentrations of NO_3^- in streamwater under HadCM3 scenarios downscaled with the BCSD (left) and the ARRM (right) techniques.

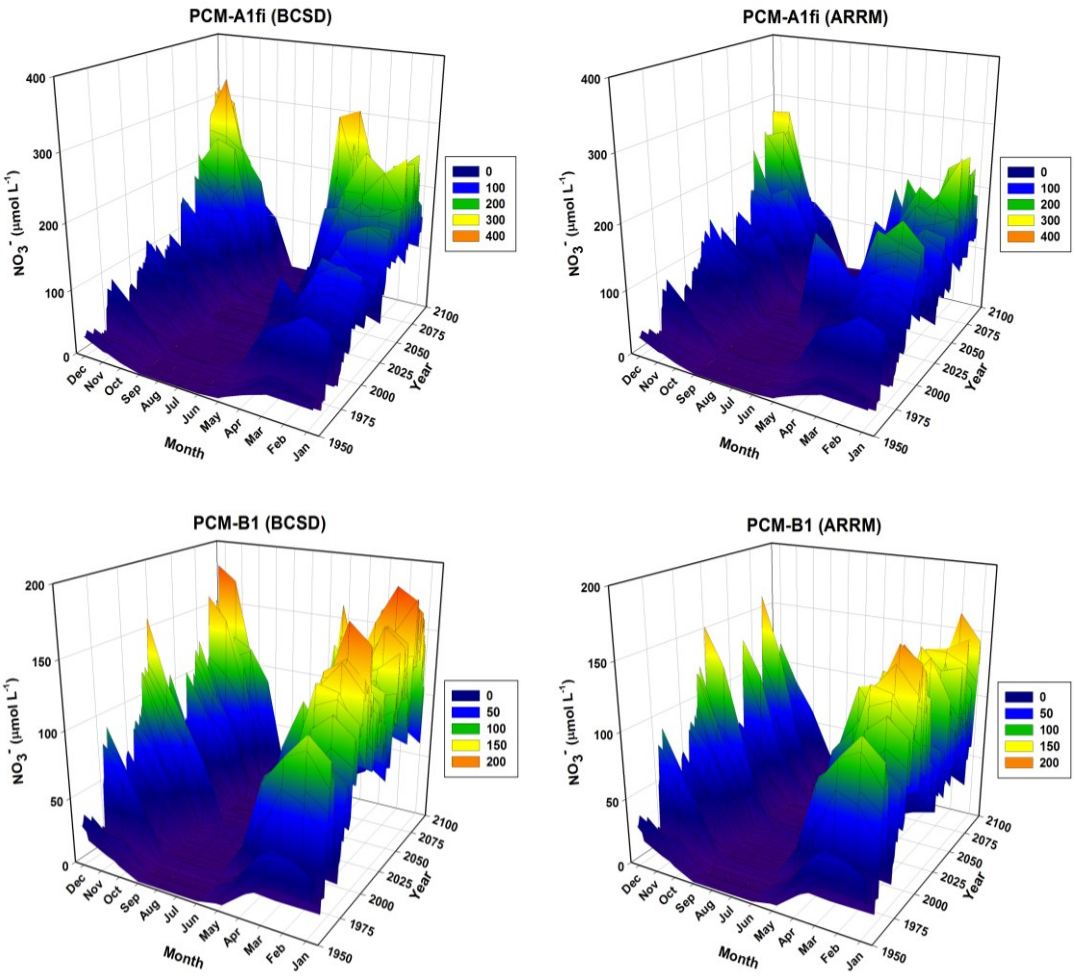

Figure 5.13. Past and future projections of monthly volume-weighted concentrations of NO_3^- in streamwater under PCM scenarios downscaled with the BCSD (left) and the ARRM (right) techniques.

5.3. Discussion

5.3.1. Future Climate Projections

The projected increases in temperature using ARRM downscaling were higher than BCSD due to the ability of the ARRM technique to better capture the number of hot days per year (over 95^{o}F or 36^{o}C) which are in the tail of the temperature distribution [*O'Brien et al.*, 2001]. An important aspect of ARRM is that it uses all the information provided by AOGCMs regarding projected changes in day-to-day variability. This approach allows the shape of the probability distribution to change over time, shifting the mean, variance, and even the skewness (symmetry) of the distribution [*O'Brien et al.*, 2001]. Although the results of this method were similar to less complex downscaling approaches at the seasonal to annual scale, ARRM downscaled projections for changes in the tail of the distribution of meteorological data can be significantly different from other downscaling methods since those approaches do not consider daily projections from AOGCMs [*O'Brien et al.*, 2001]. Overall, the temperature projections under the two downscaling techniques were closer than precipitation projections since there is generally a good match between sets of VIC grid observations and HBEF station measurements of temperature.

The ARRM downscaled projections of precipitation were much higher than BCSD values. This difference is due to two factors. First, ARRM is able to capture simulated changes in large precipitation events on daily basis, by accurately resolving the relationship at the tails of the distribution [*Stoner et al.*, 2012]. Second, the set of precipitation observations that were used for these two downscaling techniques vary significantly. The daily HBEF precipitation for WS6 (0.13 km^2) is calculated by the Theissen weighting method based on 3 rain gages located along

an elevation transect through the watershed. In contrast, VIC uses a retrospective gridded observational database to train the downscaling model to generate grids. Measured temperature and precipitation for a VIC grid cell (~10 km^2) are not from a single station, but rather are statistical interpolations among multiple stations, not all of which are necessarily in the grid cell of interest. Therefore, in a relatively small area with mountainous terrain that affects precipitation patterns like the HBEF, one would expect a single point source of precipitation data to be quite different and more variable from values for the overall 1/8° grid. A comparison of observations (graph not shown) by rank showed that the biases are rank-dependent and not time-dependent (i.e., high precipitation amounts at the HBEF are always underestimated by the VIC grid regardless of the day they occur).

The difference in projections of solar radiation is solely due to the downscaling technique selected since they both employed the same set of observations from VIC. Results from phase 1 (Chapter four) showed that PnET-BGC is sensitive to changes in meteorological inputs. Therefore, differences in climate projections associated with different downscaling techniques are manifested through marked differences in hydrochemical responses.

5.3.2. Hydrology, Stream Nitrate, and NPP

Historical changes in climate at the HBEF have altered the seasonal pattern of streamflow [*Campbell et al.*, 2011]. At the HBEF, the flow regime is snowmelt-driven with peak spring-flows in April, but model projections under both downscaling techniques indicated a decline in the snowpack, snow melt, and timing and magnitude of the snowmelt hydrograph peak. During future warmer winters with a higher rain to snow ratio, snowpack accumulation will diminish

and water will become distributed more evenly throughout the year. Although snowmelt is not the main driver of streamflow at the HBEF, it helps to recharge the groundwater supply [*Campbell et al.*, 2011] and is associated with a large percentage of the annual export of nutrients [*Likens and Bormann*, 1995]. In low elevation areas, changes in the capacity of soil and groundwater to store water will alter the risk of flooding during the snowmelt [*Hodgkins et al.*, 2003]. Compared to BCSD, the use of ARRM downscaling scenarios resulted in a deeper snowpack, higher peak discharge during snowmelt, wetter soil, and relatively higher annual streamflow, suggesting a greater chance of more intense storms and flooding, particularly when soils are saturated. Increased risk of flooding has important implications for climate change adaptation policies in the Northeast [*NECIA*, 2006].

There is a strong relationship between precipitation and streamflow at the HBEF [*Campbell et al.*, 2011], but modeled hydrologic responses to future projected increases in precipitation varied with downscaling technique. Under BCSD downscaled scenarios, the annual discharge decreased under all scenarios due to the projected higher temperature and an associated increase in evapotranspiration, coupled with the inability of the downscaling technique to capture local precipitation patterns and extreme events. In contrast, under the ARRM technique, HadCM3-A1fi and PCM-B1 scenarios showed an increase in annual streamflow while HadCM3-B1 and PCM-A1fi scenarios exhibited a slight decline. As ARRM is more effective in capturing extreme events and local precipitation patterns, all ARRM projections resulted in significantly greater stream flow than under BCSD. There is a growing body of literature that focuses on climate variability, changes in return period and intensity of extreme events rather than "soft" extremes [*Klein Tank and Können*, 2003] which are typically the 90-95th percentile [*Fowler et al.*, 2007]. Changes in precipitation variability and extreme

events elicit a strong response on the hydrological cycle. Model projections of future precipitation and stream discharge indicate an increased importance of individual storms during summer and fall due to more frequent and intense extreme rainfall events. Use of the ARRM downscaling approach had a profound effect on modeled hydrological responses. These results highlight the critical need to correctly characterize the quantity and distribution of future precipitation for accurate streamflow forecasting in the Northeast.

Projected increases in precipitation and associated higher soil moisture and WUE under ARRM downscaling, resulted in increased tree growth compared to BCSD. In PnET-BGC, the length of growing season is determined by the minimum temperature, while the maximum temperature affects photosynthesis and respiration. The difference between maximum and minimum temperatures determines vapor pressure deficit (VPD) which affects the WUE. In the absence of water stress, projected forest growth is higher compared to 20th century due to the warmer, wetter climate and a longer growing season. An increase in both maxima and minima temperatures result in a longer growing season and higher VPD, causing water stress, which offsets the enhancement of tree growth to some extent. Repeated water stress and drought during the growing season, results in decreases in projected maximum LAI, decreasing NPP. Increasing temperature can increase forest growth in two ways: by increasing the number of days with optimum photosynthetic temperature, or by alleviating N limitation through higher rates of soil N mineralization. However, the extent of these effects are limited by precipitation quantity and the seasonal pattern in soil moisture. This example illustrates the important interplay between projections of changing temperature and precipitation and their effects on the growth of forests. The selection of observations and downscaling technique can have important consequences to global change projections.

The export of elements from forested watersheds are strongly influenced by stream discharge [*Likens and Bormann*, 1995]; therefore future changes in the hydrological cycle, especially the seasonality and quantity of discharge, will likely affect water quality and nutrient loss. Soils at the HBEF have low base saturation and are sensitive to inputs of strong acid anions [*Driscoll et al.*, 2001]. Therefore, projections of elevated leaching of nitrate could re-acidify soil and streamwater in acid-sensitive regions that have been impacted by acid deposition like the HBEF [*Driscoll et al.*, 2003]. Moreover, elevated export of nitrate from forest lands could alter the nutrient status of adjacent N-growth limited coastal waters [*Driscoll et al.*, 2003]. The simulated decline in soil moisture induced mid-summer drought stress on vegetation, which could decouples the linkage between soil and vegetation. Midsummer droughts and water stress decreases N uptake by trees and increases N availability, which leads to elevated loss of NO_3^- [*Pourmokhtarian et al.*, 2012]. For model runs using ARRM downscaling, plant WUE increased and midsummer drought did not occur to the same extent as under BCSD simulations. Under ARRM simulations, higher precipitation and associated increases in soil moisture and WUE offset the effect of higher temperatures, thereby minimizing future NO_3^- loss. In PnET-BGC, the decomposition rate of soil organic matter increases exponentially with temperature and decreases linearly with decreasing soil moisture. Therefore, under ARRM downscaled scenarios of higher projected soil moisture and temperature, it might be anticipated that NO_3^- leaching would exceed projections under BCSD. However, the absence of midsummer drought and water stress due to higher precipitation, allowed plant demand for N to keep pace with the N mineralization rate. As a result, the assimilation of the additional N produced under warmer temperatures, limited NO_3^- leaching. Nevertheless under the warmest scenario (HadCM3-A1fi) after mid-century, the optimum temperature for photosynthesis is exceeded under both downscaling techniques,

resulting in similar NO_3^- leaching. Seasonal patterns of annual N export varied with the downscaling technique used; under BCSD elevated concentrations were projected in fall and with ARRM NO_3^- peaked during winter and spring snowmelt.

6. Cross-site analysis for seven headwater watersheds in northeastern U.S.

The objective of this phase of the dissertation was to assess the potential range of responses of forested ecosystems in the northeastern U.S. to future climate change through a cross-site analysis that includes simulations for seven intensive study sites. These sites have different climate conditions, vegetation, soils, historical land disturbance, and biogeochemical characteristics. The location of these watersheds creates pattern of spatial variation in climate (temperature, precipitation, and solar radiation), atmospheric deposition, site characteristics, and host of other variables. In this dissertation phase, I used the ARRM approach to downscale future global climate model output from the IPCC AR5 (see Chapter AOGCMs and Future Scenarios) along with Representative Concentration Pathway scenarios (RCP) (see Chapter AOGCMs and Future Scenarios). These scenarios were used as input to run PnET-BGC.

6.1. Introduction

There is a growing body of literature that anticipates important biophysical processes that are driven by climate to change as a linear function of increasing global temperature [*Allen et al.*, 2009; *Matthews et al.*, 2009; *Meinshausen et al.*, 2009; *Zickfeld et al.*, 2009]. Recent syntheses of available data and modeling results have increased confidence in projections of precipitation and streamflow that might respond to incremental changes in global temperature (e.g., Δ1°C, Δ2°C, Δ3°C) [*Committee on Stabilization Targets for Atmospheric Greenhouse Gas Concentrations; National Research Council*, 2011]. Thus, climate change impacts could be quantified for a

particular unit temperature change by scaling from global to local increases in temperature and coupling projections of water cycle change to the extent of global warming [*Committee on Stabilization Targets for Atmospheric Greenhouse Gas Concentrations; National Research Council*, 2011]. Each incremental increase in temperature can be linked to a "carbon climate response" for CO_2 stabilization targets [*Matthews et al.*, 2009].

The "carbon climate response" is a new metric of temperature change in response to carbon emissions which considers the net effects of both the carbon cycle and physical climate feedbacks to the Earth system [*Matthews et al.*, 2009]. It is defined as the globally averaged temperature change which corresponds to emission of 1 trillion tons of carbon (3.7 trillion tons of CO_2) [*Matthews et al.*, 2009]. Studies show that for a given amount of cumulative emissions, regardless of instantaneous rate, different AOGCMs exhibit a consistent carbon climate response [*Allen et al.*, 2009; *Matthews et al.*, 2009; *Zickfeld et al.*, 2009]. Many impacts of long-term climate change over the 21st century are expected to depend on cumulative total emissions rather than timing of emissions [*Committee on Stabilization Targets for Atmospheric Greenhouse Gas Concentrations; National Research Council*, 2011]. Implementing this approach links climate-induced impacts to global mean temperature and associated cumulative carbon emissions. Thus, this new framework for assessing climate change impacts allows policymakers to focus on potential impacts of climate change to terrestrial ecosystems over the long-term through the metric of cumulative CO_2 emissions for any given period rather than specific atmospheric carbon dioxide concentrations. This approach would orient policymakers toward long term policies of how much cumulative CO_2 should be emitted rather than specific time periods by which emission control programs should take place.

Estimates of the temperature response to cumulative emissions are based on the new metric of carbon-climate response [*Matthews et al.*, 2009]. This new metric is a generalization of climate sensitivity to carbon dioxide forcing. The carbon-climate response relates changes in global mean temperature to cumulative carbon emissions by including the response of the carbon cycle to emissions beside temperature response to carbon dioxide forcing. Studies have shown a linear response of global mean temperature to cumulative carbon emissions [*Allen et al.*, 2009; *Meinshausen et al.*, 2009; *Zickfeld et al.*, 2009] which is independent of the timing of emissions [*Matthews et al.*, 2009]. In this chapter, the projected responses of different watersheds to changing climate are normalized by future increases in temperature. These changes in ecosystem responses could ultimately be linked to corresponding total cumulative carbon emissions.

6.2.Study Sites

Seven intensively-monitored forest watersheds that encompass a range of climate, atmospheric deposition, soil conditions, and historical land disturbances across the northeastern U.S. were used for this phase of the dissertation (Table 3.1). The study watersheds include the Hubbard Brook Experimental Forest (HBEF) and Cone Pond Watershed (CPW) in the White Mountains, New Hampshire; East Bear Brook (EBB) in Maine; Sleepers River Watershed (SRW) in Vermont; Biscuit Brook (BSB) in the Catskill Mountains; and Huntington Wildlife Forest (HWF) in the Adirondack Mountains, New York; and the Fernow Experimental Forest (FEF) in the Allegheny Mountains, West Virginia (Figure 3.1).

The Hubbard Brook Experimental Forest (HBEF) is in the southern White Mountains of New Hampshire, USA (43°56'N, 71°45'W) [*Likens and Bormann*, 1995]. The site was

established as a center for hydrological research in 1955 by the U.S. Forest Service, and joined the National Science Foundation Long-Term Ecological Research (LTER) network in 1987. The climate is cool-temperate, humid continental, with mean annual temperature of 5.7°C, with an annual mean precipitation of 1,400 mm, and an annual mean discharge of 880 mm. Soils are largely well-drained Spodosols, with bedrock at an average depth of 1-2 m. Vegetation is mostly northern hardwoods with coniferous vegetation at higher elevation [*Johnson et al.*, 2000].

The Cone Pond Watershed (CPW) is located in the White Mountains of New Hampshire, USA (43°54'N, 71°36'W). The dominant vegetation is mixed conifer (80%). Less than 10% of coniferous area was cut during 1890-1910 and 1933 [*Aber and Driscoll*, 1997]. The major historical land disturbance was a fire in 1820 which burned almost all of the watershed area [*Aber and Driscoll*, 1997]. Climate is very similar to the HBEF with the mean annual precipitation of 1,280 mm and the mean annual discharge of 670 mm. Soils are mainly Typic, Lithic, and Aquic Haplorthods [*Bailey et al.*, 1995].

The East Bear Brook (EBB) is located in eastern Maine, USA (44°52'N, 68°06'W). The EBB watershed is 11.0 ha and it is the reference watershed for West Bear Brook (WBB). The major historical land disturbance was harvesting in the 1940s that only affected the deciduous vegetation of the watershed (~80-90% of the basal area) [*Norton et al.*, 1999]. The climate is typical for central Maine, with some marine influence due to proximity to the ocean [*Fernandez et al.*, 2003]. Mean annual air temperature is 5.6°C and mean annual precipitation is 1,320 mm [*Fernandez et al.*, 2007]. The dominant vegetation is northern hardwoods. The soils are coarse, loamy, mixed, frigid Typic Haplorthods developed on till averaging one meter in thickness [*Fernandez et al.*, 2003].

Sleepers River Watershed (SRW) is a 41 ha watershed northeastern Vermont, USA (44°29'N, 72°10'W). The watershed was clear-cut in 1929 [*Thorne et al.*, 1988]. The climate is continental, with Canadian air from the north and the Gulf Stream from the south strongly influencing the climate [*Shanley et al.*, 2002]. The mean annual temperature is 6°C with mean annual precipitation of 1320 mm [*Shanley et al.*, 2002] and the mean annual discharge is 740 mm. The dominant vegetation is northern hardwoods. Soil type varies across the watershed and ranges from well-drained podzolic Distrochrepts and Fragiochrepts to poorly drained boggy Fragiaquepts [*Comer and Zimmermann*, 1968]. The bedrock of quartz-mica phyllite with calcareous granulite, which underlies 99% of the basin, is covered with a fine silty calcareous till with a depth of 1 to 3 m [*Shanley et al.*, 2002].

The Biscuit Brook (BSB) watershed is located in the Catskill Mountains, New York, USA (41°59'N, 74°30'W). The watershed has not been logged since the 1920s [*Murdoch et al.*, 1998]. Vegetation is primarily northern hardwood forest. The mean annual air temperature is 4.3°C, with mean annual precipitation of 1,750 mm [*Murdoch et al.*, 1998]. The mean annual discharge is 970 mm. Soils are primarily acidic Inceptisols with low exchangeable base cations [*Murdoch et al.*, 1998].

The Huntington Wildlife Forest (HWF) is located in the central Adirondacks, New York, USA (44°00'N, 74°13'W). The watershed was heavily cut about 1917 and the maximum age of trees is about 100 years [*Mitchell et al.*, 2001]. The dominant vegetation is northern hardwoods (72%), while mixed hardwood-conifer and conifer forest covers 18% and 10%, respectively. The mean annual temperature is 4.4°C. Mean annual precipitation is 1210 mm [*Shepard et al.*, 1989] and mean annual discharge is 830 mm. Soils include Becket-Mundal series sandy loams (coarse-

loamy, mixed, frigid typic Haplorthods) with an average depth of less than 1 m [*Mitchell et al.*, 2001].

The Fernow Experimental Forest (FEF) is in the Allegheny Mountains, West Virginia, USA (39°03'N, 79°41'W). The forest was logged between 1903 and 1911. The mean annual temperature is 9.2°C [*Adams et al.*, 1994]. The mean annual precipitation is 1,460 mm with mean annual discharge of 710 mm. The dominant vegetation is central hardwoods. Average soil depth is around 1 m. Soils are moderately deep and well-drained and formed in parent material weathered from inter-bedded shale, siltstone and sandstone [*Adams et al.*, 1994]. The dominant soil type is a Calvin channery silt loam (loamy-skeletal, mixed, mesic Typic Dystrochrept) [*Adams et al.*, 1994].

6.3. Model Output Analysis

I extracted monthly PnET-BGC output along with site-specific projected and mean global surface air temperatures from two emissions scenarios for each of four AOGCMs (total of eight runs) from 2012 through 2100. I computed the annual global mean temperature for each emission scenarios for each of the four AOGCMs. Then I calculated the absolute values and average percentage changes of each model output for 2070-2100 relative to measured (or simulated when there was no measurement) values of 1970-2000. Then I compared those parameters versus projected increase in annual mean temperature for each site. The state variables considered for this analysis include streamflow, evapotranspiration, drought index (DWater), Net Primary Productivity (NPP), soil humus carbon pool, streamwater nitrate, and acid neutralizing capacity (ANC). The DWater term (ranges from 0 to 1, unitless) is an estimate

of the degree of stomatal closure due to sub-optimal water availability. DWater is a model-calculated metric of soil water stress on stomatal closure compared to the condition in the absence of water stress (DWater=1). Soil water stress (DWater) and actual evapotranspiration are functions of plant water demand and available soil water for each time step of simulation (monthly for this analysis). If the plant water demand is higher than available soil water for a month, water stress occurs and the value of DWater decreases to less than 1 (e.g., a DWater value of 0.9 indicates that there is a 10% shortage of available soil water for trees in that month of model simulation). Therefore, if the sum of DWater for all months of an annual simulation is 12, there is no water stress for any month during that year. An annual DWater value less than 12 indicates that trees experience water stress in some months over an annual simulation which in turn affects stomatal closure, decreases photosynthesis and ultimately decreases NPP. For this analysis I compared DWater values from simulations by subtracting simulated DWater values for an annual period from a reference condition of 12 (i.e., no water stress) (Δ DWater). Therefore, the more negative the Δ DWater values the greater the water stress experienced by trees.

6.4. Results

6.4.1. Future Climate Projections

Statistically downscaled AOGCM climate projections for the two CO_2 emission scenarios for all Northeast sites indicate increases in average air temperature ranging from 1.2 to 8.5°C by the end of the century, depending on the AOGCM, greenhouse gas emission trajectory selected, and study site (Table 6.1, Figure 6.1). The greatest temperature increase is projected by HadGEM-RCP8.5 (8.5°C), while MRI-CGCM3-RCP4.5 shows the most modest temperature

increase (1.2°C). Across the sites, the Fernow Experimental Forest (FEF) shows the lowest and highest increase in temperature (1.2 to 8.5°C), therefore has the maximum variability in projected changes in temperature (SD = 2.3°C). The variability for all other sites is 1.8°C, with the exception of the Huntington Wildlife Forest (HWF) (SD = 2.0°C). Across all eight climate scenarios, HadGEM-RCP8.5 and HadGEM-RCP4.5 show the greatest (SD = 0.8°C) and the lowest (SD = 0.3°C) variability in projected changes in temperature, respectively. The high emission scenarios (RCP8.5) show higher variability across sites and AOGCM simulations (SD = 1.5°C) compared to low emission scenarios (RCP4.5) (SD = 1.1°C).

Precipitation projections are highly variable, ranging from a 5.7 cm decrease to 56.5 cm increase compared to the long-term annual measurements (Table 6.1). The greatest precipitation increase is projected by HadGEM-RCP8.5 (56.5 cm) for Biscuit Brook (BSB), while HadGEM-RCP4.5 shows a decline in projected precipitation for the FEF (Table 6.1, Figure 6.2). Across all sites, BSB shows the highest variability in projected changes in precipitation (SD = 13.1 cm), while the HWF has the lowest variability (SD = 3.4 cm). Across all eight climate scenarios, HadGEM-RCP8.5 and MRI-CGCM3-RCP4.5 exhibit maximum (SD = 19.9 cm) and minimum (SD = 5.9 cm) variability in projected changes in precipitation, respectively. High and low emission scenarios show the same variability in projected changes in precipitation.

All the sites except the FEF show a positive relationship between AOGCM projections of temperature and precipitation (Figure 6.3). The maximum slope of precipitation response to increases in temperature was for the BSB (6.5 cm $°C^{-1}$) while the FEF has the lowest slope (-0.45 cm $°C^{-1}$). The regression between projections of changes in temperature and precipitation is statistically significant ($P < 0.05$) across all sites except for the CPW and FEF. The overall regression line for the relationship between projected changes in precipitation with temperature

change for all sites is statistically significant ($P < 0.1$) with a slope of 2.15 cm °C^{-1} (r^2=0.06). The HBEF shows the strongest significant regression (r^2=0.78, $P < 0.05$) between temperature and precipitation followed by the SRW (r^2=0.73, $P < 0.1$) and EBB (r^2=0.6, $P < 0.05$), while other sites do not show statistically significant relationship between projected changes in precipitation with temperature change.

Table 6.1. Summary of climate projections of change in annual air temperature and annual precipitation from statistically downscaled AOGCM output. The value shown for each scenario is the difference between the mean of measured values for the reference period (1970-2000) and the simulation period 2070-2100. Note that for sites that do not have measured values for the entire period of 1970-2000, measured data for a shorter period are used.*

Study Watershed	Climate Variable	1970-2000*	2070-2100							
		Observed	CCSM4		HadGEM2		MIROC5		MRI-CGCM3	
			RCP 8.5	RCP 4.5	RCP 8.5	RCP 4.5	RCP 8.5	RCP 4.5	RCP 8.5	RCP 4.5
Bear Brook	**Temperature (°C)**	**6.6**	4.9	2.6	6.3	4.6	8.0	4.4	4.6	2.3
	Annual Precipitation (cm)	**131**	42.8	42.2	54.2	52.7	55.5	51.8	54.1	37.2
Sleepers River*	**Temperature (°C)**	**4.7**	4.0	1.7	6.4	4.0	6.5	3.4	3.6	1.6
	Annual Precipitation (cm)	**125**	27.3	17.8	33.5	36.1	34.9	23.2	21.8	12.2
Huntington Forest	**Temperature (°C)**	**4.7**	5.4	3.0	7.4	4.9	8.0	4.8	4.2	2.3
	Annual Precipitation (cm)	**107**	6.2	3.5	6.5	6.0	13.0	5.4	10.0	2.7
Hubbard Brook	**Temperature (°C)**	**5.7**	4.8	2.5	6.6	4.4	7.2	4.1	4.1	2.0
	Annual Precipitation (cm)	**144**	23.6	19.1	24.6	26.5	30.2	21.3	22.3	15.8
Cone Pond*	**Temperature (°C)**	**5.7**	4.8	2.5	6.6	4.4	7.3	4.1	4.2	2.1
	Annual Precipitation* (cm)	**127**	29.7	32.3	45.9	46.0	27.3	22.7	22.0	16.3
Biscuit Brook*	**Temperature (°C)**	**5.3**	4.6	2.3	6.6	4.5	6.9	3.9	3.8	1.9
	Annual Precipitation (cm)	**155**	29.0	26.9	56.5	36.2	52.8	44.8	39.9	18.5
Fernow	**Temperature (°C)**	**9.4**	4.9	2.5	8.5	4.0	6.5	4.0	2.7	1.2
	Annual Precipitation (cm)	**147**	14.0	2.5	3.3	-5.7	22.3	16.1	33.4	9.6

*Sleepers River temperature and precipitation data are from 1991-2000.

*Cone Pond precipitation data are from 1990-2000.

*Biscuit Brook temperature and precipitation data are from 1984-2000.

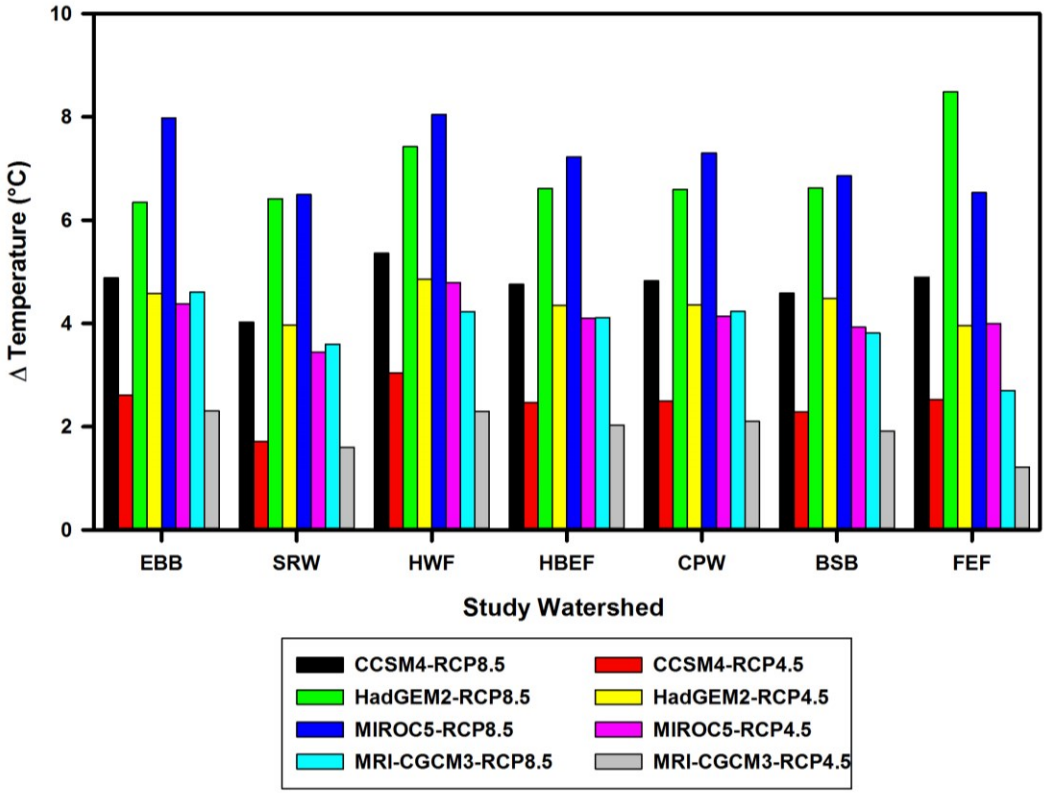

Figure 6.1. Projected changes in mean annual air temperature from statistically downscaled AOGCM output for study watersheds for individual AOGCM simulations under different emission scenarios. The value shown for each scenario is the difference between the mean of simulated annual values for the period 2070-2100 and measured annual values the reference period (1970-2000). EBB: East Bear Brook watershed; SRW: Sleepers River Watershed; HWF: Huntington Wildlife Forest; HBEF: Hubbard Brook Experimental Forest; CPW: Cone Pond Watershed; BSB: Biscuit Brook watershed; FEF: Fernow Experimental Forest.

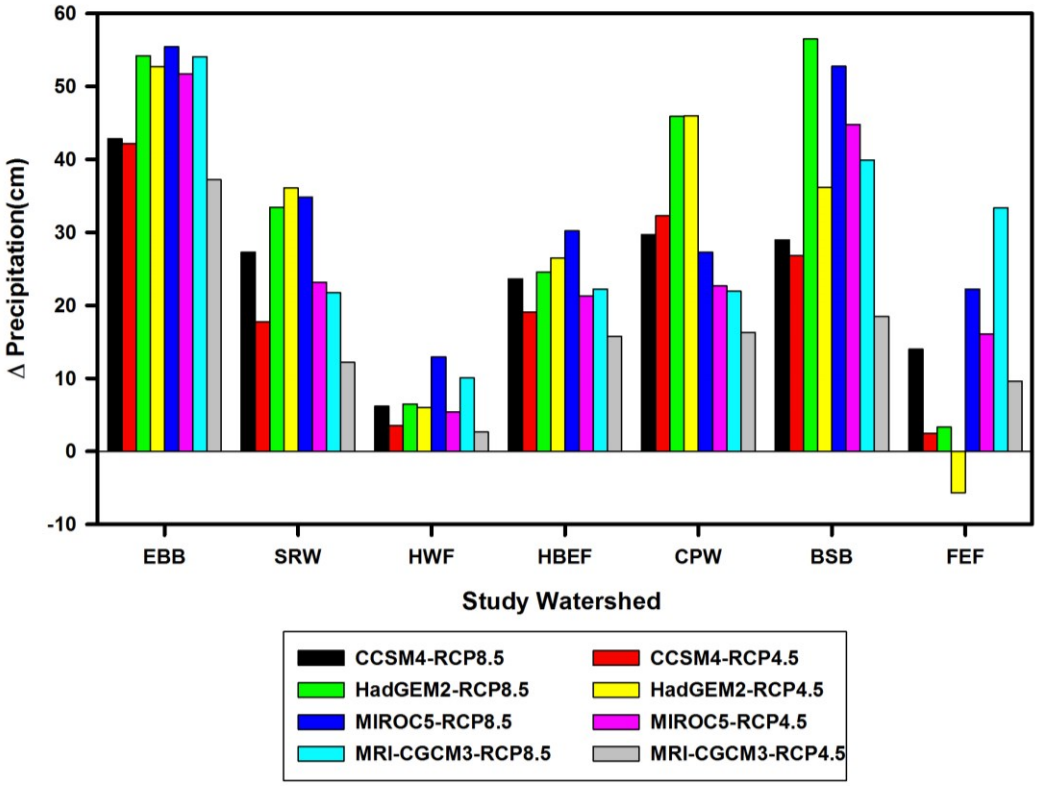

Figure 6.2. Projected changes in mean annual precipitation from statistically downscaled AOGCM output for study watersheds for individual AOGCM simulations under different emission scenarios. The value shown for each scenario is the difference between the mean of annual simulated values for the period 2070-2100 and annual measured values the reference period (1970-2000). EBB: East Bear Brook watershed; SRW: Sleepers River Watershed; HWF: Huntington Wildlife Forest; HBEF: Hubbard Brook Experimental Forest; CPW: Cone Pond Watershed; BSB: Biscuit Brook watershed; FEF: Fernow Experimental Forest.

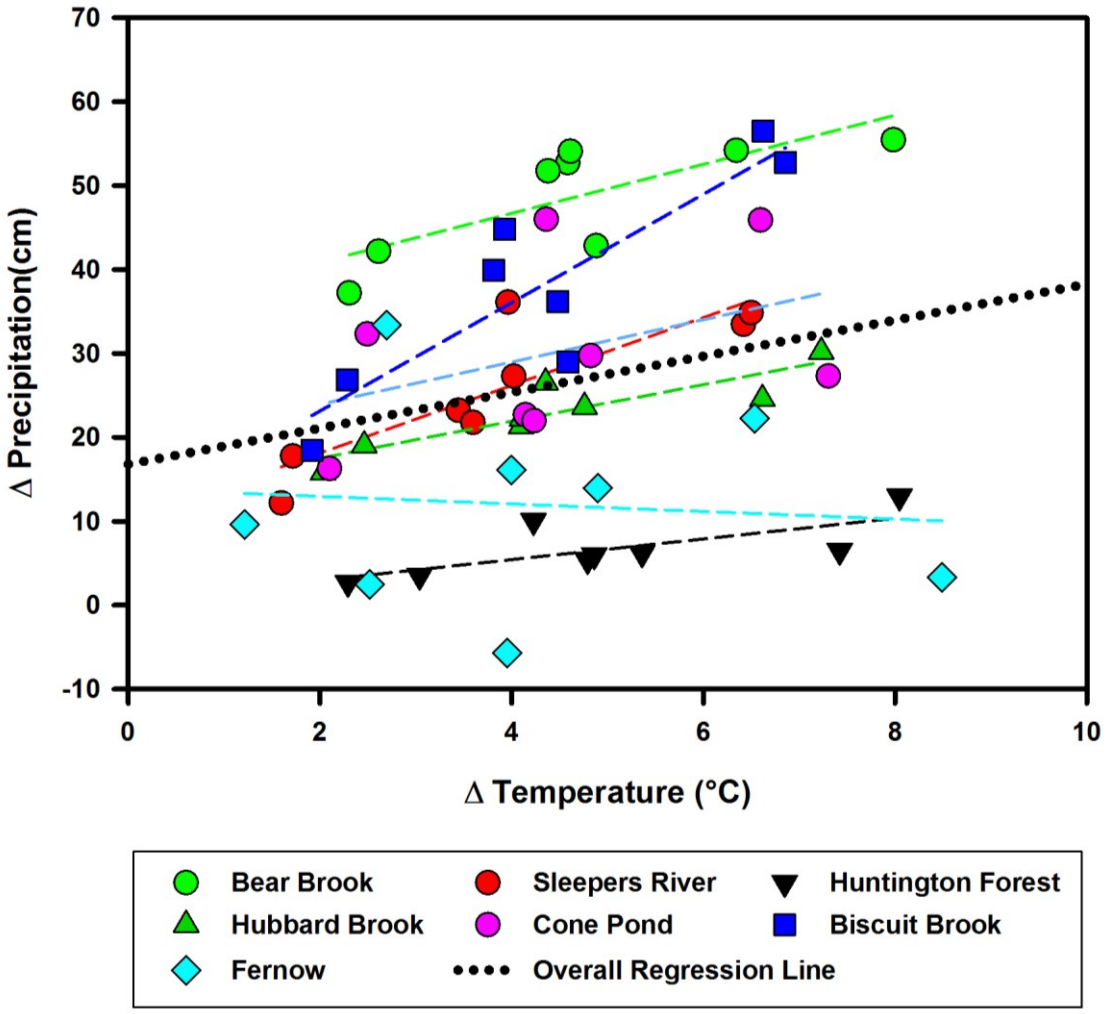

Figure 6.3. Regression analysis between projected increases in mean annual temperature and annual precipitation for the period of 2070-2100 compared to the reference period of 1970-2000. The black dotted line shows the overall regression line for all data.

6.4.2. Hydrology and Water Balance

Based on PnET-BGC model results, climate change is projected to cause substantial long term shifts in annual precipitation and hydrologic patterns across all sites except for the FEF. The extent of these changes depend on AOGCMs, emission scenarios, and site characteristics and location. The most notable trend in streamflow under the eight different scenarios across all sites (except the FEF) was a seasonal shift toward higher winter flows and lower spring flows (data not shown). The FEF shows a seasonal shift in hydrology toward higher winter flows only under HadGEM2-RCP8.5 which has the highest projected changes in temperature (8.5°C) across all sites and all scenarios.

The model projections of mean annual streamflow are highly variable, ranging from a significant decrease at HWF and FEF to significant increases among the rest of the sites except for the HBEF which shows both increases and decreases in annual streamflow depending on the scenario and emissions trajectory (Figure 6.4). The highest increase in projected annual streamflow occurred under HadGEM-RCP4.5 for CPW (Spruce-Fir site) with an increase of 477 mm yr^{-1}. In contrast, the largest projected annual decrease in streamflow also occurred under HadGEM-RCP4.5 but for FEF (central hardwood site) by -219 mm yr^{-1}. There were no significant differences between average projected annual changes in streamflow under high (RCP8.5) and low (RCP4.5) emissions scenarios for any of the study sites (Figure 6.5). Under high emission scenarios, FEF shows the greatest variability in projected annual streamflow (SD = 126 mm yr^{-1}) across AOGCM simulations of high emission scenarios, while SRW shows the minimum variability (SD = 7.8 mm yr^{-1}). In contrast, under low emission scenarios, CPW shows the greatest variability (SD = 108 mm yr^{-1}) and HWF the lowest variability (SD = 9.2 mm yr^{-1}) in projections of annual discharge. Comparison of projected changes in mean annual streamflow

across all sites, indicates that on average high emission scenarios have higher variability (SD = 68 mm yr^{-1}) than low emission scenarios (SD = 54 mm yr^{-1}).

The model simulations of evapotranspiration (ET) show increases under all scenarios and across all sites, although the response is highly variable across sites, AOGCM simulations and scenarios. The highest and lowest increase in mean annual ET for all sites occurred under MIROC5-RCP8.5 and MRI-CGCM3-RCP4.5, respectively (Figure 6.6). Among all sites, the high emission scenarios (RCP8.5) show a higher increase in projected mean annual ET compared to low emission scenarios (RCP4.5) with the FEF showing the highest increase in mean annual ET (Figure 6.7). The highest increase in mean annual ET is projected for the BSB (44.4 cm yr^{-1}) under MIROC5-RCP8.5 scenario and the modest projected for the HWF (6.2 cm yr^{-1}) under the MRI-CGCM3-RCP4.5 scenario. Under high emission scenarios, the BSB simulations show the highest variability in projected mean annual ET (SD = 8.4 cm yr^{-1}), while the CPW exhibits the lowest variability (SD = 2.8 cm yr^{-1}). Under low emission scenarios, the FEF and HWF show the highest (SD = 8.4 cm yr^{-1}) and the lowest (SD = 2.2 cm yr^{-1}) variability, respectively. The variability in projected ET increases with higher ET values (Figure 6.7). Across all sites a comparison of ET between high and low emission scenarios based on percentage change rather than absolute change, show the same pattern except that the BSB exhibits the highest relative change in mean annual ET (Figure 6.8). The regression analysis between projected increases in the percentage change in mean annual ET and mean annual temperature shows a significant ($P < 0.05$) positive relationship ($r^2=0.2$) across all sites (Figure 6.9). All individual sites except the FEF and HWF, exhibited a significant positive relationship ($P < 0.05$) between percentage change in mean annual ET and mean annual change in temperature, with the SRW having the

strongest relationship (r^2=0.9), and HWF (*P value* = 0.06) having the weakest relationship (r^2=0.48).

The model projections of drought index (DWater) indicate significant changes in water deficit for plants under all future CO_2 emission scenarios with different AOGCMs across all sites, except for the CPW (Spruce-fir site) and the FEF under the MRI-CGCM3-RCP4.5 scenario (Figure 6.10). On average across all sites, the high emission scenarios (RCP8.5) projected greater water stress (Δ DWater = -0.4) with higher variability, due to higher temperature projections, compared to low emissions scenarios (RCP4.5) (Δ DWater = -0.2) (Figure 6.11). The highest projected water stress (Δ DWater = -0.72) occurred for the BSB under the CCSM4-RCP8.5 scenario, while the FEF shows reduction of water stress (Δ DWater = +0.02) under the MRI-CGCM3-RCP4.5 scenario which has the lowest projected increase in mean annual air temperature across all sites and scenarios (1.2°C). The FEF responses under both high and low emission scenarios show the highest variability in projected water stress among all study sites (SD = 0.3) and the CPW exhibits the lowest variability (SD = 0.0). A comparison of DWater across all sites based on percentage change shows a similar pattern to values expressed in terms of absolute change (data not shown). The regression analysis between projected increases in changes in mean annual DWater and mean annual temperature show a significant ($P < 0.05$) negative relationship (r^2=0.2) across all sites (Figure 6.12). Across all sites, the HWF and HBEF showed a significant negative relationship ($P < 0.05$), with the HWF having the strongest significant relationship (r^2=0.93) and the BSB and SRW exhibiting the weakest significant relationship ($P < 0.1$). There is no significant relationship of change in mean annual DWater with change in mean annual temperature for the EBB, CPW, and FEF. The CPW did not exhibit water

stress as change in DWater with simulated increases in temperature because water stress is limited in spruce-fir vegetation.

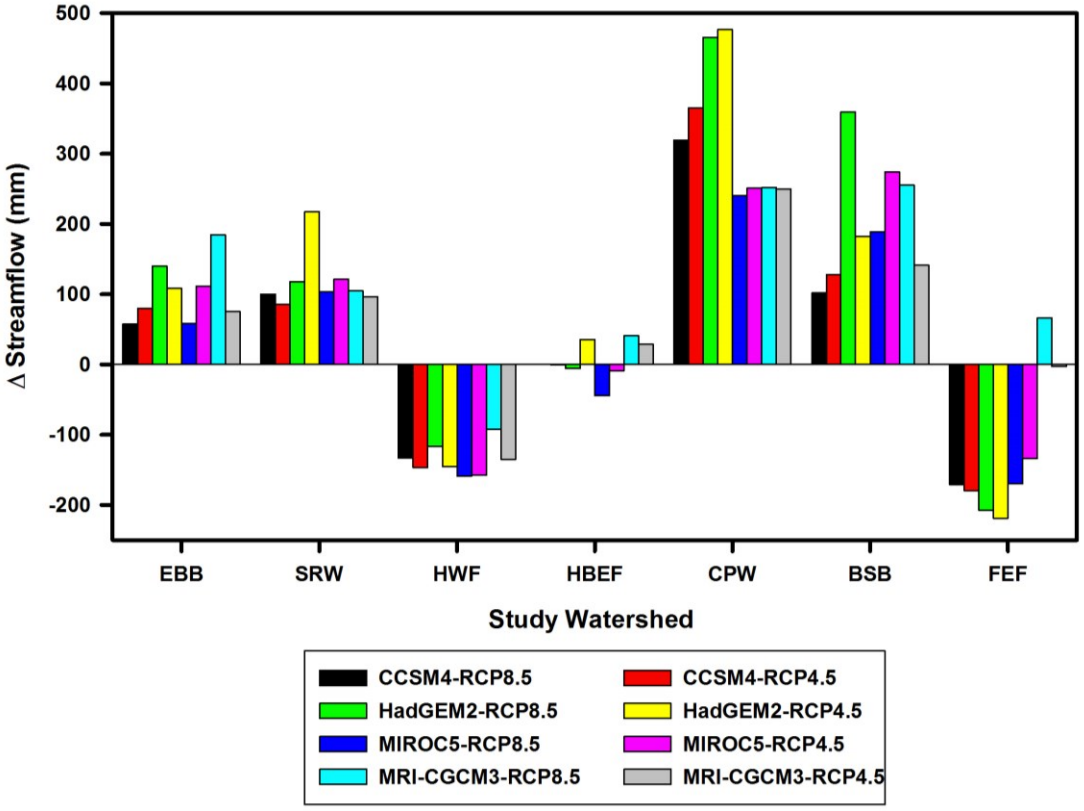

Figure 6.4. Projected changes in mean annual streamflow from PnET-BGC output for study watersheds for individual AOGCM simulations under different emission scenarios. The value shown for each scenario is the difference between the mean of simulated annual values for the period 2070-2100 and the mean of measured annual values for the reference period (1970-2000). EBB: East Bear Brook watershed; SRW: Sleepers River Watershed; HWF: Huntington Wildlife Forest; HBEF: Hubbard Brook Experimental Forest; CPW: Cone Pond Watershed; BSB: Biscuit Brook watershed; FEF: Fernow Experimental Forest.

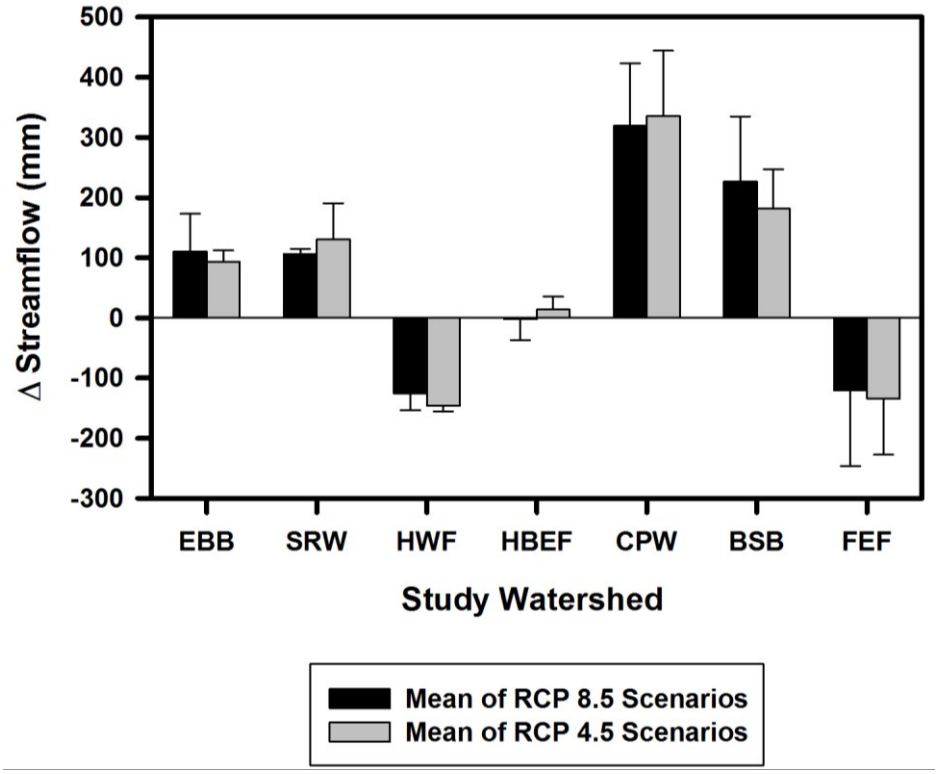

Figure 6.5. Average projected changes in mean annual streamflow under high (RCP8.5) and low (RCP4.5) emissions scenarios for study watersheds. The value shown for each scenario is the average difference between the mean of simulated values for the period 2070-2100 and mean annual measured values for the reference period (1970-2000). The error bars represent the variation of four AOGCMs under each emissions scenario for each site. EBB: East Bear Brook watershed; SRW: Sleepers River Watershed; HWF: Huntington Wildlife Forest; HBEF: Hubbard Brook Experimental Forest; CPW: Cone Pond Watershed; BSB: Biscuit Brook watershed; FEF: Fernow Experimental Forest.

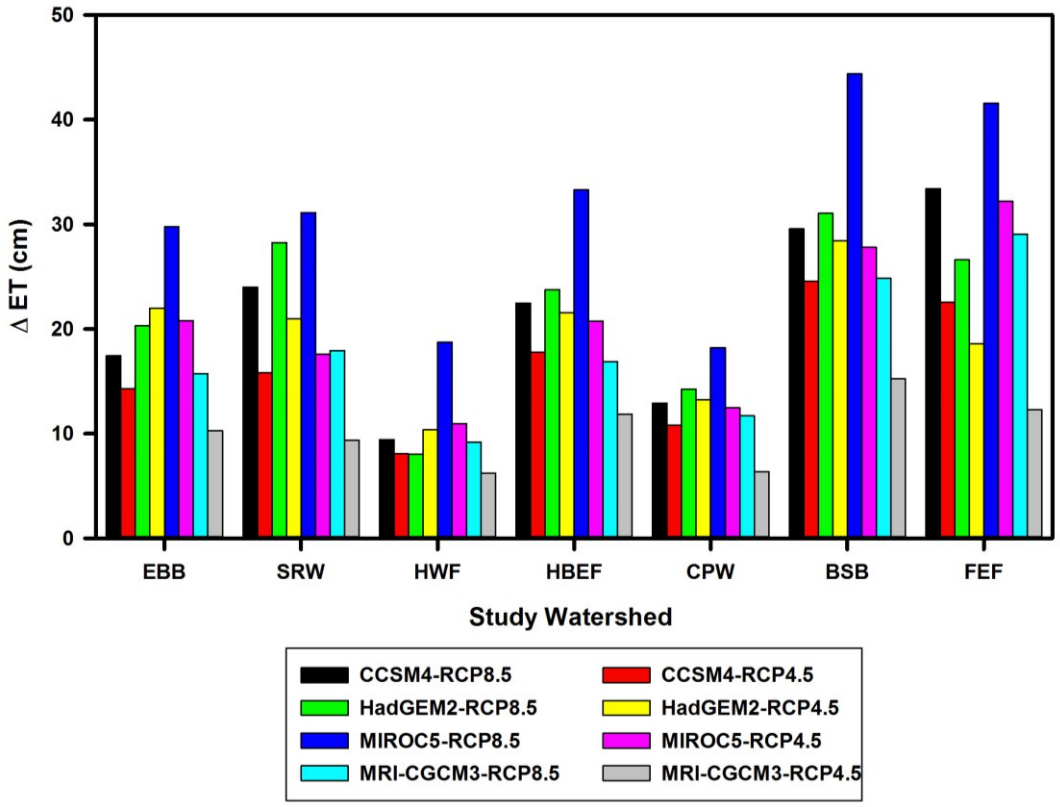

Figure 6.6. Changes in projected mean annual evapotranspiration from PnET-BGC output for study watersheds for individual AOGCM simulations under different emission scenarios. The value shown for each scenario is the difference between the mean of annual simulated values for the period 2070-2100 compared with the reference period (1970-2000). EBB: East Bear Brook watershed; SRW: Sleepers River Watershed; HWF: Huntington Wildlife Forest; HBEF: Hubbard Brook Experimental Forest; CPW: Cone Pond Watershed; BSB: Biscuit Brook watershed; FEF: Fernow Experimental Forest.

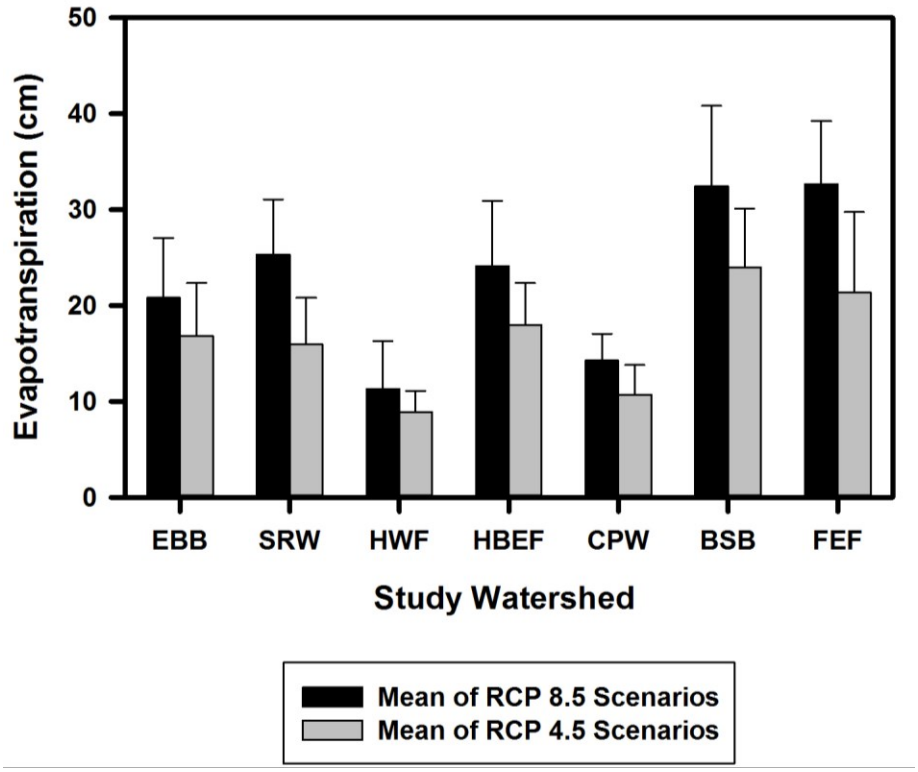

Figure 6.7. Changes in projected mean annual evapotranspiration under high (RCP8.5) and low (RCP4.5) emissions scenarios for study watersheds. The value shown for each scenario is the average difference between the mean of simulated values for the period 2070-2100 compared to the reference period (1970-2000). The error bars represent the variation of four AOGCMs under each emissions scenario for each site. EBB: East Bear Brook watershed; SRW: Sleepers River Watershed; HWF: Huntington Wildlife Forest; HBEF: Hubbard Brook Experimental Forest; CPW: Cone Pond Watershed; BSB: Biscuit Brook watershed; FEF: Fernow Experimental Forest.

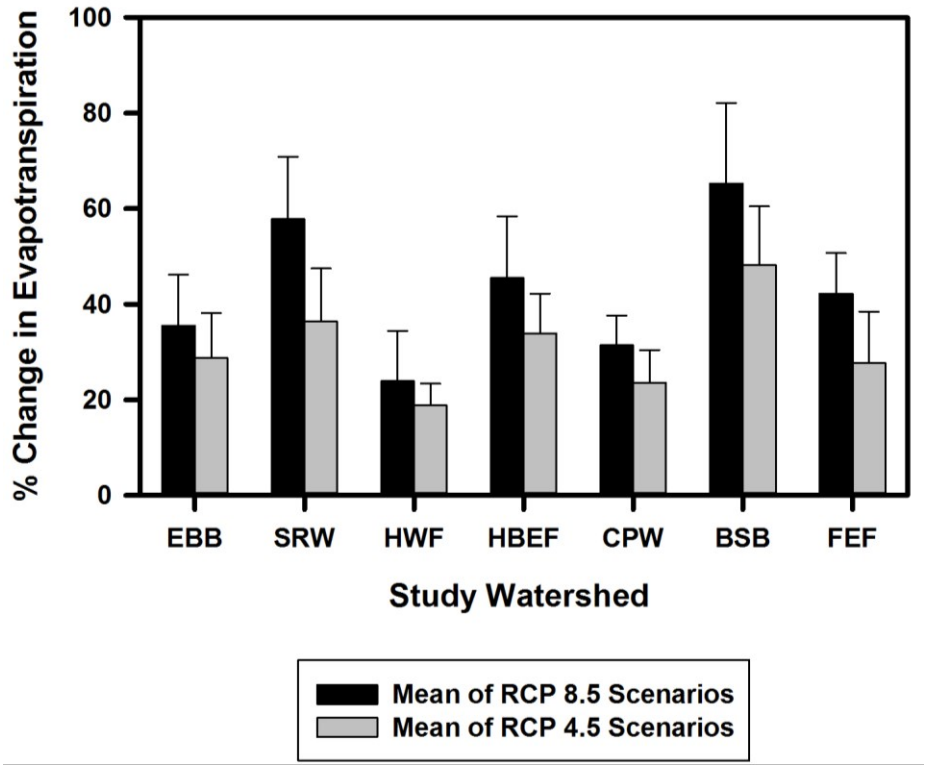

Figure 6.8. Percentage changes in mean annual evapotranspiration projections under high (RCP8.5) and low (RCP4.5) emissions scenarios for study watersheds. The value shown for each scenario is the difference between the mean of simulated values for the period 2070-2100 compared to the reference period (1970-2000). The error bars represent the variation of four AOGCMs under each emissions scenario for each site. EBB: East Bear Brook watershed; SRW: Sleepers River Watershed; HWF: Huntington Wildlife Forest; HBEF: Hubbard Brook Experimental Forest; CPW: Cone Pond Watershed; BSB: Biscuit Brook watershed; FEF: Fernow Experimental Forest.

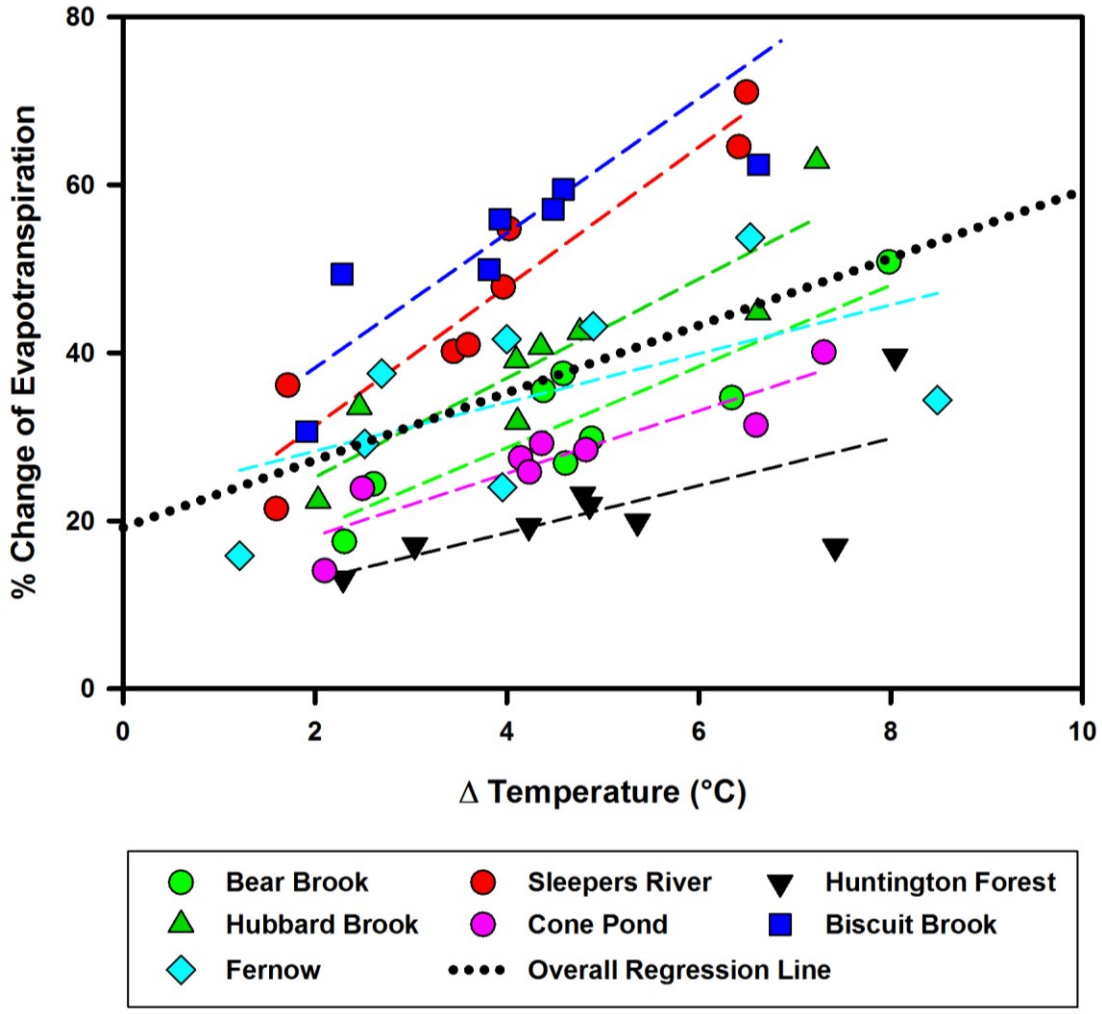

Figure 6.9. Regression analysis between projected increase in mean annual simulated percentage change in evapotranspiration and annual temperature for the period of 2070-2100 compared with the reference period (1970-2000). The black dotted line shows the overall regression line for all data.

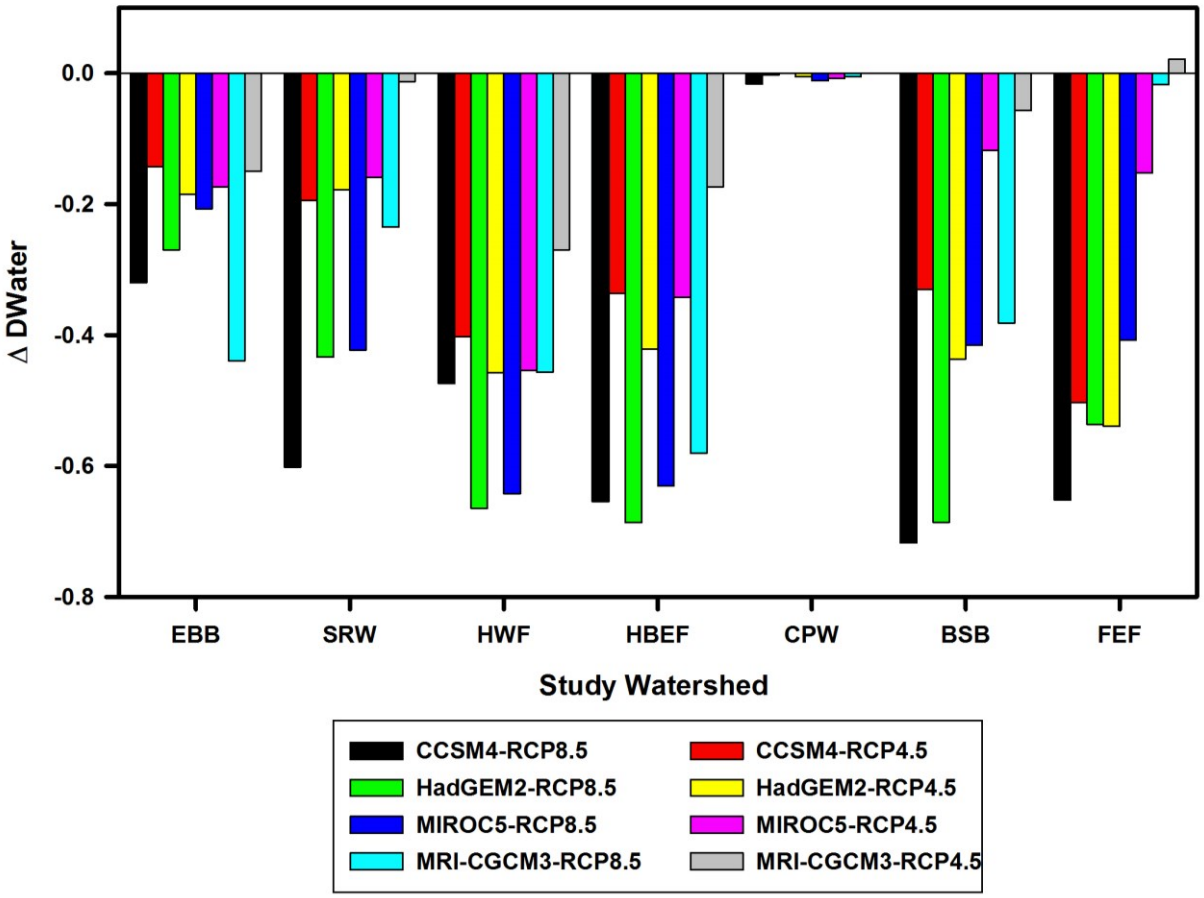

Figure 6.10. Changes in projected mean annual water stress index (DWater) from PnET-BGC output for study watersheds for individual AOGCM simulations under different emission scenarios. The value shown for each scenario is the difference between the mean of simulated values for the period 2070-2100 compared with the reference period (1970-2000). Negative values indicate water stress. EBB: East Bear Brook watershed; SRW: Sleepers River Watershed; HWF: Huntington Wildlife Forest; HBEF: Hubbard Brook Experimental Forest; CPW: Cone Pond Watershed; BSB: Biscuit Brook watershed; FEF: Fernow Experimental Forest.

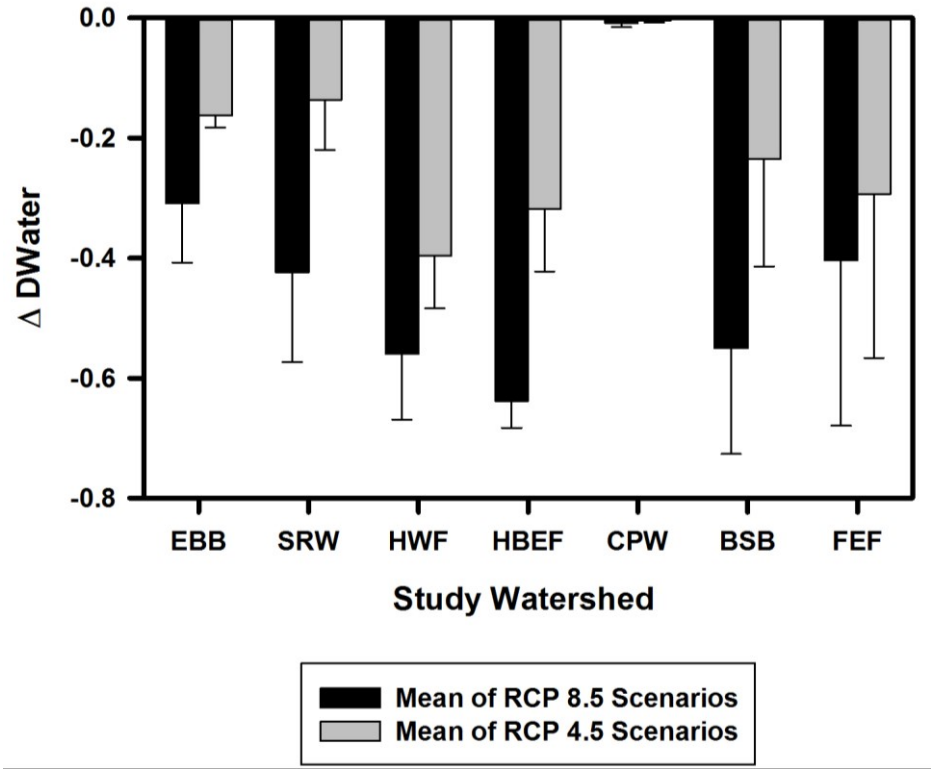

Figure 6.11. Changes in projected mean annual water stress index (DWater) under high (RCP8.5) and low (RCP4.5) emissions scenarios for the study watersheds. The value shown for each scenario is the average difference between the mean annual simulated values for the 2070-2100 period compared with the reference period (1970-2000). The error bars represent the variation of four AOGCMs under each emissions scenario for each site. EBB: East Bear Brook watershed; SRW: Sleepers River Watershed; HWF: Huntington Wildlife Forest; HBEF: Hubbard Brook Experimental Forest; CPW: Cone Pond Watershed; BSB: Biscuit Brook watershed; FEF: Fernow Experimental Forest.

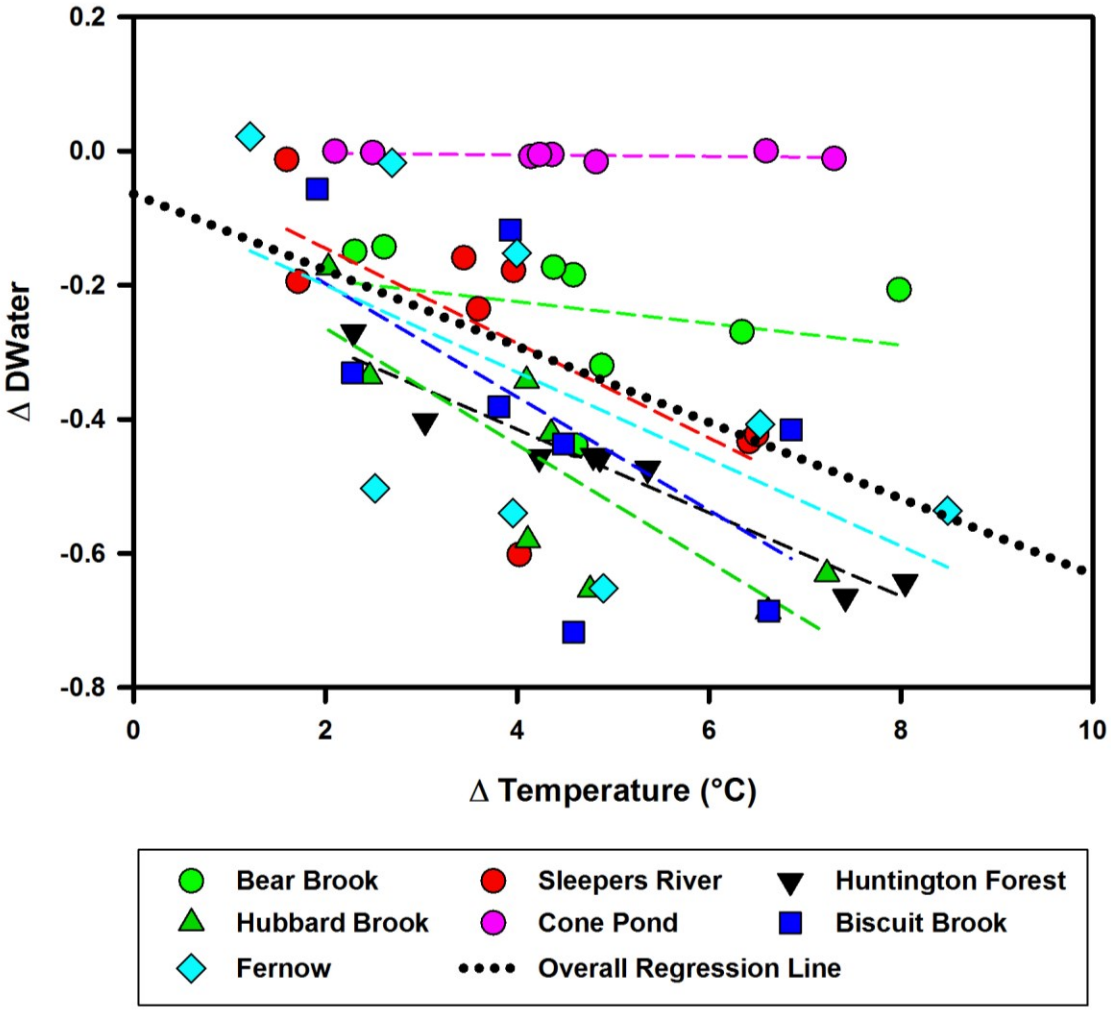

Figure 6.12. Regression analysis between projected change in mean annual simulated water stress index (DWater) and increase in mean annual temperature for the period of 2070-2100 compared with the reference period (1970-2000). The black dotted line shows the overall regression line for all data.

6.4.3. Net Primary Productivity (NPP) and the Soil Carbon Pool

Future model projections of mean annual net primary productivity (NPP) across all sites are highly variable. Simulations show both increases and decreases in mean annual NPP depending on AOGCMs, emissions scenarios and study site (Figure 6.13). The model simulations suggest the highest increase in mean annual NPP of 681 g C m^{-2} yr^{-1} occurs at the BSB under the MIROC5-RCP8.5 scenario. While the largest decrease of 295 g C m^{-2} yr^{-1} occurs at the FEF under the CCSM4-RCP8.5 scenario. On average across all sites, the low emission scenarios (RCP4.5) from the four AOGCMs projected higher NPP due to the lower temperature projections (Figure 6.14). Under the RCP8.5 scenarios, the FEF shows the highest variability in NPP response (SD = 359 g C m^{-2} yr^{-1}), while the CPW exhibits the lowest variability (SD = 79 g C m^{-2} yr^{-1}). Under the RCP4.5 scenarios, the FEF and CPW show the highest (SD = 263 gC m^{-2} yr^{-1}) and the lowest (SD = 55 gC m^{-2} yr^{-1}) variability, respectively. A comparison of all sites based on percentage change of NPP rather than absolute change, reveals a similar pattern for increase in NPP (BSB 54%), while the HWF shows the greatest decline (25%) under the CCSM4-RCP8.5 scenario (graph not shown). There is no significant relationship (*P value* > 0.05, r^2=0.006) between the projected increases in mean annual temperature and percentage changes in NPP across all sites (Figure 6.15). The SRW in the only site that shows a significant positive relationship (*P value* < 0.1, r^2=0.45) (data not shown).

The model simulations of the soil humus carbon pool show significant declines across all sites under all scenarios, with high variability across sites, AOGCMs and scenarios. The model output projected the greatest decline in the humus carbon pool for the HWF (6745 g C m^{-2}) under the CCSM4-RCP8.5 scenario and a smallest decline for the SRW (555 g C m^{-2}) under MRI-CGCM3-RCP4.5 (Figure 6.16). The projected decline in the humus carbon pool under high

emissions scenarios (RCP8.5) are on average 60% greater compared to low emissions scenarios (RCP4.5) (Figure 6.17). Under the high emission scenarios, the FEF shows the highest variability (SD = 1799 g C m^{-2}), while the CPW exhibits the lowest variability (SD = 525 g C m^{-2}). Under the low emission scenarios, the HWF and FEF show the highest (SD = 1405 g C m^{-2}) and the lowest (SD = 394 g C m^{-2}) variability, respectively. A comparison of all sites based on percentage change in the humus carbon pool show a pattern of decline similar to when values are expressed on an absolute base, but the EBB shows the highest percentage decline (61.4%) in soil humus under MIROC5-RCP8.5 (graph not shown). The regression analysis between projected changes in the mean annual humus carbon pool with mean annual temperature change shows a significant negative relationship (*P value* < 0.05, r^2=0.58) across all sites (Figure 6.18). The regression analysis shows significant (*P value* < 0.05) negative relationship between the soil humus pool and mean annual air temperature at each site with a r^2 ranging from 0.66 (HWF) to 0.91 (SRW). The SRW shows the highest relationship (r^2=0.91) while the HWF shows the lowest relationship (r^2=0.66). The slopes of the regression lines are very similar across all sites with the exception of the spruce-fir CPW which shows the smallest change in the soil humus pool with increases in air temperature. Note the regression analysis based on percentage change in the humus carbon pool rather than relative change, indicates a similar slope for the CPW compared with the other sites (Figure 6.19).

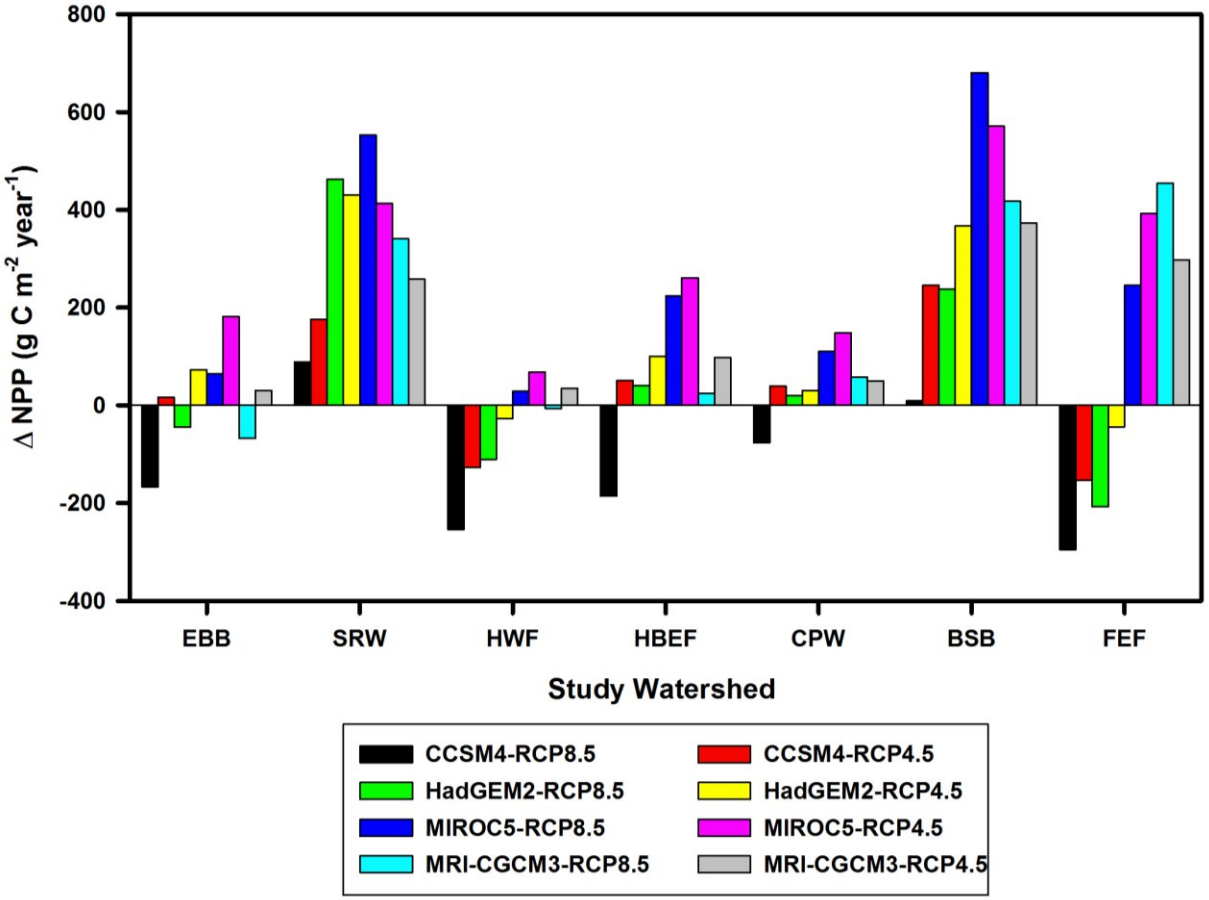

Figure 6.13. Projected changes in mean annual net primary productivity (NPP) for study watersheds for individual AOGCM simulations under different emission scenarios. The value shown for each scenario is the difference between the mean of simulated values for the period 2070-2100 compared with the reference period (1970-2000). EBB: East Bear Brook watershed; SRW: Sleepers River Watershed; HWF: Huntington Wildlife Forest; HBEF: Hubbard Brook Experimental Forest; CPW: Cone Pond Watershed; BSB: Biscuit Brook watershed; FEF: Fernow Experimental Forest.

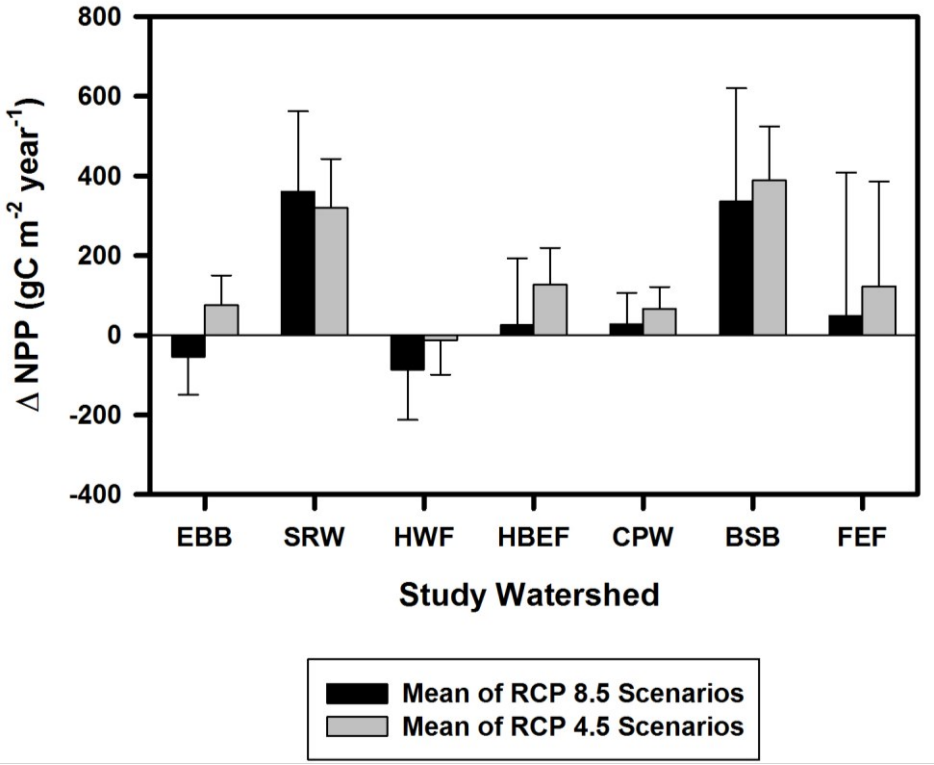

Figure 6.14. Projected changes in mean annual net primary productivity (NPP) under high (RCP8.5) and low (RCP4.5) emissions scenarios for study watersheds. The value shown for each scenario is the average difference between the mean of simulated values for the period 2070-2100 compared with the reference period (1970-2000). The error bars represent the variation of four AOGCMs under each emissions scenario for each site. EBB: East Bear Brook watershed; SRW: Sleepers River Watershed; HWF: Huntington Wildlife Forest; HBEF: Hubbard Brook Experimental Forest; CPW: Cone Pond Watershed; BSB: Biscuit Brook watershed; FEF: Fernow Experimental Forest.

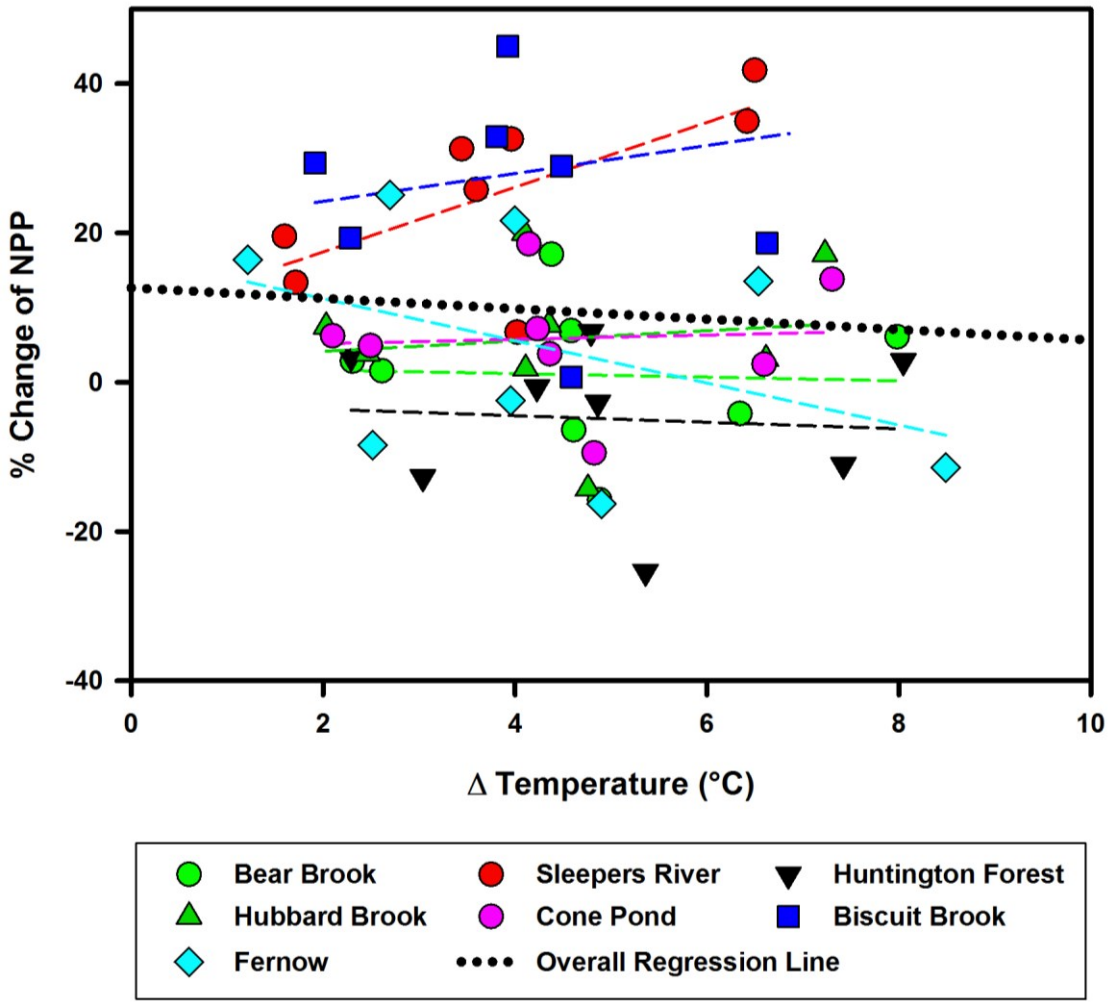

Figure 6.15. Regression analysis between projected percent changes in net primary productivity (NPP) with projected increase in mean annual temperature for the period of 2070-2100 compared with the reference period (1970-2000). The black dotted line shows the overall regression line for all data.

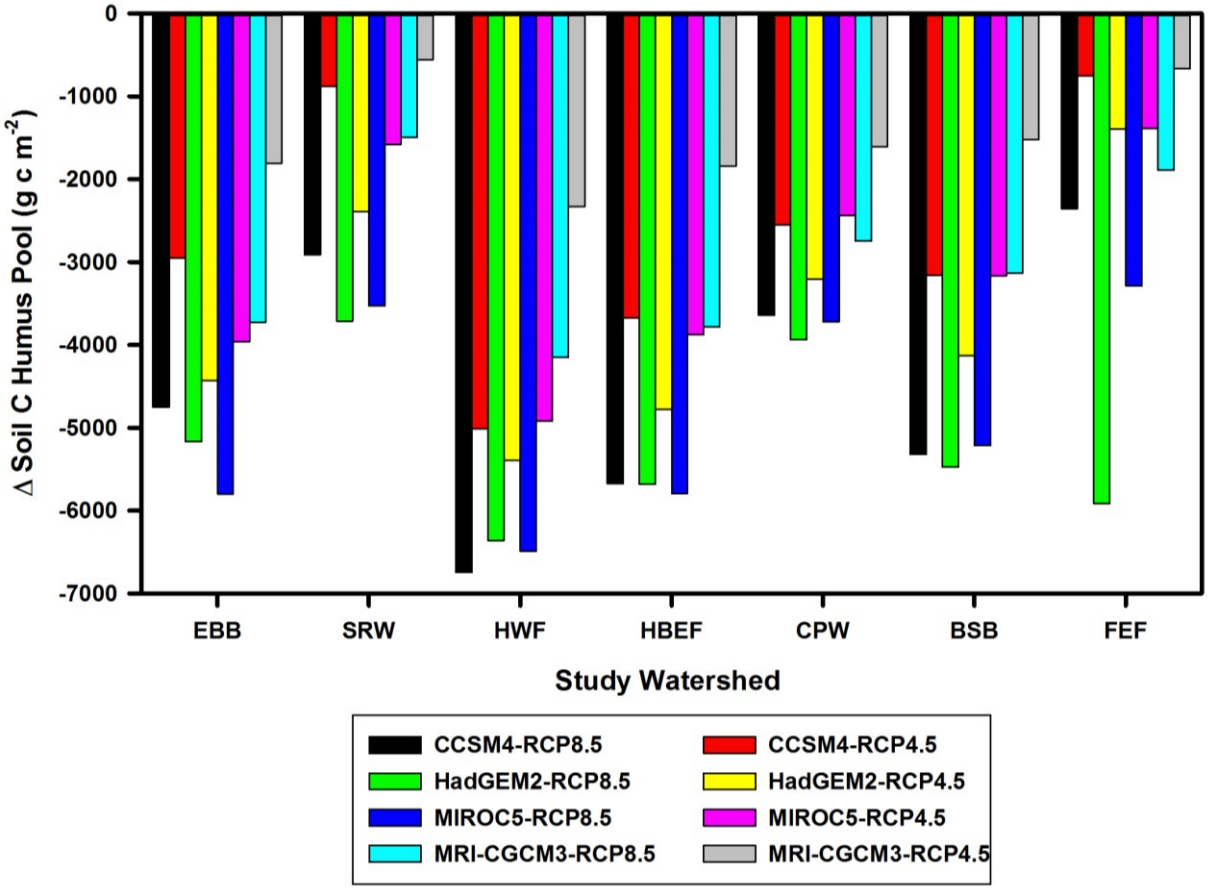

Figure 6.16. Projected changes in mean annual soil humus carbon pool for study watersheds for individual AOGCM simulations under different emission scenarios. The value shown for each scenario is the difference between the annual mean of projections for 2070-2100 and the mean of simulated values for the reference period (1970-2000). EBB: East Bear Brook watershed; SRW: Sleepers River Watershed; HWF: Huntington Wildlife Forest; HBEF: Hubbard Brook Experimental Forest; CPW: Cone Pond Watershed; BSB: Biscuit Brook watershed; FEF: Fernow Experimental Forest.

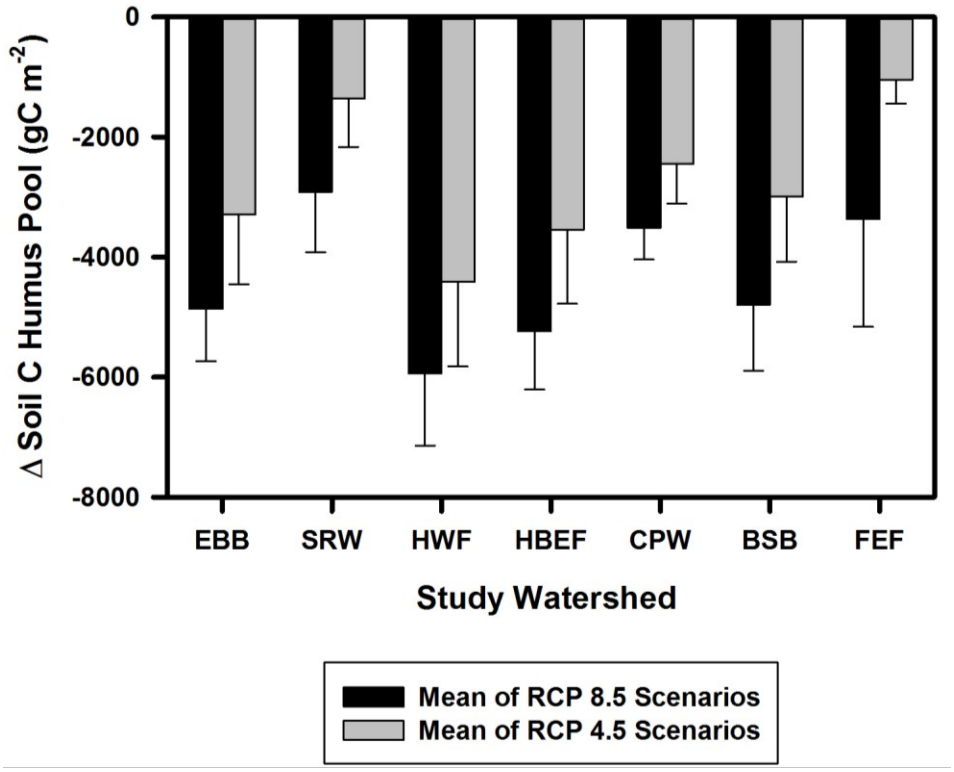

Figure 6.17. Projected changes in the mean annual soil humus carbon pool under high (RCP8.5) and low (RCP4.5) emissions scenarios for the study watersheds. The value shown for each scenario is the average difference between the mean annual simulated values for 2070-2100 compared with the reference period (1970-2000). The error bars represent the variation of four AOGCMs under each emissions scenario for each site. EBB: East Bear Brook watershed; SRW: Sleepers River Watershed; HWF: Huntington Wildlife Forest; HBEF: Hubbard Brook Experimental Forest; CPW: Cone Pond Watershed; BSB: Biscuit Brook watershed; FEF: Fernow Experimental Forest.

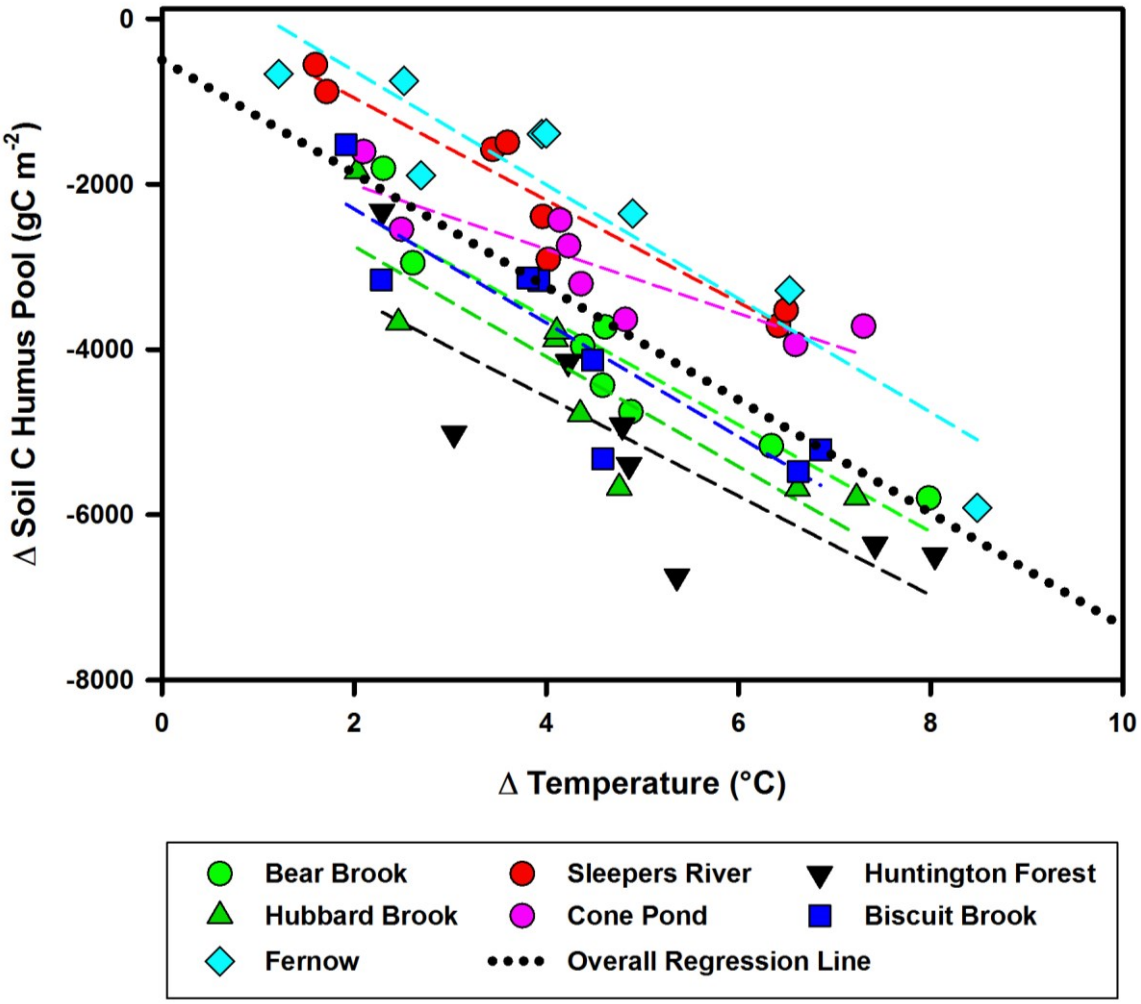

Figure 6.18. Regression analysis between projected changes in annual soil humus carbon pool (gC m^{-2}) and increase in mean annual temperature for the period of 2070-2100 compared with values for the reference period (1970-2000). The black dotted line shows the overall regression line for all data.

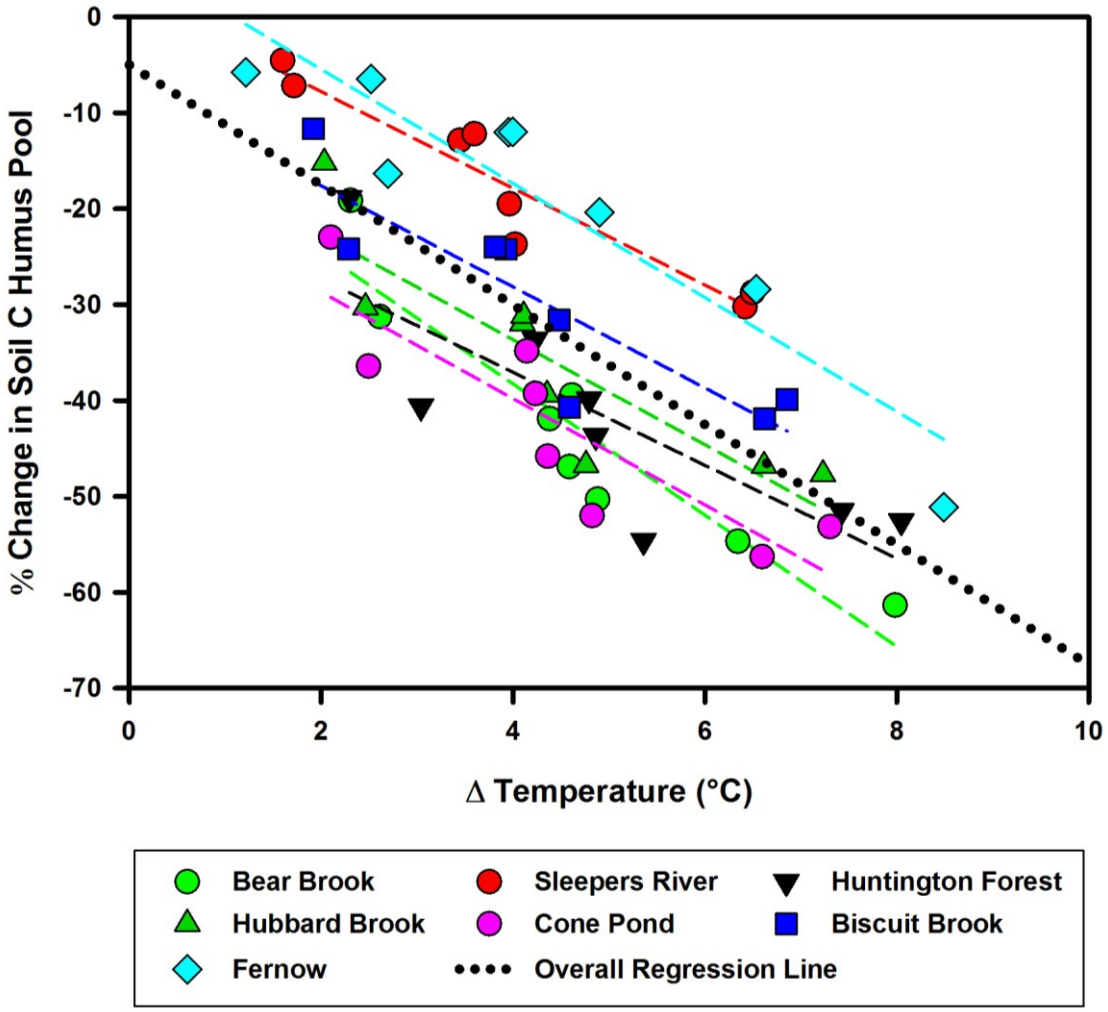

Figure 6.19. Regression analysis between projected percent changes in the mean annual humus carbon pool and mean annual temperature for the period of 2070-2100 compared with the reference period (1970-2000). The black dotted line shows the overall regression line for all data.

6.4.4. Streamwater Chemistry

Model simulations show an increase in annual volume weighted NO_3^- responses across all sites and all scenarios, with the exception of the FEF which shows a decrease under three scenarios (Figure 6.20). Climate change projections indicate substantial temporal shifts in streamwater NO_3^- responses across all sites and the extent of these changes depends on the AOGCMs, emission scenarios, and site characteristics and location. The model simulations of stream NO_3^- for the FEF exhibit marked variability across AOGCM simulations and scenarios with the highest and lowest changes in projected annual volume weighted NO_3^- responses of 210 and -22 μmol L^{-1} under HadGEM-RCP8.5 and MIROC5-RCP8.5, respectively compared to all other sites. Across all sites except the FEF, the average changes in annual volume weighted NO_3^- concentrations under high emissions scenarios (RCP8.5) are approximately double the changes under low emissions scenarios (RCP4.5) (Figure 6.21). Under the high emission scenarios, the FEF shows the highest variability (SD = 104 μmol L^{-1}), while the CPW exhibits the lowest variability (SD = 8.3 μmol L^{-1}). Under the low emission scenarios, the FEF and SRW show the highest (SD = 23.5 μmol L^{-1}) and the lowest (SD = 6.4 μmol L^{-1}) variability, respectively. The HWF is the most sensitive watershed to climate change projections of stream NO_3^- and shows the highest increase in annual volume weighted NO_3^- concentrations in response to all projections due to the lowest increase in future projections of precipitation (Figure 6.20).

Future model projections of mean annual volume-weighted stream acid neutralizing capacity (ANC) show decreases across most sites under all scenarios. Exceptions in this pattern are evident for the EBB and CPW which show increases in ANC under some scenarios (Figure 6.22). The highest increase of 27 μeq L^{-1} in ANC projected for the EBB occurs under the MRI-CGCM3-RCP4.5 scenario. The highest decline in ANC is simulated for the SRW under

HadGEM2-RCP8.5 by 176 μeq L^{-1}. The variation in projected mean annual volume-weighted ANC across AOGCM simulations and scenarios is highest for the SRW compared to other sites. High and low emission scenarios for SRW had standard deviations of 42 μeq L^{-1} and 66 μeq L^{-1}, respectively. The EBB and HBEF with standard deviations of 3.1 μeq L^{-1} and 4.2 μeq L^{-1} showed the lowest variability under high and low emission scenarios, respectively. The CPW is the only site that shows a decrease under the high emission scenario and increase under the low emission scenario (Figure 6.22). The high emission scenarios on average doubled the rate of decline in stream ANC at CPW compared to low emissions scenarios (Figure 6.23).

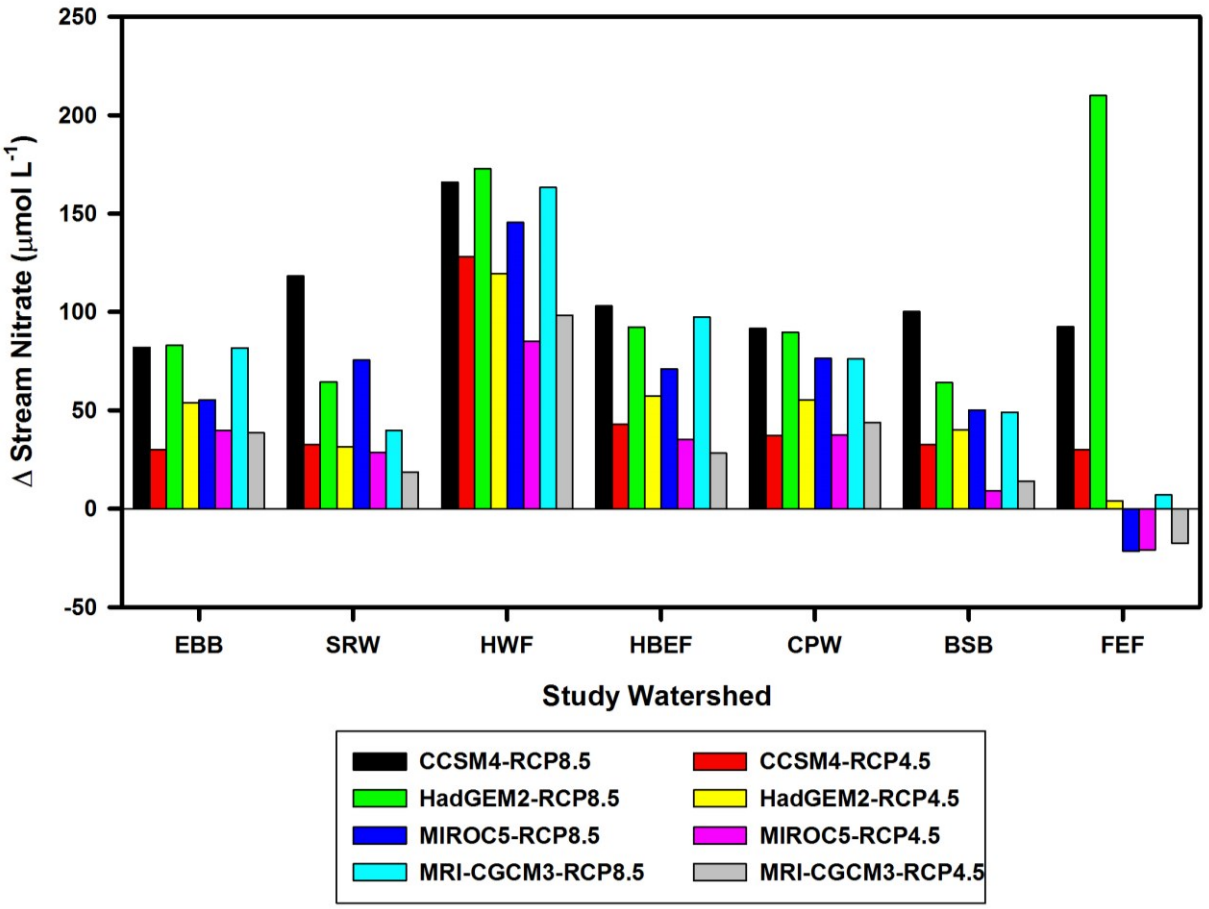

Figure 6.20. Projected changes in mean annual volume weighted NO_3^- concentrations (μmol L^{-1}) for study watersheds for individual AOGCM simulations under different emission scenarios. The value shown for each scenario is the difference between the mean of annual simulated values for the period 2070-2100 and measured values for the reference period (1970-2000). EBB: East Bear Brook watershed; SRW: Sleepers River Watershed; HWF: Huntington Wildlife Forest; HBEF: Hubbard Brook Experimental Forest; CPW: Cone Pond Watershed; BSB: Biscuit Brook watershed; FEF: Fernow Experimental Forest.

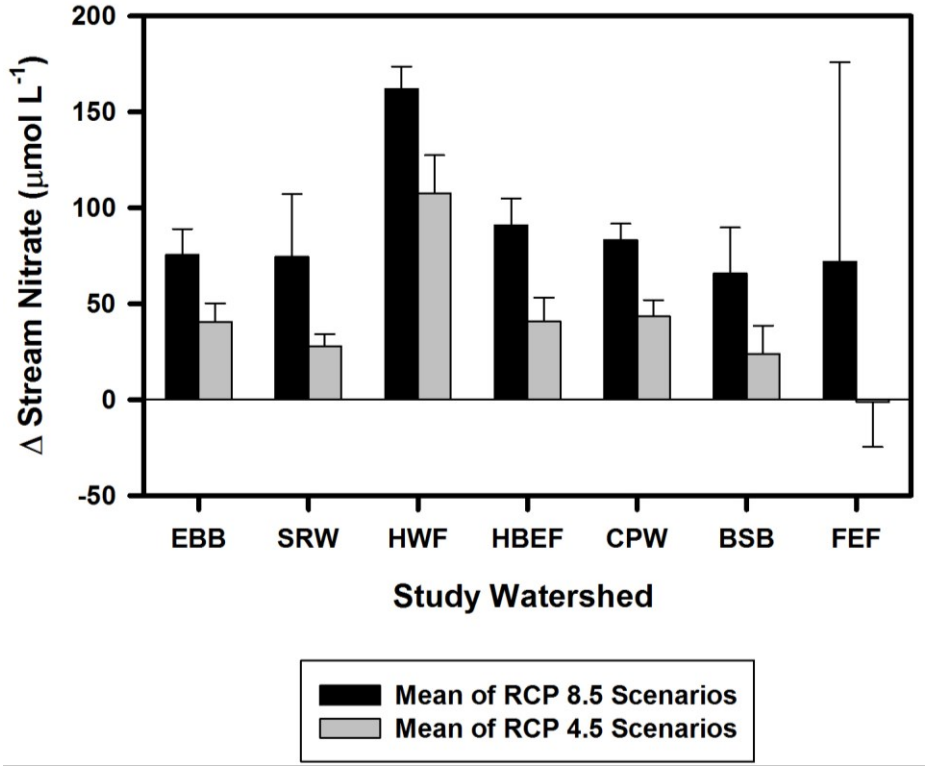

Figure 6.21. Projected changes in mean annual volume weighted NO_3^- concentrations (μmol L^{-1}) of AOGCM projections under high (RCP8.5) and low (RCP4.5) emissions scenarios for study watersheds. The value shown for each scenario is the average annual difference between the simulated values for the period 2070-2100 and the mean of measured values for the reference period (1970-2000). The error bars represent the variation of four AOGCMs under each emissions scenario for each site. EBB: East Bear Brook watershed; SRW: Sleepers River Watershed; HWF: Huntington Wildlife Forest; HBEF: Hubbard Brook Experimental Forest; CPW: Cone Pond Watershed; BSB: Biscuit Brook watershed; FEF: Fernow Experimental Forest.

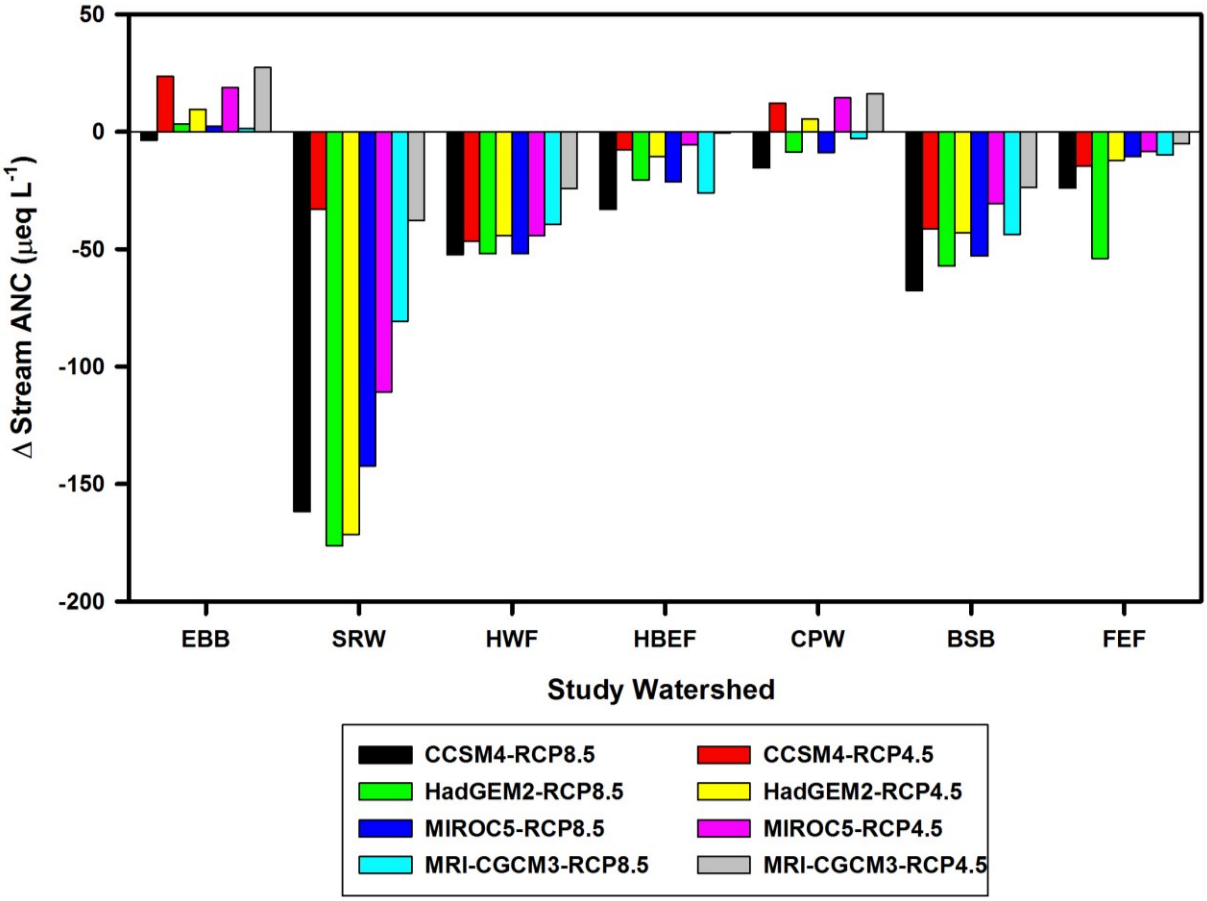

Figure 6.22. Projected changes in mean annual volume weighted ANC (μeq L^{-1}) for study watersheds for individual AOGCM simulations under different emission scenarios. The value shown for each scenario is the difference between simulated values for the period 2070-2100 and the mean of measured values for the reference period (1970-2000). EBB: East Bear Brook watershed; SRW: Sleepers River Watershed; HWF: Huntington Wildlife Forest; HBEF: Hubbard Brook Experimental Forest; CPW: Cone Pond Watershed; BSB: Biscuit Brook watershed; FEF: Fernow Experimental Forest.

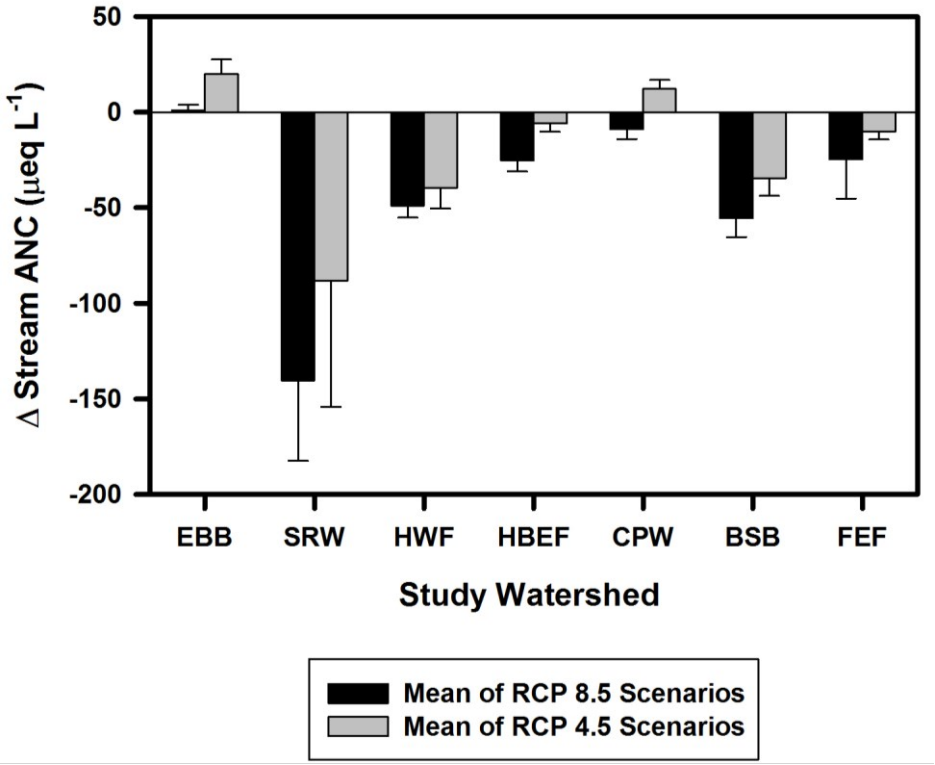

Figure 6.23. Projected changes in mean annual volume weighted ANC (μeq L^{-1}) under high (RCP8.5) and low (RCP4.5) emissions scenarios for study watersheds. The value shown for each scenario is the difference between simulated values for the period 2070-2100 and the mean of measured values for the reference period (1970-2000). The error bars represent the variation of four AOGCMs under each emissions scenario for each site. EBB: East Bear Brook watershed; SRW: Sleepers River Watershed; HWF: Huntington Wildlife Forest; HBEF: Hubbard Brook Experimental Forest; CPW: Cone Pond Watershed; BSB: Biscuit Brook watershed; FEF: Fernow Experimental Forest.

6.5. Discussion

6.5.1. Future Climate Projections

Projected changes in temperature and precipitation across all the Northeast sites are the main drivers of hydrological and biogeochemical responses, which are manifested differently depending on vegetation, soils, site characteristics, elevation, and historical land disturbances. There is a strong negative correlation (*P value* < 0.05, r = -0.91) between measured mean annual air temperature for the period of 1970-2000 and projected percent increases in mean annual temperature of 2070-2100 across all sites and all scenarios. This trend indicates that the relative change in temperature at colder sites is greater compared to changes at warmer sites. Therefore, the FEF which has the highest measured mean annual temperature (9.4°C) across all sites, is projected to experience less warming compared to colder sites like the SRW (6°C) and HWF (4.7°C). Note that removing the FEF from the correlation analysis still yields the same significant correlation but with a slightly higher P-Value (*P value* < 0.1, r = -0.76). There is no spatial gradient with latitude in projected increases in temperature, although for a given site projected air temperature increases with increasing emissions. The average variability of projected increases in temperature across all sites is higher (SD = 0.6°C) under high emission scenarios compared to low emission scenarios (SD = 0.4°C). The average variability of projected increases in temperature for a given climate scenario across all sites is lower (SD = 0.5°C) compared to average variability of all scenarios (four AOGCMs and two emission trajectory) for a given site (SD = 1.9°C). This trend indicates how differences in historical climate are manifested through increased variability among scenarios for a given site.

There is no clear spatial pattern in projected increases in precipitation under future emissions. One might expect that the projected increases in precipitation would be greatest at sites experiencing relatively high precipitation compared to sites with lower mean annual precipitation. Although there is no statistically significant trend between measured mean annual precipitation of 1970-2000 and projected increases in precipitation for the period of 2070-2100, sites which are currently receiving higher precipitation are projected to get wetter. The exception to this pattern is the FEF. The FEF has the second highest mean annual precipitation of 1,460 mm after the BSB (1,750 mm). However, the average projected increases in mean annual precipitation of all climate change scenarios for the FEF is 119 mm which is the second lowest projected increase among sites (after the HWF). Even the HadGEM-RCP4.5 scenario shows a decline in future precipitation. The average variability of projected increases in precipitation for a given climate scenario across all study sites is higher (SD = 15.8 cm) compared to the average variability of all scenarios (four AOGCMs and two emission trajectory) for a given site (SD = 8.5 cm). Therefore, the downscaling of AOGCM projections of precipitation decreases the variability of those scenarios. This is an important finding because it indicates that station-based downscaling could decrease the variability and therefore uncertainty in precipitation projections to some extent. Since precipitation projections have more inter-annual variability and uncertainty than temperature projections, more attention should be given to temperature-driven changes as metrics for climate change impact assessments. Although this is not to say that projected changes in precipitation will not have a profound impact on the structure and function of northern forest watersheds.

6.5.2. Hydrology

Results from Phase 1 of this dissertation for the HBEF indicate that changes in temperature and precipitation are the main drivers of the forest ecosystem response to changing climate. Across all study sites, the FEF, HWF, and CPW did not fit this conceptual model and showed varied responses. The FEF and HWF did not show any significant relationship of changes in mean annual ET and projected increases in mean annual temperature (chapter 6.4.2). The CPW is the only spruce-fir forest and did not exhibit water stress like other study sites. The FEF is the only study site with central hardwood vegetation and also soils have the highest water holding capacity (WHC) of 30 cm of the study sites (12 cm). These differences in the characteristics of the three study sites are responsible for their different responses to changing climate compared to the conceptual model observed for HBEF and at most sites. Although, the FEF and HWF have similar historical land disturbance (100 years old harvesting), but they have different background climate conditions, vegetation and WHC. The FEF has the highest and lowest projected changes in temperature across all sites and is the only site that shows a decrease in projected precipitation under one climate scenario (HadGEM2-RCP4.5). The average projected increases in precipitation for the HWF are the lowest across all sites.

At the FEF, simulations suggest a complete loss of snow pack under all scenarios toward the end of 21st century and higher temperatures compared to other sites. Higher variability in projections of temperature and precipitation at the FEF results in a scattered response of ET to future changes in temperature compared to other sites (no statistically significant relationship between projected changes in ET and air temperature). The higher WHC at the FEF also mitigates the effects of higher temperatures to some extent by supplying water for plant transpiration demand during the extended growing season. The HWF response of ET to increases

in air temperature is driven by a lack of available water for transpiration during the growing season since it has the lowest projected increase in precipitation of any of the modeled sites despite similar increases in temperature. A lack of precipitation during the extended growing season, increases water stress on trees, decreasing photosynthetic rate and therefore decreasing ET. The weaker response of ET to future increases in temperature at the CPW is due to the different tree vegetation (spruce-fir). The spruce-fir forest has a lower optimum temperature for photosynthesis than northern hardwoods and increases in temperature above the temperature optimum that are projected for the CPW will cause temperature stress on vegetation and a decline in photosynthesis and forest productivity which leads to lower ET. Future projections for the CPW watershed do not exhibit water stress. Therefore spruce-fir watersheds experience temperature stress before water stress can occur under future climate projections. The spruce-fir forest also has higher foliar respiration in response to increases in temperature compared to northern hardwoods [*Aber and Federer*, 1992]. Lastly, the spruce-fir forest at the CPW has a lower photosynthetic capacity due to lower foliar N and therefore lower transpirational demand compared to northern hardwoods which can eliminate water stress. Therefore, projected increases in ET for the coniferous forest of CPW is only driven by temperature through the lengthening of the growing season rather than precipitation since trees do not experience water stress under future climate projections.

PnET-BGC calculates the ET and water stress for each month as a function of available soil water and plant water demand. *Aber and Federer*, [1992] derived a relationship for the response of tree photosynthesis to changes in temperature, providing parameter values for different tree species classes based on literature. They define a multiplier between 0 and 1 to depict the effect of temperature on gross photosynthesis. The photosynthesis relationship is a

parabolic function with minimum and optimum temperature values set as parameters for different tree types. They determined the optimum temperature for gross photosynthesis is 24°C and 20°C for northern hardwoods and spruce-fir, respectively [*Aber and Federer*, 1992; *Aber et al.*, 1995; *Ollinger et al.*, 2009]. They also characterize foliar respiration as a function of gross photosynthesis which increases with temperature as a Q_{10} factor of 2 [*Aber and Federer*, 1992; *Ollinger et al.*, 2009]. The Q_{10} is a measure of the temperature dependency of a rate process (e.g., change in foliar respiration if temperature increases by 10°C). A projected lengthening of the growing season and associated increases in evapotranspiration due to higher temperature, could limit available soil water and ultimately lead to water stress on plants, despite projected increases in precipitation. Model simulations under lower emissions scenarios for the Northeast where hydrology is strongly driven by snowmelt (except FEF), indicate that projected increases in annual ET largely occur during the late spring, summer and early fall due to the extended growing season. Under the higher emissions scenarios, the increases in ET continue into winter causing a substantial increase in annual ET. Across other sites, the projected increases in winter ET are due to a decline in snowpack associated with higher temperature and increases in the percentage of precipitation occurring as rain versus snow. Increases in ET result in water stress on plants and decrease streamflow during summer. This hydrologic change has important implications for the health, structure and productivity of forest and aquatic ecosystems and the services they provide, and the availability of water to supply downstream urban centers during summer months.

The projections of water stress across all sites and under all climate change scenarios, although highly variable with AOGCM and scenario, suggest a general increasing trend of dry growing season conditions. This trend is driven by decreases in mean monthly soil moisture

during summer and early fall as a result of increased ET which is consistent with projected low summer discharge. The high variability in water stress projections is consistent with high variability in projections of increases in precipitation across sites and AOGCM projections and among scenarios. During summer drought, ET continues to consume surface water resources exacerbating short supply. The greater the soil water deficit, the lower the tree productivity which in turn decouples soil-vegetation processes and decreases nutrient retention. Even short term water stress on plants during the growing season can hamper productivity, carbon and nitrogen sequestration, and disrupt element cycling.

The seasonal pattern of streamflow across all sites except the FEF, project more winter and early spring high-flow and lower summer flows. There will more precipitation during late fall, winter and early spring and lower precipitation in summer. In sites where snow is more prevalent (e.g., HWF, SRW, HBR, CPW), the snow pack will develop later in the season and melt earlier in the Spring. Projected increases in late winter/early spring soil moisture have important implications for future water management in the Northeast. The combination of wetter winters and warmer summers, pose a significant risk to forest ecosystem productivity and the services they provide. Four out of the seven study sites (EBB, SRW, CPW, BSB) show significant increases in projected mean annual streamflow. This could pose a risk of flooding for urban centers downstream especially since the precipitation projections suggest higher intensity rainfall events with shorter return period. Under future projected increases in precipitation and annual streamflow, any possible disturbance of forested watersheds and impact on vegetation could cause higher risks of flood and removal of soil and nutrients. Increased risk of flooding has important implications for climate change adaptation policies in the Northeast [*NECIA*, 2006]. In contrast, at the HWF and FEF, projections of mean annual streamflow show significant decline

due to smaller projected increases in precipitation at the HWF and higher projected increases in temperature at the FEF, which could cause summer drought for agricultural land downstream and pose pressure on water supply and resources especially during summer. Finally at the HBEF the projected response is highly variable ranging from increases to decreases in mean annual streamflow depending on the climate change scenario. This level of complexity in the hydrologic response of watersheds to changing climate will challenge our ability to respond and adapt to this critical dimension of global change.

6.5.3. Net Primary Productivity

Model simulations indicate a longer growing season across all sites and under all future climate scenarios. In PnET-BGC the length of growing season is defined as total growing degree days, which is defined as the number of the days that minimum air temperature is above 0°C. Under projected future climate change, the longer and more productive growing season is due to a combination of higher temperatures and precipitation (more availability of water). Future projections of changes in temperature show an average increase of 25% in the number of growing days across all sites and all AOGCMs for the period of 2070-2100 compared to the reference period of 1970-2000. This expansion in the growing season is greater under high emission scenarios (mean = 33%, SD = 15%) compared to low emission scenarios (mean = 16%, SD = 8%). Among all AOGCMs, the HadGEM2 and MIROC5 indicate the highest increases in projected growing days and therefore the longest growing seasons across all sites (average of 35%). Note that an enhancement of tree growth can be limited if temperatures exceed optimum values for photosynthesis and/or if availability of water becomes limiting during the extended growing season. Projected increases in temperature and precipitation drive increases in

evapotranspiration in Northeast forest watersheds. Model projections for all sites under all scenarios indicate significant increases in ET toward the end of the 21st century, the extent of which is strongly a function of projected increases in temperature. The model projections show significant increases in both evaporation and transpiration under future changing climate, although increases in transpiration exceed increases in evaporation due to longer growing seasons and warmer temperatures in northeastern forest sites.

Although the model projections of NPP varied substantially across all sites and among all scenarios, root and foliar NPP decrease across most sites while wood biomass increases. The projected reduction in root and foliar NPP is due to water stress while increase in wood NPP is driven by the longer growing season and higher rates of photosynthesis due to warmer temperature in the absence of water stress. Decreases in foliar and root NPP cause a significant decline in inputs of litter which causes declines in the humus carbon pool across all sites. If these projections hold up, the ability of forested ecosystems to sequester carbon could decrease due to a lack of aboveground growth. In contrast, in the absence of water stress, the efficiency of photosynthesis will increase under future climate change and create a strong sink for carbon. The CPW shows the smallest decline in foliar NPP of the seven study sites evaluated. Although, the projected temperature stress to CPW and decline in productivity has important implications for the spruce-fir forests of the Northeast. Possible changes in productivity and composition of these forests could impact the economy of the region (wood products industry) and disrupt the services these ecosystems provide. If the projected temperature stress occurs in spruce-fir forests of the Northeast, it is likely that other tree species with higher temperature tolerance will replace them over 21st century. The SRW is the only site that shows an increase in NPP under all scenarios and a positive relationship between NPP and mean annual temperature. This response at SRW is

due to lower projected increase in temperature (the SRW has the lowest projected increase) coupled with large projected increases in precipitation compared to other sites. Therefore, the SRW benefits from a warmer, wetter climate and longer growing season. Variability in projected changes in NPP, forest productivity and shifts in C storage in plants was evident across all these sites, which is an important finding that has implications for the future of forest ecosystems and carbon management in the Northeast.

6.5.4. Biogeochemistry

Model projections of the soil humus C pool across all sites and under all scenarios show significant declines with projected increases in temperature. In PnET-BGC, the decomposition rate of soil organic matter is depicted to increase exponentially with temperature and has a positive linear relationship with soil moisture. Therefore, temperature is the main driver of projected decreases in the humus C pool under future climate conditions. The projected decrease in the humus C pool has important implications for the capacity of forested ecosystems to sequester carbon and for soil processes under changing climate over the 21st century. This process is one of the largest sources of uncertainty in projections of terrestrial ecosystem responses to changing climate. The magnitude of this uncertainty could be large enough to prevent differentiation between forest ecosystems acting as potential sources or sinks of carbon [*Cox et al.*, 2000; *Friedlingstein et al.*, 2006].

Changes in the balance of precipitation and ET could substantially impact forest growth and productivity which in turn could alter the magnitude and timing of hydrology and biogeochemical cycles [*Campbell et al.*, 2009]. Changes in the timing and amount of precipitation could impact forest nutrient cycling, and over multiple decades, the species

composition of the forest [*Huntington et al.*, 2009]. The projected increase in the growing season under a warmer climate could impact forest nutrient cycles by increasing the rate of nutrient uptake from the soil by vegetation [*Huntington et al.*, 2009]. With increases in the productivity and growth rate of forests, the total amount of sequestrated nutrients (e.g., N, calcium) could increase. In addition, the lack of snowpack during winter under projected climate change at sites where snow is a prominent form of precipitation, could increase water infiltration during the winter [*Huntington et al.*, 2009] and leaching losses of nutrients.

Model simulations projected increases in mean annual volume weighted NO_3^- across all sites and all scenarios except for three scenarios at the FEF. Elevated export of NO_3^- from forest lands could alter the nutrient status of adjacent N-growth limited coastal waters [*Driscoll et al.*, 2003]. A strong positive response between nitrogen mineralization and temperature in combination with a decoupling of plant-soil interactions under future climate enhances net nitrification and NO_3^- leaching. The pattern of biogeochemical response is evident across modeled sites. Sites like the SRW that have relatively large soil pools of exchangeable base cations, can neutralize strong acid anions in leachate. Watersheds like the HBEF that have acidic soils, exhibit marked acidification of soil and water associated with projected NO_3^- leaching. The differences among sites is the manifestation of differences in rates of atmospheric N deposition as well as the degree of soil N depletion caused by past forest disturbance.

The new framework of climate change impacts based on increases in temperature provides a practical approach for decision makers and policy managers to assess and quantify the potential effects on forested ecosystems and their services. This approach clearly links climate change impacts on forested watersheds to averaged local and global warming and to future emission controls, providing useful guidelines for policymakers and water resources managers

on cumulative CO_2 emissions projected changes in temperature and associated ecosystem effects. Therefore, policies could be formed by considering total cumulative emissions, associated impacts, and uncertainties. Climate change policies for adaptation and mitigation could be also framed around this approach. This framework provides scientific support for evaluating the impact of different impacts on forest production, soils and water quantity and quality.

This framework provides new insights of climate change impacts on forested ecosystems with associated uncertainty related to projected temperature change which is different from uncertainties associated with equivalent carbon dioxide concentrations (e.g., the lack of information on aerosol forcing in climate impact studies). Further, since the range of effects is expressed as an incremental temperature change, policymakers can decide an appropriate target for emission stabilization which will limit these effects on forested ecosystems. Moreover, each degree of temperature increase can be translated into a best estimate of associated CO_2-equivalent concentrations. Through this approach, we can link a range of potential ecosystem impacts to a cumulative carbon framework to help guide management decisions [*Allen et al.*, 2009; *Matthews et al.*, 2009; *Meinshausen et al.*, 2009; *Zickfeld et al.*, 2009].

7. Synthesis and Future Research Recommendations

Climate change is already affecting the Northeast. Projected increases in temperature and changes in the quantity and seasonality of precipitation will likely have impacts on ecosystem structure, function and sustainability [*Hayhoe et al.*, 2007; *NECIA*, 2006]. The projected pattern of temperature change is more consistent than precipitation [*NECIA*, 2006]. The results from all three phases of this dissertation indicate that potential changes in climate could affect the structure and function of forested watersheds and services they provide. For this dissertation, I took advantage of long-term, comprehensive records of meteorological, hydrological and biogeochemical data available for seven intensive study sites in the northeastern U.S. Thorough characterization and available data from these sites provided me with detailed information for model calibration and quantitative hydrological and biogeochemical data to help validate processes and rates depicted in PnET-BGC. All sites are relatively undisturbed with the exception of air pollution and climate change. Due to their relative small size and high elevation, they enable assessment of small changes in hydrological and biogeochemical cycles under changing climate. Therefore, these watersheds that are sensitive to small changes in climate can serve as surrogate for larger and more resistant catchments at broader scales and improve the understanding of climate change impacts at regional scales. Changes in climate are manifested differently at each site depending on climate change scenarios, and site characteristics such as climate, dominant vegetation, soils, and historical land disturbances. Since the study sites are scattered across the Northeast region, I was able to investigate the spatial pattern among these sites through cross-site analysis.

Water quantity and quality and changes in seasonality of streamflow are influenced by meteorological conditions and long-term changes in climate [*Mitchell et al.*, 1996; *Murdoch et*

al., 1998]. Stream discharge is the main driver of the export of solutes from forested watersheds [*Likens and Bormann*, 1995], therefore future changes in the hydrological cycle, especially annual discharge and its seasonality, will affect water quality and nutrient losses from forested watersheds. Small headwater watersheds regulate and provide water for downstream larger bodies of water. They provide habitat for aquatic organisms as well as irrigation water for agriculture and drinking water for urban areas. Forest ecosystems in the Northeast provide wood for timber products, paper and energy, maple syrup, and recreational services while regulating trace gas exchange, sequestrating carbon and nitrogen and limiting nutrient losses from soil. Quantitatively assessing the impacts of climate change on forest ecosystems is critical to provide scientific evidence for policy makers and managers to help guide emission control programs to ensure that ecosystems continue providing their services under changing climate and climate adaptation programs.

In phase 1 of my dissertation, I assessed the hydrochemical responses of the HBEF to projected changes in climate with and without invoking the effects of CO_2 on vegetation. The results indicated a broad range of hydrologic and biogeochemical responses to changing climate. This phase provided an indication of the direction and extent of changes that might be expected under different climate scenarios. A sensitivity analysis was conducted that showed that the model output is sensitive to changes in climatic inputs. Temperature and precipitation are both important drivers of projected responses, although invoking CO_2 effects on vegetation could offset the effects of increasing temperature to some extent. Simulations suggest that under future climate there will likely be an increase in annual discharge and its distribution as well as quality. Model projections indicated a decline in the snowpack, snow melt, and timing and magnitude of the snowmelt hydrograph peak. During future warmer winters with a higher rain to snow ratio,

snowpack accumulation will diminish and water will become distributed more evenly throughout the year. Summer flows will be lower due to higher ET demand and a longer growing season, likely increasing soil water stress. Under water stress, plants close their stomata and their photosynthetic capacity decreases which causes a decoupling of soil-plant linkages. Higher temperatures result in higher rates of net mineralization. Less uptake of NH_4^+ by tress and increases in net nitrification leads to elevated leaching of NO_3^- and acidification of soil and surface water. Also the soil C humus pool is projected to decline significantly due to increases in temperature. Findings from this chapter underscore the important interplay between projections of changing temperature and precipitation and their effects on tree growth in the Northern Forest.

In phase two, I investigated the differences in two common statistical downscaling techniques: Bias Correction-Spatial Disaggregation (BCSD) (Grid-based) and Asynchronous Regional Regression Model (ARRM) (station-based) as well as in two sets of observations for "training" these downscaling techniques. I found the ARRM technique is more effective in mimicking observed precipitation quantity and temporal patterns at the local scale. This finding has important implications on assessment of climate change impacts at the small watershed scale. In mountainous areas with complex terrain, downscaling applications using the VIC grid approach, which averages meteorology over the 1/8° grid, underestimates precipitation. This finding is important since results from phase 1 showed that model output is sensitive to climate inputs. Moreover, a lack of precipitation during the extended growing season could increase water stress on plants and lead to elevated NO_3^- leaching from soil and stream water. Downscaling under the ARRM techniques showed limited drought response under future climate change. ARRM downscaling scenarios resulted in a deeper snowpack, higher peak discharge during snowmelt, wetter soil, and relatively higher annual streamflow, suggesting a greater

chance of more intense storms and flooding, particularly when soils are saturated in low elevation areas. An ensemble of AOGCMs projected that extreme precipitation events would increase by 67% in the Northeast [*Hayhoe et al.*, 2007; *NECIA*, 2006]. These extreme events could damage infrastructures and ecosystems impacting people, local businesses and the economy. These findings have important implications for climate change adaptation and mitigation policies in the Northeast. These results highlight the critical need to correctly characterize the quantity and distribution of future precipitation for accurate streamflow forecasting in the Northeast. The selection of observations and downscaling technique can have important consequences to global change projections.

Phase 3 of this dissertation provides an analysis of the responses of seven different forested watersheds in the Northeast to different AOGCM simulations and different emission scenarios. Considering the dynamic nature of climate change both in time and space, it is challenging to generalize the long-term climatic shifts across the Northeast. Nevertheless, comparing and contrasting an array of watersheds with a wide range of characteristics provides important insights on the potential range of responses of these diverse ecosystems. Their historical land disturbance, vegetation and soil characteristics are important factors that influence the differences in their responses to changing climate. Changes in climate could significantly impact forest growth and productivity which in turn could alter the magnitude and timing of hydrological and biogeochemical cycles [*Campbell et al.*, 2009]. These close linkages between climate change and vegetation are manifested in complex patterns across these sites which could ultimately alter the structure and function of these forests and the services they provide. The Northern Forest has been impacted by air pollution through inputs of acid deposition and soil and surface water acidification [*Driscoll et al.*, 2001]. While emission controls have diminished these

impacts and some ecosystems have started to show recovery [*Driscoll et al.*, 2001], model projections suggest that under future climate, enhanced net mineralization of N and nitrification could increase leaching of NO_3^- which could offset and reverse the recovery of the acid-base status of acid impacted ecosystems. Findings from this phase suggest that climate change could potentially result in the mobilization of soil N, elevated NO_3^- leaching and acidification of soil and surface water. Note weathering rates and soil percent base saturation of different sites affect the magnitude of responses. If northern hardwood species are replaced by more temperature and drought tolerant species, this effect could be mitigated to some extent. Forests experiencing temperature or water stress could be susceptible to secondary stresses such as insects or disease.

The findings of this chapter provide a new framework for assessing climate change impacts based on incremental increases in temperature. Across all sites, model projections of decreases in soil C and N pools showed a strong negative relationship with temperature. The responses of other state variables (e.g., NPP, streamwater discharge) are non linear due to effects of precipitation quantity and soil water and linkages with temperature change. Nevertheless, this framework could help guide policy makers and managers to make appropriate decisions to mitigate effects and ensure the continuation of ecosystem services and facilitate adaptation to changing climate. Finally, it is essential that experimental forested watersheds such as those investigated in this dissertation be maintained and preserved. Long-term monitoring and measurements of meteorology, biomass, hydrology, and stream chemistry at these intensive sites is not only necessary for model parameterization and testing but it is essential to detect climate change signals over time.

While the results of this dissertation provide insights into climate change impacts on forested watersheds in the northeastern U.S., there are still many areas of uncertainty regarding

climate change impacts on forested ecosystems. The following research suggestions could provide needed contributions to the overall assessments of climate change impacts on forests and their watersheds:

- Studying the interactions of changing air pollution (e.g., tropospheric ozone, atmospheric deposition) and climate change across these watersheds;
- Implementing RCPs projections of changes in emissions (e.g., N, S) instead of the assumption of "business-as-usual" of atmospheric emissions and deposition;
- Cross-site analysis of model projections of high elevation forest watersheds across the U.S.;
- Implementing simulations depicting multiple soil layers rather than current single-layer;
- Linking the model PnET-BGC to forest models in order to consider possible changes and shifts in composition of trees and species;
- Assessing possible nutrient limitation under CO_2 fertilization effects on vegetation growth; and
- Evaluating the major drivers across site differences that affect the response to climate change.

8. Conclusions

In phase 1 of the dissertation, I evaluated the hydrochemical response of a northern hardwood forest watershed to projected changes in climate and atmospheric CO_2. A sensitivity analysis shows that model output is sensitive to climatic drivers that have changed in recent decades and are expected to change more in the upcoming decades (temperature, precipitation, solar radiation). As model calculations suggest that future changes in climate induce water stress (decreases in summer soil moisture due to shifts in hydrology and increased evapotranspiration), an uncoupling of plant-soil linkages and element cycling that can increase net mineralization/nitrification and soil and water NO_3^- leaching and acidification. Forest fertilization associated with increases in CO_2 appears to mitigate this perturbation somewhat. Moving forward, there is a critical need to better understand the interplay among multiple disturbances and legacies of these ecosystems in order to project their response to global change.

Phase 2 provides new insights into the importance of the careful selection of statistical downscaling techniques and appropriate observations for "training" those techniques. It also introduces new sets of uncertainties beyond those generally associated with AOGCMs used for climate change impacts assessments in small forested watersheds. In this phase I compared and contrasted projections of temperature and precipitation derived from BCSD and ARRM downscaling techniques, and two different sets of observations; VIC grid and station-based. I evaluated how their differences were manifested through biogeochemical responses of a forested watershed using the PnET-BGC model. The choice of downscaling method had a profound effect on watershed hydrology, which in turn affected forest growth and stream chemistry. These projected changes were directly related to the ability of the downscaling technique to mimic observed precipitation, emphasizing the need for careful selection of observations for "training"

the downscaling technique as well as selecting a downscaling technique that appropriately suits the scale and topography of watershed. For climate projections of small watersheds, particularly for sites situated in complex, mountainous terrain, it is important to use point observations from within (or in close proximity to) the watershed in conjunction with the ARRM downscaling technique since this method relies on measurements from an observation station within or near the watershed boundaries. These measurements capture the actual variability of meteorological conditions for that watershed which improves the ability of the downscaling technique to mimic the local climate patterns especially for small watersheds situated in complex terrain.

Phase 3 of this study provides insights into how climate change manifests differently through an array of forested ecosystems with a wide range of characteristics. I compared and contrasted potential responses of seven forested ecosystems in the northeastern U.S. to future climate change and conducted a cross-site analysis. I evaluated different site characteristics and how they affect watershed responses to potential future changes in climate. I investigated the responses of these watersheds and linked them to projected increases in mean annual temperature. Results indicate that vegetation plays an important role since it regulates the hydrological and biogeochemical cycles. All forest watershed sites show significant increases in evapotranspiration under future climate change due to warmer temperatures and an extended growing season. Model projections for sites where snow is currently prevalent, indicated the extent of snowpack accumulation will diminish significantly or disappear by the end of the 21st century. This change could impact local economies and businesses that depend on winter recreational activities, and put pressure on water supplies. Model simulations showed that under climate change, northern hardwoods forests experience drought and water stress during the growing season which affect their productivity and the rate of carbon, nitrogen and nutrient

assimilation. In contrast, the spruce-fir forests are susceptible to temperature stress due to their lower optimum temperature for photosynthesis than hardwood forests. This perturbation could affect the pulp and paper industry. Under a changing climate spruce-fir forests may be replaced with more temperature tolerant species. The streamflow projections are highly variable across sites with some showing significant increases in annual water yield, while others indicate decreases. As a result, forests across the Northeast and their downstream urban centers could face risks of both flooding or drought. This variability in response challenges policy makers and water resource and forest managers. One of the insights of this part of the dissertation is projected changes in NPP, carbon allocation in plants, and the humus C pool which could significantly affect the ability of these forests to sequester carbon and alter soil processes over the 21st century.

9. References

Aber, J. D., and C. T. Driscoll (1997), Effects of land use, climate variation, and N deposition on N cycling and C storage in northern hardwood forests, *Global Biogeochem. Cycles*, *11*(4), 639–648, doi:10.1029/97GB01366.

Aber, J. D., and C. A. Federer (1992), A Generalized, Lumped-Parameter Model of Photosynthesis, Evapotranspiration and Net Primary Production in Temperate and Boreal Forest Ecosystems, *Oecologia*, *92*(4), 463–474, doi:10.1007/BF00317837.

Aber, J. D., S. V. Ollinger, C. A. Federer, P. B. Reich, M. L. Goulden, D. W. Kicklighter, J. M. Melillo, and R. G. Lathrop Jr (1995), Predicting the effects of climate change on water yield and forest production in the northeastern United States, *Clim Res*, *05*(3), 207–222, doi:10.3354/cr0005207.

Aber, J. D., P. B. Reich, and M. L. Goulden (1996), Extrapolating Leaf CO_2 Exchange to the Canopy: A Generalized Model of Forest Photosynthesis Compared with Measurements by Eddy Correlation, *Oecologia*, *106*(2), 257–265, doi:10.1007/BF00328606.

Aber, J. D., S. V. Ollinger, and C. T. Driscoll (1997), Modeling Nitrogen Saturation in Forest Ecosystems in Response to Land Use and Atmospheric Deposition, *Ecological Modelling*, *101*(1), 61–78, doi:10.1016/S0304-3800(97)01953-4.

Aber, J. D., S. V. Ollinger, C. T. Driscoll, G. E. Likens, R. T. Holmes, R. J. Freuder, and C. L. Goodale (2002), Inorganic Nitrogen Losses from a Forested Ecosystem in Response to Physical, Chemical, Biotic, and Climatic Perturbations, *Ecosystems*, *5*(7), 648–658, doi:10.1007/s10021-002-0203-2.

Aber, J. D., C. L. Goodale, S. V. Ollinger, M.-L. Smith, A. H. Magill, M. E. Martin, R. A. Hallett, and J. L. Stoddard (2003), Is Nitrogen Deposition Altering the Nitrogen Status of Northeastern Forests?, *BioScience*, *53*(4), 375–389, doi:10.1641/0006-3568(2003)053[0375:INDATN]2.0.CO;2.

Adams, M. B., J. N. Kochenderfer, F. Wood, T. R. Angradi, and P. Edwards (1994), *Forty years of hydrometeorological data from the Fernow Experimental Forest, West Virginia*, US Department of Agriculture, Forest Service, Northeastern Forest Experiment Station.

Ainsworth, E. A., and S. P. Long (2005), What Have We Learned from 15 Years of Free-Air CO2 Enrichment (FACE)? A Meta-Analytic Review of the Responses of Photosynthesis, Canopy Properties and Plant Production to Rising CO2, *New Phytologist*, *165*(2), 351–371, doi:10.1111 /j.1469-8137.2004.01224.x.

Ainsworth, E. A., and A. Rogers (2007), The response of photosynthesis and stomatal conductance to rising [CO2]: mechanisms and environmental interactions, *Plant, Cell & Environment*, *30*(3), 258–270, doi:10.1111/j.1365-3040.2007.01641.x.

Ainsworth, E. A., P. A. Davey, G. J. Hymus, B. G. Drake, and S. P. Long (2002), Long-Term Response of Photosynthesis to Elevated Carbon Dioxide in a Florida Scrub-Oak Ecosystem, *Ecological Applications*, *12*(5), 1267–1275.

Allen, M. R., D. J. Frame, C. Huntingford, C. D. Jones, J. A. Lowe, M. Meinshausen, and N. Meinshausen (2009), Warming caused by cumulative carbon emissions towards the trillionth tonne, *Nature*, *458*(7242), 1163–1166, doi:10.1038/nature08019.

Bailey, S. W., C. T. Driscoll, and J. W. Hornbeck (1995), Acid-base chemistry and aluminum transport in an acidic watershed and pond in New Hampshire, *Biogeochemistry*, *28*(2), 69–91.

Beerling, D. J. (1996), Ecophysiological responses of woody plants to past CO2 concentrations, *Tree Physiology*, *16*(4), 389 –396, doi:10.1093/treephys/16.4.389.

Campbell, J. L. et al. (2009), Consequences of climate change for biogeochemical cycling in forests of northeastern North America, *Canadian Journal of Forest Research*, *39*(2), 264–284, doi:10.1139/X08-104.

Campbell, J. L., C. T. Driscoll, A. Pourmokhtarian, and K. Hayhoe (2011), Streamflow responses to past and projected future changes in climate at the Hubbard Brook Experimental Forest, New Hampshire, United States, *Water Resour. Res.*, *47*, 15 PP., doi:201110.1029/2010WR009438.

Chen, L., and C. T. Driscoll (2005), A two-layer model to simulate variations in surface water chemistry draining a northern forest watershed, *Water Resour. Res. (W09425)*, *41*(9), 8 PP., doi:10.1029/2004WR003625.

Clark, J. M., S. H. Bottrell, C. D. Evans, D. T. Monteith, R. Bartlett, R. Rose, R. J. Newton, and P. J. Chapman (2010), The importance of the relationship between scale and process in understanding long-term DOC dynamics, *Science of The Total Environment*, *408*(13), 2768–2775, doi:10.1016/j.scitotenv.2010.02.046.

Collins, W. J. et al. (2011), Development and evaluation of an Earth-System model – HadGEM2, *Geoscientific Model Development*, *4*(4), 1051–1075, doi:10.5194/gmd-4-1051-2011.

Comer, G., and R. Zimmermann (1968), Low-flow and basin characteristics of two streams in northern Vermont, *Journal of Hydrology*, *7*(1), 98–108.

Committee on Stabilization Targets for Atmospheric Greenhouse Gas Concentrations; National Research Council (2011), *Climate Stabilization Targets: Emissions, Concentrations, and Impacts over Decades to Millennia*, The National Academies Press.

Cox, P. M., R. A. Betts, C. D. Jones, S. A. Spall, and I. J. Totterdell (2000), Acceleration of global warming due to carbon-cycle feedbacks in a coupled climate model, *Nature*, *408*(6809), 184–187, doi:10.1038/35041539.

Cramer, W. et al. (2001), Global response of terrestrial ecosystem structure and function to CO2 and climate change: results from six dynamic global vegetation models, *Global Change Biology*, *7*(4), 357–373, doi:10.1046/j.1365-2486.2001.00383.x.

Curtis, P. S., and X. Wang (1998), A meta-analysis of elevated CO2 effects on woody plant mass, form, and physiology, *Oecologia*, *113*(3), 299–313, doi:10.1007/s004420050381.

Curtis, P. S., C. S. Vogel, K. S. Pregitzer, D. R. Zak, and J. A. Teeri (1995), Interacting Effects of Soil Fertility and Atmospheric CO2 on Leaf Area Growth and Carbon Gain Physiology in Populus x euramericana (Dode) Guinier, *New Phytologist*, *129*(2), 253–263, doi:10.1111/j.1469-8137.1995.tb04295.x.

Dail, D., E. Davidson, and J. Chorover (2001), Rapid Abiotic Transformation of Nitrate in an Acid Forest Soil, *Biogeochemistry*, *54*(2), 131–146, doi:10.1023/A:1010627431722.

Davis, G., J. Whipple, S. Gherini, C. Chen, R. Goldstein, A. Johannes, P. Chan, and R. Munson (1987), Big Moose Basin: Simulation of Response to Acidic Deposition, *Biogeochemistry*, *3*(1), 141–161, doi:10.1007/BF02185190.

DeGaetano, A. T., and R. J. Allen (2002), Trends in Twentieth-Century Temperature Extremes across the United States, *Journal of Climate*, *15*(22), 3188–3205.

Delworth, T. L. et al. (2006), GFDL's CM2 Global Coupled Climate Models. Part I: Formulation and Simulation Characteristics, *Journal of Climate*, *19*(5), 643–674, doi:10.1175/JCLI3629.1.

Dettinger, M. D., D. R. Cayan, M. K. Meyer, and A. E. Jeton (2004), Simulated hydrologic responses to climate variations and change in the Merced, Carson, and American River basins, Sierra Nevada, California, 1900–2099, *Climatic Change*, *62*(1-3), 283–317.

Drake, B. G., M. A. Gonzalez-Meler, and S. P. Long (1997), More Efficient Plants: A Consequence of Rising Atmospheric CO2?, *Annu. Rev. Plant. Physiol. Plant. Mol. Biol.*, *48*(1), 609–639, doi:10.1146/annurev.arplant.48.1.609.

Driscoll, C. T., G. B. Lawrence, A. J. Bulger, T. J. Butler, C. S. Cronan, C. Eagar, K. F. Lambert, G. E. Likens, J. L. Stoddard, and K. C. Weathers (2001), Acidic Deposition in the Northeastern United States: Sources and Inputs, Ecosystem Effects, and Management Strategies, *BioScience*, *51*(3), 180–198, doi:10.1641/0006-3568(2001)051[0180:ADITNU]2.0.CO;2.

Driscoll, C. T. et al. (2003), Nitrogen Pollution in the Northeastern United States: Sources, Effects, and Management Options, *Bioscience*, *53*(4), 357–374, doi:10.1641/0006-3568(2003)053[0357:NPITNU]2.0.CO;2.

Ellsworth, D. S. (1999), CO2 Enrichment in a Maturing Pine Forest: Are CO2 Exchange and Water Status in the Canopy Affected?, *Plant, Cell & Environment*, *22*, 461–472, doi:10.1046/j.1365-3040.1999.00433.x.

Ellsworth, D. S., R. Oren, C. Huang, N. Phillips, and G. R. Hendrey (1995), Leaf and canopy responses to elevated CO2 in a pine forest under free-air CO2 enrichment, *Oecologia*, *104*(2), 139–146, doi:10.1007/BF00328578.

Evans, C., P. Chapman, J. Clark, D. Monteith, and M. Cresser (2006), Alternative explanations for rising dissolved organic carbon export from organic soils, *Global Change Biology*, *12*, 2044–2053, doi:10.1111/j.1365-2486.2006.01241.x.

Farquhar, G., and S. Wong (1984), An Empirical Model of Stomatal Conductance, *Functional Plant Biol.*, *11*(3), 191–210.

Farrior, C. E., R. Dybzinski, Simon A. Levin, and S. W. Pacala (2013), Competition for Water and Light in Closed-Canopy Forests: A Tractable Model of Carbon Allocation with Implications for Carbon Sinks., *The American Naturalist*, *181*(3), 314–330, doi:10.1086/669153.

Fernandez, I. J., L. E. Rustad, S. A. Norton, J. S. Kahl, and B. J. Cosby (2003), Experimental Acidification Causes Soil Base-Cation Depletion at the Bear Brook Watershed in Maine, *Soil Sci. Soc. Am. J.*, *67*(6), 1909–1919.

Fernandez, I. J., J. E. Karem, S. A. Norton, and L. E. Rustad (2007), Temperature, soil moisture, and streamflow at The Bear Brook Watershed in Maine (BBWM),

Findlay, S. E. G. (2005), Increased Carbon Transport in the Hudson River: Unexpected Consequence of Nitrogen Deposition?, *Frontiers in Ecology and the Environment*, *3*(3), 133–137.

Fowler, H. J., S. Blenkinsop, and C. Tebaldi (2007), Linking climate change modelling to impacts studies: recent advances in downscaling techniques for hydrological modelling, *International Journal of Climatology*, *27*(12), 1547–1578, doi:10.1002/joc.1556.

Freeman, C., C. D. Evans, D. T. Monteith, B. Reynolds, and N. Fenner (2001), Export of organic carbon from peat soils, *Nature*, *412*(6849), 785, doi:10.1038/35090628.

Freeman, C., N. Fenner, N. J. Ostle, H. Kang, D. J. Dowrick, B. Reynolds, M. A. Lock, D. Sleep, S. Hughes, and J. Hudson (2004), Export of dissolved organic carbon from peatlands under elevated carbon dioxide levels, *Nature*, *430*(6996), 195–198, doi:10.1038/nature02707.

Friedlingstein, P. et al. (2006), Climate–Carbon Cycle Feedback Analysis: Results from the C4MIP Model Intercomparison, *J. Climate*, *19*(14), 3337–3353, doi:10.1175/JCLI3800.1.

Garnett, M. H., P. Ineson, and A. C. Stevenson (2000), Effects of burning and grazing on carbon sequestration in a Pennine blanket bog, UK, *The Holocene*, *10*(6), 729 –736, doi:10.1191/09596830094971.

Gbondo-Tugbawa, S. S., C. T. Driscoll, J. D. Aber, and G. E. Likens (2001), Evaluation of an integrated biogeochemical model (PnET-BGC) at a northern hardwood forest ecosystem, *Water Resour. Res.*, *37*(4), 1057–1070, doi:10.1029/2000WR900375.

Gent, P. R., G. Danabasoglu, L. J. Donner, M. M. Holland, E. C. Hunke, S. R. Jayne, D. M. Lawrence, R. B. Neale, P. J. Rasch, and M. Vertenstein (2011), The community climate system model version 4, *Journal of Climate*, *24*(19), 4973–4991.

Goodale, C. L., J. D. Aber, and P. M. Vitousek (2003), An Unexpected Nitrate Decline in New Hampshire Streams, *Ecosystems*, *6*(1), 0075–0086, doi:10.1007/s10021-002-0219-0.

Goodale, C. L., J. D. Aber, P. M. Vitousek, and W. H. McDowell (2005), Long-Term Decreases in Stream Nitrate: Successional Causes Unlikely; Possible Links to DOC?, *Ecosystems*, *8*(3), 334–337, doi:10.1007/s10021-003-0162-8.

Hamlet, A. F., and D. P. Lettenmaier (1999), EFFECTS OF CLIMATE CHANGE ON HYDROLOGY AND WATER RESOURCES IN THE COLUMBIA RIVER BASIN1, *JAWRA Journal of the American Water Resources Association*, *35*(6), 1597–1623, doi:10.1111/j.1752-1688.1999.tb04240.x.

Hayhoe, K. et al. (2004), Emissions Pathways, Climate Change, and Impacts on California, *Proceedings of the National Academy of Sciences of the United States of America*, *101*(34), 12422–12427, doi:10.1073/pnas.0404500101.

Hayhoe, K. et al. (2007), Past and Future Changes in Climate and Hydrological Indicators in the US Northeast, *Climate Dynamics*, *28*(4), 381–407, doi:10.1007/s00382-006-0187-8.

Hayhoe, K., C. Wake, B. Anderson, X.-Z. Liang, E. Maurer, J. Zhu, J. Bradbury, A. DeGaetano, A. Stoner, and D. Wuebbles (2008), Regional Climate Change Projections for the Northeast USA, *Mitigation and Adaptation Strategies for Global Change*, *13*(5), 425–436, doi:10.1007/s11027-007-9133-2.

Hodgkins, G. A., R. W. Dudley, and T. G. Huntington (2003), Changes in the Timing of High River Flows in New England over the 20th Century, *Journal of Hydrology*, *278*(1-4), 244–252, doi:10.1016/S0022-1694(03)00155-0.

Houlton, B. Z., C. T. Driscoll, T. J. Fahey, G. E. Likens, P. M. Groffman, E. S. Bernhardt, and D. C. Buso (2003), Nitrogen Dynamics in Ice Storm-Damaged Forest Ecosystems: Implications for Nitrogen Limitation Theory, *Ecosystems*, *6*(5), 431–443, doi:10.1007/s10021-002-0198-1.

Huntington, T. G., G. A. Hodgkins, B. D. Keim, and R. W. Dudley (2004), Changes in the Proportion of Precipitation Occurring as Snow in New England (1949–2000), *Journal of Climate*, *17*(13), 2626–2636.

Huntington, T. G., A. D. Richardson, K. J. McGuire, and K. Hayhoe (2009), Climate and hydrological changes in the northeastern United States: recent trends and implications for

forested and aquatic ecosystems This article is one of a selection of papers from NE Forests 2100: A Synthesis of Climate Change Impacts on Forests of the Northeastern US and Eastern Canada., *Canadian Journal of Forest Research*, *39*(2), 199–212.

Huybrechts, P. (2001), *Changes in Sea Level Rise. Climate Change 2001: The Scientific Basis. Contribution of Working Group I to the Third Assessment Report of the Intergovernmental Panel on Climate (IPCC)*, Cambridge University Press, Cambridge; New York.

Intergovernmental Panel on Climate Change (IPCC) (2007), *Climate Change 2007: The Physical Science Basis. Contribution of Working Group I to the Fourth Assessment Report of the Intergovernmental Panel on Climate Change. Edited by S. Solomon, D. Qin, M. Manning, Z. Chen, M. Marquis, K.B. Averyt, M. Tignor, and H.L. Miller*, Cambridge University Press, Cambridge, United Kingdom and New York, NY, USA.

Janssen, P. H. M., and P. S. C. Heuberger (1995), Calibration Of Process-Oriented Models, *Ecological Modelling*, *83*(1-2), 55–66, doi:10.1016/0304-3800(95)00084-9.

Jarvis, A. J., and W. J. Davies (1998), The coupled response of stomatal conductance to photosynthesis and transpiration, *Journal of Experimental Botany*, *49*(Special Issue), 399 –406, doi:10.1093/jxb/49.Special_Issue.399.

Johnson, C. E., A. H. Johnson, and T. G. Siccama (1991), Whole-Tree Clear-Cutting Effects on Exchangeable Cations and Soil Acidity, *Soil Sci Soc Am J*, *55*(2), 502–508, doi:10.2136/sssaj1991.03615995005500020035x.

Johnson, C. E., C. T. Driscoll, T. G. Siccama, and G. E. Likens (2000), Element Fluxes and Landscape Position in a Northern Hardwood Forest Watershed Ecosystem, *Ecosystems*, *3*(2), 159–184, doi:10.1007/s100210000017.

Jones, C. et al. (2013), Twenty-First-Century Compatible CO2 Emissions and Airborne Fraction Simulated by CMIP5 Earth System Models under Four Representative Concentration Pathways, *J. Climate*, *26*(13), 4398–4413, doi:10.1175/JCLI-D-12-00554.1.

Jørgensen, S. E. (1988), *Fundamentals of Ecological Modeling, Dev. Environ. Model.*, Elsevier Science, New York, USA.

Karl, T. R., J. M. Melillo, and T. C. Peterson (2009), *Global climate change impacts in the United States*, Cambridge University Press.

Keenan, T. F., E. Davidson, A. M. Moffat, W. Munger, and A. D. Richardson (2012), Using model-data fusion to interpret past trends, and quantify uncertainties in future projections, of terrestrial ecosystem carbon cycling, *Global Change Biology*, *18*(8), 2555–2569, doi:10.1111/j.1365-2486.2012.02684.x.

Keenan, T. F., D. Y. Hollinger, G. Bohrer, D. Dragoni, J. W. Munger, H. P. Schmid, and A. D. Richardson (2013), Increase in forest water-use efficiency as atmospheric carbon dioxide concentrations rise, *Nature*, *499*(7458), 324–327.

Klein Tank, A., and G. Können (2003), Trends in indices of daily temperature and precipitation extremes in Europe, 1946-99, *Journal of Climate*, *16*(22), 3665–3680.

Lewis, J. D., D. T. Tissue, and B. R. Strain (1996), Seasonal response of photosynthesis to elevated CO2 in loblolly pine (Pinus taeda L.) over two growing seasons, *Global Change Biology*, *2*(2), 103–114, doi:10.1111/j.1365-2486.1996.tb00055.x.

Liang, X., D. P. Lettenmaier, E. F. Wood, and S. J. Burges (1994), A simple hydrologically based model of land surface water and energy fluxes for general circulation models, *J. Geophys. Res.*, *99*(D7), 14415–14428, doi:10.1029/94JD00483.

Liang, X., L. Li, A. Dai, and K. E. Kunkel (2004a), Regional climate model simulation of summer precipitation diurnal cycle over the United States, *Geophysical Research Letters*, *31*(24).

Liang, X.-Z., L. Li, K. E. Kunkel, M. Ting, and J. X. L. Wang (2004b), Regional Climate Model Simulation of U.S. Precipitation during 1982–2002. Part I: Annual Cycle, *J. Climate*, *17*(18), 3510–3529, doi:10.1175/1520-0442(2004)017<3510:RCMSOU>2.0.CO;2.

Likens, G. E., and F. H. Bormann (1995), *Biogeochemistry: of a Forested Ecosystem*, Springer-Verlag, New York, USA.

Likens, G. E., F. H. Bormann, N. M. Johnson, D. W. Fisher, and R. S. Pierce (1970), Effects of Forest Cutting and Herbicide Treatment on Nutrient Budgets in the Hubbard Brook Watershed-Ecosystem, *Ecological Monographs*, *40*(1), 23–47, doi:10.2307/1942440.

Likens, G. E., C. T. Driscoll, D. C. Buso, T. G. Siccama, C. E. Johnson, G. M. Lovett, D. F. Ryan, T. Fahey, and W. A. Reiners (1994), The Biogeochemistry of Potassium at Hubbard Brook, *Biogeochemistry*, *25*(2), 61–125, doi:10.1007/BF00000881.

Luo, Y. et al. (2004), Progressive Nitrogen Limitation of Ecosystem Responses to Rising Atmospheric Carbon Dioxide, *BioScience*, *54*(8), 731–739, doi:10.1641/0006-3568(2004)054[0731:PNLOER]2.0.CO;2.

Luthi, D. et al. (2008), High-resolution carbon dioxide concentration record 650,000-800,000[thinsp]years before present, *Nature*, *453*(7193), 379–382, doi:10.1038/nature06949.

Matthews, H. D., N. P. Gillett, P. A. Stott, and K. Zickfeld (2009), The proportionality of global warming to cumulative carbon emissions, *Nature*, *459*(7248), 829–832, doi:10.1038/nature08047.

Maurer, E. P., and H. G. Hidalgo (2008), Utility of daily vs. monthly large-scale climate data: an intercomparison of two statistical downscaling methods, *Hydrol. Earth Syst. Sci.*, *12*(2), 551–563, doi:10.5194/hess-12-551-2008.

Maurer, E. P., A. W. Wood, J. C. Adam, D. P. Lettenmaier, and B. Nijssen (2002), A Long-Term Hydrologically Based Dataset of Land Surface Fluxes and States for the Conterminous United States*, *J. Climate*, *15*(22), 3237–3251, doi:10.1175/1520-0442(2002)015<3237:ALTHBD>2.0.CO;2.

McCarthy, H. R., R. Oren, K. H. Johnsen, A. Gallet-Budynek, S. G. Pritchard, C. W. Cook, S. L. LaDeau, R. B. Jackson, and A. C. Finzi (2010), Re-assessment of plant carbon dynamics at the Duke free-air CO2 enrichment site: interactions of atmospheric [CO2] with nitrogen and water availability over stand development, *New Phytologist*, *185*(2), 514–528, doi:10.1111/j.1469-8137.2009.03078.x.

Meinshausen, M., N. Meinshausen, W. Hare, S. C. B. Raper, K. Frieler, R. Knutti, D. J. Frame, and M. R. Allen (2009), Greenhouse-gas emission targets for limiting global warming to 2[thinsp][deg]C, *Nature*, *458*(7242), 1158–1162, doi:10.1038/nature08017.

Melillo, J. M., J. Borchers, and J. Chaney (1995), Vegetation/Ecosystem Modeling and Analysis Project:Comparing biogeography and biogeochemistry models in a continental-scale study of terrestrial ecosystem responses to climate change and CO2 doubling, *Global Biogeochemical Cycles*, *9*(4), 407–437, doi:10.1029/95GB02746.

Mitchell, M. J., C. T. Driscoll, J. S. Kahl, P. S. Murdoch, and L. H. Pardo (1996), Climatic Control of Nitrate Loss from Forested Watersheds in the Northeast United States, *Environ. Sci. Technol.*, *30*(8), 2609–2612, doi:10.1021/es9600237.

Mitchell, M. J., P. J. McHale, S. Inamdar, and D. J. Raynal (2001), Role of within-lake processes and hydrobiogeochemical changes over 16 years in a watershed in the Adirondack Mountains of New York State, USA, *Hydrol. Process.*, *15*(10), 1951–1965, doi:10.1002/hyp.249.

Monteith, D. T. et al. (2007), Dissolved Organic Carbon Trends Resulting from Changes in Atmospheric Deposition Chemistry, *Nature*, *450*(7169), 537–540, doi:10.1038/nature06316.

Moss, R., M. Babiker, S. Brinkman, E. Calvo, T. Carter, J. Edmonds, I. Elgizouli, S. Emori, L. Erda, and K. Hibbard (2008), Towards new scenarios for analysis of emissions, climate change, impacts, and response strategies: IPCC Expert Meeting Report, 19–21 September 2007, *Noordwijkerhout, The Netherlands*, 155.

Moss, R. H. et al. (2010), The next generation of scenarios for climate change research and assessment, *Nature*, *463*(7282), 747–756, doi:10.1038/nature08823.

Murdoch, P. S., D. A. Burns, and G. B. Lawrence (1998), Relation of Climate Change to the Acidification of Surface Waters by Nitrogen Deposition, *Environmental Science & Technology*, *32*(11), 1642–1647, doi:10.1021/es9708631.

Nakićenović, N., J. Alcamo, G. Davis, B. de Vries, J. Fenhann, S. Gaffin, K. Gregory, A. Grübler, T. Y. Jung, and T. Kram (2000), *Special Report on Emissions Scenarios: A Special Report of Working Group III of the Intergovernmental Panel on Climate Change*, 1st ed., Cambridge University Press, Cambridge, UK, and New York, NY.

NECIA (2006), *Northeast Climate Impact Assessment (NECIA). 2006. Climate Change in the U.S. Northeast. A Report of the Northeast Climate Impacts Assessment. Cambridge, Massachusetts: Union of Concerned Scientists (UCS).*, UCS Publications, Cambridge, MA, USA.

Norby, R. J., and D. R. Zak (2011), Ecological Lessons from Free-Air CO2 Enrichment (FACE) Experiments, *Annual Review of Ecology, Evolution, and Systematics*, *42*(1), 181–203, doi:10.1146/annurev-ecolsys-102209-144647.

Norby, R. J., S. D. Wullschleger, C. A. Gunderson, D. W. Johnson, and R. Ceulemans (1999), Tree responses to rising CO2 in field experiments: implications for the future forest, *Plant, Cell & Environment*, *22*(6), 683–714, doi:10.1046/j.1365-3040.1999.00391.x.

Norby, R. J., J. M. Warren, C. M. Iversen, B. E. Medlyn, and R. E. McMurtrie (2010), CO2 enhancement of forest productivity constrained by limited nitrogen availability, *Proceedings of the National Academy of Sciences*, *107*(45), 19368 –19373, doi:10.1073/pnas.1006463107.

Norton, S. et al. (1999), The Bear Brook Watershed, Maine (BBWM), USA, *Environ Monit Assess*, *55*(1), 7–51, doi:10.1023/A:1006115011381.

Nowak, R. S., D. S. Ellsworth, and S. D. Smith (2004), Functional Responses of Plants to Elevated Atmospheric CO2: Do Photosynthetic and Productivity Data from FACE Experiments Support Early Predictions?, *New Phytologist*, *162*(2), 253–280, doi:10.1111/j.1469-8137.2004.01033.x.

O'Brien, T. P., D. Sornette, and R. L. McPherron (2001), Statistical asynchronous regression: Determining the relationship between two quantities that are not measured simultaneously, *J. Geophys. Res.*, *106*(A7), 13247–13259, doi:10.1029/2000JA900193.

Ollinger, S. V., J. D. Aber, and P. B. Reich (1997), Simulating Ozone Effects on Forest Productivity: Interactions Among Leaf-, Canopy-, and Stand-Level Processes, *Ecological Applications*, *7*(4), 1237–1251, doi:10.1890/1051-0761(1997)007[1237:SOEOFP]2.0.CO;2.

Ollinger, S. V., J. D. Aber, P. B. Reich, and R. J. Freuder (2002), Interactive Effects of Nitrogen Deposition, Tropospheric Ozone, Elevated CO2 and Land Use History on the Carbon

Dynamics of Northern Hardwood Forests, *Global Change Biol*, *8*(6), 545–562, doi:10.1046/j.1365-2486.2002.00482.x.

Ollinger, S. V., C. L. Goodale, K. Hayhoe, and J. P. Jenkins (2009), Potential Effects of Climate Change and Rising CO2 on Ecosystem Processes in Northeastern U.S. Forests, *Mitigation and Adaptation Strategies for Global Change*, *14*(1), 101–106, doi:10.1007/s11027-008-9157-2.

Peñuelas, J., J. G. Canadell, and R. Ogaya (2011), Increased water-use efficiency during the 20th century did not translate into enhanced tree growth, *Global Ecology and Biogeography*, *20*(4), 597–608, doi:10.1111/j.1466-8238.2010.00608.x.

Pope, V. D., M. L. Gallani, P. R. Rowntree, and R. A. Stratton (2000), The Impact of New Physical Parametrizations in the Hadley Centre Climate Model: HadAM3, *Climate Dynamics*, *16*(2), 123–146, doi:10.1007/s003820050009.

Pourmokhtarian, A., C. T. Driscoll, J. L. Campbell, and K. Hayhoe (2012), Modeling potential hydrochemical responses to climate change and increasing CO2 at the Hubbard Brook Experimental Forest using a dynamic biogeochemical model (PnET-BGC), *Water Resour. Res.*, *48*(7), W07514, doi:10.1029/2011WR011228.

Riahi, K., S. Rao, V. Krey, C. Cho, V. Chirkov, G. Fischer, G. Kindermann, N. Nakicenovic, and P. Rafaj (2011), RCP 8.5—A scenario of comparatively high greenhouse gas emissions, *Climatic Change*, *109*(1-2), 33–57, doi:10.1007/s10584-011-0149-y.

Saxe, H., D. S. Ellsworth, and J. Heath (1998), Tree and forest functioning in an enriched CO2 atmosphere, *New Phytologist*, *139*(3), 395–436, doi:10.1046/j.1469-8137.1998.00221.x.

Schecher, W. D., and C. T. Driscoll (1995), ALCHEMI: A chemical equilibrium model to assess the acid-base chemistry and speciation of aluminum in dilute solutions. R. Loeppert, A.P. Schwab and S. Goldberg (eds.). In: Chemical Equilibrium and Reaction Models. Soil Sci. Soc. America, Madison, WI, *SSSA Special Publication 42*, 325–356.

Shanley, J. B., C. Kendall, T. E. Smith, D. M. Wolock, and J. J. McDonnell (2002), Controls on old and new water contributions to stream flow at some nested catchments in Vermont, USA, *Hydrol. Process.*, *16*(3), 589–609, doi:10.1002/hyp.312.

Shepard, J. P., M. J. Mitchell, T. J. Scott, Y. M. Zhang, and D. J. Raynal (1989), Measurements of wet and dry deposition in a Northern Hardwood forest, *Water Air Soil Pollut*, *48*(1-2), 225–238, doi:10.1007/BF00282380.

Solomon, S., D. Qin, M. Manning, Z. Chen, M. Marquis, K. B. Averyt, M. Tignor, and H. L. Miller (2007), *IPCC. Climate Change 2007: The Physical Science Basis. Contribution of Working Group I to the Fourth Assessment Report of the Intergovernmental Panel on Climate Change.*

Stewart, I. T., D. R. Cayan, and M. D. Dettinger (2005), Changes toward Earlier Streamflow Timing across Western North America, *Journal of Climate*, *18*(8), 1136–1155.

Stoner, A. M. K., K. Hayhoe, X. Yang, and D. J. Wuebbles (2012), An asynchronous regional regression model for statistical downscaling of daily climate variables, *International Journal of Climatology*, n/a–n/a, doi:10.1002/joc.3603.

Strain, B. R., and F. A. Bazzaz (1983), Terrestrial plant communities, in *CO2 and Plants*, edited by E. R. Lemon, pp. 177–222, Westview Press, Boulder, Colorado, USA.

Taylor, K. E., R. J. Stouffer, and G. A. Meehl (2009), A summary of the CMIP5 experiment design, *WCRP, submitted*.

Thomson, A. et al. (2011), RCP4.5: a pathway for stabilization of radiative forcing by 2100, *Climatic Change*, *109*(1-2), 77–94, doi:10.1007/s10584-011-0151-4.

Thorne, J., J. Anderson, and K. Horiuchi (1988), Cation cycling in a base-poor and base-rich northern hardwood forest ecosystem, *Journal of environmental quality*, *17*(1), 95–101.

Tryhorn, L., and A. DeGaetano (2011), A comparison of techniques for downscaling extreme precipitation over the Northeastern United States, *Int. J. Climatol.*, *31*(13), 1975–1989, doi:10.1002/joc.2208.

VanRheenen, N. T., A. W. Wood, R. N. Palmer, and D. P. Lettenmaier (2004), Potential implications of PCM climate change scenarios for Sacramento–San Joaquin River Basin hydrology and water resources, *Climatic Change*, *62*(1-3), 257–281.

Venterea, R. T., P. M. Groffman, M. S. Castro, L. V. Verchot, I. J. Fernandez, and M. B. Adams (2004), Soil Emissions of Nitric Oxide in Two Forest Watersheds Subjected to Elevated N Inputs, *Forest Ecology and Management*, *196*(2-3), 335–349, doi:10.1016/j.foreco.2004.03.028.

Vuuren, D. et al. (2011), The representative concentration pathways: an overview, *Climatic Change*, *109*(1-2), 5–31, doi:10.1007/s10584-011-0148-z.

Wake, C. P., and A. Markham (2005), Indicators of Climate Change in the Northeast 2005. Clean Air—Cool Planet.,

Washington, W. M. et al. (2000), Parallel Climate Model (PCM) Control and Transient Simulations, *Climate Dynamics*, *16*(10), 755–774, doi:10.1007/s003820000079.

Watanabe, M. et al. (2010), Improved Climate Simulation by MIROC5: Mean States, Variability, and Climate Sensitivity, *J. Climate*, *23*(23), 6312–6335, doi:10.1175/2010JCLI3679.1.

Wolfe, D. W., M. D. Schwartz, A. N. Lakso, Y. Otsuki, R. M. Pool, and N. J. Shaulis (2005), Climate Change and Shifts in Spring Phenology of Three Horticultural Woody Perennials

in Northeastern USA, *International Journal of Biometeorology*, *49*(5), 303–309, doi:10.1007/s00484-004-0248-9.

Wood, A. W., E. P. Maurer, A. Kumar, and D. P. Lettenmaier (2002), Long-range experimental hydrologic forecasting for the eastern United States, *Journal of Geophysical Research: Atmospheres*, *107*(D20), ACL 6–1–ACL 6–15, doi:10.1029/2001JD000659.

Wood, A. W., L. R. Leung, V. Sridhar, and D. P. Lettenmaier (2004), Hydrologic Implications of Dynamical and Statistical Approaches to Downscaling Climate Model Outputs, *Climatic Change*, *62*(1-3), 189–216, doi:10.1023/B:CLIM.0000013685.99609.9e.

Worrall, F., T. Burt, and R. Shedden (2003), Long term records of riverine dissolved organic matter, *Biogeochemistry*, *64*(2), 165–178, doi:10.1023/A:1024924216148.

Yanai, R. D., M. A. Vadeboncoeur, S. P. Hamburg, M. A. Arthur, C. B. Fuss, P. M. Groffman, T. G. Siccama, and C. T. Driscoll (2013), From Missing Source to Missing Sink: Long-Term Changes in the Nitrogen Budget of a Northern Hardwood Forest, *Environ. Sci. Technol.*, doi:10.1021/es4025723.

Yukimoto, S., Y. Adachi, and M. Hosaka (2012), A new global climate model of the Meteorological Research Institute: MRI-CGCM3: model description and basic performance (special issue on recent development on climate models and future climate projections), *Journal of the Meteorological Society of Japan*, *90*, 23–64.

Zhai, J., C. T. Driscoll, T. J. Sullivan, and B. J. Cosby (2008), Regional application of the PnET-BGC model to assess historical acidification of Adirondack lakes, *Water Resour. Res. (W01421)*, *44*(1), 9 PP., doi:10.1029/2006WR005532.

Zhu, J., and X.-Z. Liang (2005), Regional climate model simulation of US soil temperature and moisture during 1982–2002, *Journal of geophysical research*, *110*(D24), D24110.

Zickfeld, K., M. Eby, H. D. Matthews, and A. J. Weaver (2009), Setting cumulative emissions targets to reduce the risk of dangerous climate change, *Proceedings of the National Academy of Sciences*, *106*(38), 16129–16134.

10. Vita

Afshin Pourmokhtarian
apourmok@syr.edu
151 Link Hall, Civil and Environmental Engineering
Syracuse University, Syracuse, NY 13244

EDUCATION

- **Ph.D., Civil and Environmental Engineering**
  - Syracuse University, Syracuse, New York, October 2013
  - Dissertation Topic: *"Biogeochemical modeling of soil and surface water responses to climate change in the Northeastern U.S"*
  - *Advisor: Dr. Charles T. Driscoll*

- **Master of Science, Civil and Environmental Engineering**
  - Tarbiat Modares University, Tehran, Iran, June 2005
  - Thesis Topic: *"Biological corrosion prevention in concrete sewer pipes by adding industrial waste materials as an additive"*

- **Bachelor of Engineering, Civil Engineering**
  - Tehran University, Tehran, Iran, May 2002

JOURNAL PUBLICATIONS

- **Pourmokhtarian, A., Driscoll, C. T., Campbell, J. L., Hayhoe, K.**, (2013) '*A comparison of Gridded Quantile Mapping vs. Station Based Downscaling Approaches on Potential Hydrochemical Responses of Forested Watersheds to Climate Change Using a Dynamic Biogeochemical Model (PnET-BGC)*' Environmental Science and Technology (*In Preparation*)

- **Pourmokhtarian, A., Driscoll, C. T., Campbell, J. L., Hayhoe, K.**, (2013) '*New Framework for Assessment of Climate Change Impacts on Forested Watershed*' Nature Climate Change (*In Preparation*)

- **Pourmokhtarian, A., Driscoll, C. T., Campbell, J. L., Hayhoe, K.**, (2012) '*Modeling Potential Hydrochemical Responses to Climate Change and Rising CO_2 at the Hubbard Brook Experimental Forest Using a Dynamic Biogeochemical Model (PnET-BGC)*' Water Resources Research, VOL. 48, W07514, doi:10.1029/2011WR011228

- **Campbell, J. L., Driscoll, C. T., Pourmokhtarian, A., Hayhoe, K.**, (2011) '*Streamflow Responses to Past and Projected Future Changes in Climate at the Hubbard Brook Experimental Forest, New Hampshire, USA*' Water Resources Research, VOL. 47, W02514, doi:10.1029/2010WR009438

- **Tominaga, K., Aherne, J., Watmough, S. A., Alveteg, M., Cosby, B. J., Driscoll, C. T., Posch, M., Pourmokhtarian, A.**, (2010) '*Predicting Acidification Recovery at the Hubbard Brook Experimental Forest, New Hampshire: Evaluation of Four Models*' Environmental Science & Technology, 44 (23), pp 9003–9009, DOI: 10.1021/es102243j

BOOK CHAPTER

- **Bytnerowicz, A., Fenn, M., McNulty, S., Yuan, F., Pourmokhtarian, A., Driscoll, C. T., Tom, M.,** (2012) '*Interactive effects of air pollution and climate change on forest ecosystems in the United States – current understanding and future scenarios*' Elsevier Physical Sciences Series, Book Project for Series "Developments in Environmental Science"

HIGHLIGHTS AND SUMMARIES OF PUBLICATIONS

- Research Highlights of Nature Climate Change (2012), Hydrology, '*Catchment interactions*', Nature Climate Change 2, 486 (2012) doi:10.1038/nclimate1619

- NSF Discovery (07-25-2012), 'Acid Rain: Scourge of the Past or Trend of the Present? New connection between climate change and acidification of Northeast's forests and streams', http://www.nsf.gov/discoveries/disc_summ.jsp?cntn_id=124955&org=BIO

- Featured on Science360 radio (August 2012), 'Acid Rain Flashback!'

CONFERENCE PRESENTATIONS

- **Stoner, A., Hayhoe, K., Pourmokhtarian, A., Driscoll, C. T., Campbell, J. L.**, (2013) '*Developing High-Resolution Climate Projections at the Watershed Scale: A Hubbard Brook Case Study*' American Geophysical Union (AGU) 2013 Fall Meeting, Oral Presentation, December 9-13, 2013, San Francisco, CA

- **Driscoll, C. T., Groffman, P. M., Campbell, J. L., Pourmokhtarian, A., Templer, P.H., Fahey, T. J.**, (2013) '*Effects of changing climate on the structure and function of the Northern Forest: long-term measurements, experiments and future model projections from the Hubbard Brook Experimental Forest, New Hampshire, USA*' The International Symposium on Forest Soils: Linking Ecosystem Processes and Management to Forest Biodiversity and Functions (ISFS 2013), Oral Presentation, September 16-20, 2013, Shenyang, China.

- **Pourmokhtarian, A., Driscoll, C. T., Campbell, J. L., Hayhoe, K.**, (2013) '*New Framework for Assessment of Climate Change Impacts on Forested Watershed*' 50th Annual Hubbard Brook Cooperators' Meeting, Oral Presentation, Hubbard Brook, NH

- **Bytnerowicz, A., Fenn, M., McNulty, S., Yuan, F., Pourmokhtarian, A., Driscoll, C.T., and Meixner, T.**, (2013) '*Interactive effects of air pollution and climate change on forests in the United States*', Research Group 7.01 '*Impacts of Air pollution and Climate Changes on Forest ecosystems*', IUFRO Congress for Latin America (IUFROLAT), Oral Presentation, June 12-15, 2013, Costa Rica

- **Pourmokhtarian, A., Driscoll, C. T., Campbell, J. L., Hayhoe, K.**, (2013) '*A comparison of Gridded Quantile Mapping vs. Station Based Downscaling Approaches on Potential Hydrochemical Responses of Forested Watersheds to Climate Change Using a Dynamic Biogeochemical Model (PnET-BGC)*' Northeastern Ecosystem Research Cooperative (NERC) 2013 Spring Meeting, Poster Presentation, March 19-20, 2013, Saratoga Springs, NY

- **Pourmokhtarian, A., Driscoll, C. T., Campbell, J. L., Hayhoe, K.**, (2012) '*A comparison of Gridded Quantile Mapping vs. Station Based Downscaling Approaches on Potential Hydrochemical Responses of Forested Watersheds to Climate Change Using a Dynamic Biogeochemical Model (PnET-BGC)*' American Geophysical Union (AGU) 2012 Fall Meeting, Poster Presentation, December 3-7, 2012, San Francisco, CA

- **Pourmokhtarian, A., Driscoll, C. T., Campbell, J. L., Hayhoe, K.**, (2012) '*Modeling potential impacts of climate change on future streamflow and chemistry at the Hubbard Brook Experimental Forest (HBR), New Hampshire, United States*' Long Term Ecological Research (LTER) All Scientists Meeting (ASM) 2012: The Unique Role of the LTER Network in the Anthropocene: Collaborative Science Across Scales, Poster Presentation, September 10-13, 2012, Estes Park, CO

- **Pourmokhtarian, A., Driscoll, C. T., Campbell, J. L., Hayhoe, K.**, (2012) '*Cross site analysis of northern forested watersheds responses to future changes in climate and CO_2 using a dynamic biogeochemical model (PnET-BGC)*' Long Term Ecological Research (LTER) All Scientists Meeting (ASM) 2012: The Unique Role of the LTER Network in the Anthropocene: Collaborative Science Across Scales, Poster Presentation, September 10-13, 2012, Estes Park, CO

- **Pourmokhtarian, A., Driscoll, C. T., Campbell, J. L., Hayhoe, K.**, (2012) '*Comparison Between Gridded Quantile Mapping vs Station Based Downscaling Approaches on Potential Hydrochemical Responses of Forested Watersheds to Climate Change Using PnET-BGC Model*' 49th Annual Hubbard Brook Cooperators' Meeting, Oral Presentation, Hubbard Brook, NH

- **Pourmokhtarian, A., Driscoll, C. T., Campbell, J. L., Hayhoe, K.**, (2012) '*Identifying key indicators of forested watersheds responses to climate change and increasing CO_2 effects in the northeastern U.S. using a dynamic biogeochemical model (PnET-BGC) and cross site analysis*' Nunan Lecture and Research Day, Poster Presentation, April 13, 2012, L.C. Smith College of Engineering, Syracuse University, Syracuse, NY

- **Pourmokhtarian, A., Driscoll, C. T., Campbell, J. L., Hayhoe, K.**, (2011) '*Cross site analysis of forested watersheds in the northeastern U.S. to climate change and increasing CO_2 over the 21st century using a dynamic biogeochemical model (PnET-BGC)*' American Geophysical Union (AGU) 2011 Fall Meeting, Oral Presentation, December 5-9, 2011, San Francisco, CA

- **Driscoll, C. T., Pourmokhtarian, A., Campbell, J. L., Hayhoe, K., Wu, W.** (2011) '*Modeling of the Hydrochemical Response of High Elevation Forest Watersheds to Climate Change and Atmospheric Deposition Using a Biogeochemical Model (PnET-BGC)*' EPA STAR Meeting, Oral Presentation, September 20-22, 2011, Washington D.C.

- **Pourmokhtarian, A., Driscoll, C. T., Campbell, J. L., Hayhoe, K.**, (2011) '*Modeling Biogeochemical Effects of Interactions of Future Climate Change with Forest Cutting*' 48th Annual Hubbard Brook Cooperators' Meeting, Oral Presentation, Hubbard Brook, NH

- **Pourmokhtarian, A., Driscoll, C. T., Campbell, J. L.**, (2011) '*Impacts of Climate Change and Rising CO_2 on Elemental Mass Balances over the 21st century at the Hubbard Brook Experimental Forest (HBEF), NH*' Nunan Lecture and Research Day, Poster Presentation, April 8, 2011, L.C. Smith College of Engineering, Syracuse University, Syracuse, NY

- **Pourmokhtarian, A., Driscoll, C. T., Campbell, J. L.,** (2011) '*Impacts of Climate Change and Rising CO_2 on Elemental Mass Balances over the 21st century at the Hubbard Brook Experimental Forest (HBEF), NH*' 21st Annual Great Lakes Research Consortium (GLRC) Student/Faculty Conference, Oral Presentation, March 18-19, 2011, SUNY College of Environmental Science and Forestry, Syracuse, NY

- **Pourmokhtarian, A., Driscoll, C. T., Campbell, J. L., Hayhoe, K.**, (2010) '*Changes in Element Fluxes under Climate Change at Hubbard Brook over 21st Century*' 47th Annual Hubbard Brook Cooperators' Meeting, Oral Presentation, Hubbard Brook, NH

- **Campbell, J. L., Driscoll, C. T., Pourmokhtarian, A., Hayhoe, K.**, (2010) '*Streamflow Responses to Past and Projected Future Changes in Climate at Hubbard Brook*' 47th Annual Hubbard Brook Cooperators' Meeting, Oral Presentation, Hubbard Brook, NH

- **Pourmokhtarian, A., Driscoll, C. T., Campbell, J. L.**, (2010) '*Hydrochemical Modeling Effort: Could Invoking Long-Term CO_2 Fertilization Effects Offset Future Temperature-Induced Effects on Soil and Surface Water Chemistry at Hubbard Brook Experimental Forest (HBEF) in NH?*' Nunan Lecture and Research Day, Poster Presentation, April 9, 2010, L.C. Smith College of Engineering, Syracuse University, Syracuse, NY

- **Pourmokhtarian, A., Driscoll, C. T., Campbell, J. L.**, (2010) '*Hydrochemical Modeling Effort: Could Invoking Long-Term CO_2 Fertilization Effects Offset Future Temperature-Induced Effects on Soil and Surface Water Chemistry at Hubbard Brook Experimental Forest (HBEF) in NH?*' 25th Anniversary of CASE (Center for Advanced Systems and Engineering) Conference, Poster Presentation, April 8-9, 2010, L.C. Smith College of Engineering, Syracuse University, Syracuse, NY

- **Pourmokhtarian, A., Driscoll, C. T., Campbell, J. L.,** (2010) '*Modeling Potential Hydrochemical Responses to Climate Change and Rising CO_2 at the Hubbard Brook Experimental Forest (HBEF), New Hampshire Using PnET-BGC*' 20th Annual Great Lakes Research Consortium (GLRC) Student/Faculty Conference, Oral Presentation,

March 19-20, 2010, SUNY College of Environmental Science and Forestry, Syracuse, NY

- **Pourmokhtarian, A. (*Invited Speaker*), Driscoll, C. T., Campbell, J. L., Hayhoe, K.**, (2009) '*Potential effects of Rising CO_2 and Climate Change Interactions with Atmospheric Deposition in Northeastern U.S. over the 21st Century Using a Dynamic Biogeochemical Model (PnET-BGC)*' American Geophysical Union (AGU) 2009 Fall Meeting, Oral Presentation, December 14-18, 2009, San Francisco, CA

- **Sebestyen, S. D., Campbell, J. L., Shanley, J. B., Pourmokhtarian, A., Driscoll, C. T., Boyer, E. W.**, (2009) '*Stream Nitrate Responses to Hydrological Forcing and Climate Change in Northern Forests of the USA*' American Geophysical Union (AGU) 2009 Fall Meeting, Oral Presentation, December 14-18, 2009, San Francisco, CA

- **Campbell, J. L., Driscoll, C. T., Pourmokhtarian, A.**, (2009) '*The Impact of Climate Change on Past and Future streamflow at the Hubbard Brook Experimental Forest*' American Geophysical Union (AGU) 2009 Fall Meeting, Poster Presentation, December 14-18, 2009, San Francisco, CA

- **Pourmokhtarian, A., Driscoll, C. T.**, (2009) '*Interactions of Climate Change with Acidic Deposition in a Forest Watershed over the 21st Century Using a Dynamic Biogeochemical Model (PnET-BGC)*' National Atmospheric Deposition Program (NADP) Annual Meeting and Scientific Symposium, Oral Presentation, October 6-8, 2009, Saratoga Springs, NY

- **Driscoll, C. T., Driscoll, K. M., Roy, K. M., Zhou, Q., Pourmokhtarian, A., Sullivan, T. J., Mitchell, M. J.**, (2009) '*Linkages Among Acidic and Hg Deposition and Climate Change in Adirondack Ecosystems*' National Atmospheric Deposition Program (NADP) Annual Meeting and Scientific Symposium, Oral Presentation, October 6-8, 2009, Saratoga Springs, NY

- **Zhou, Q., Driscoll, C. T., Pourmokhtarian, A., Sullivan, T. J., Cosby B. J.**, (2009) '*Developing the Critical Loads for the Acidification of Some Lake- Watersheds in the Adirondack Region of New York*' National Atmospheric Deposition Program (NADP) Annual Meeting and Scientific Symposium, Poster Presentation, October 6-8, 2009, Saratoga Springs, NY

- **Pourmokhtarian, A., Driscoll, C. T., Campbell, J. L., Hayhoe, K.**, (2009) '*Biogeochemical Modeling of Soil and Surface Water Responses to Climate Change in the Northeastern U.S. using PnET-BGC*' Long Term Ecological Research (LTER) All Scientists Meeting (ASM) 2009: Integrating Science and Society in a World of Constant Change, Oral Presentation, September 14-16, 2009, Estes Park, CO

- **Pourmokhtarian, A., Driscoll, C. T., Campbell, J. L., Hayhoe, K.**, (2009) '*Modeling of the Hydrochemical Response of High Elevation Forest Watersheds to Climate Change and Atmospheric Deposition Using a Biogeochemical Model (PnET-BGC)*' Long Term Ecological Research (LTER) All Scientists Meeting (ASM) 2009: Integrating Science

and Society in a World of Constant Change, Oral Presentation, September 14-16, 2009, Estes Park, CO

- **Pourmokhtarian, A., Driscoll, C. T., Campbell, J. L.,** (2009) '*Modeling Hydrochemical Responses to Climate Change at the Hubbard Brook Experimental Forest over the 21st Century Using a Dynamic Biogeochemical Model (PnET-BGC)*' Long Term Ecological Research (LTER) All Scientists Meeting (ASM) 2009: Integrating Science and Society in a World of Constant Change, Poster Presentation, September 14-16, 2009, Estes Park, CO

- **Campbell, J. L., Driscoll, C. T., Pourmokhtarian, A.,** (2009) '*Climate-induced changes in streamflow at the Hubbard Brook Experimental Forest*' Long Term Ecological Research (LTER) All Scientists Meeting (ASM) 2009: Integrating Science and Society in a World of Constant Change, Poster Presentation, September 14-16, 2009, Estes Park, CO

- **Pourmokhtarian, A., Driscoll, C. T., Campbell, J. L.**, (2009) '*Could long-term CO_2 fertilization offset future effects of increases in temperature on soil and surface water chemistry at Hubbard Brook Experimental Forest?*' 46th Annual Hubbard Brook Cooperators' Meeting, Oral Presentation, Hubbard Brook, NH

- **Driscoll, C. T., Pourmokhtarian, A., Pardo, L. H.**, (2009) '*Critical Loads of Acidity at Hubbard Brook*' 46th Annual Hubbard Brook Cooperators' Meeting, Oral Presentation, Hubbard Brook, NH

- **Tominaga, K., Aherne, J., Watmough, S. A., Alveteg, M., Cosby, B. J., Driscoll, C. T., Posch, M., Pourmokhtarian, A.**, (2009) '*Predicting future soil and stream chemistry using an ensemble of acidification models at Hubbard Brook*' 46th Annual Hubbard Brook Cooperators' Meeting, Oral Presentation, Hubbard Brook, NH

- **Tominaga, K., Aherne, J., Watmough, S. A., Alveteg, M., Cosby, B. J., Driscoll, C. T., Kiekbusch, J., Posch, M., Pourmokhtarian, A., Weis, W., Huber, C.**, (2009) '*Modeling acidification recovery at long-term monitoring sites: a multi-model evaluation*' 6th International Symposium on Ecosystem Behavior BIOGEOMON, 29 June-3 July 2009, University of Helsinki, Helsinki, Finland

- **Pourmokhtarian, A., Driscoll, C. T., Campbell, J. L., Hayhoe, K.**, (2009) '*Assessing the Hydrochemical Response of High Elevation Forest Watersheds to Climate Change and Atmospheric Deposition Using a Biogeochemical Model (PnET-BGC)*' American Geophysical Union (AGU) 2009 Joint Assembly: The Meeting of the Americas, Oral Presentation, May 24-27, 2009, Toronto, Ontario, Canada

- **Pourmokhtarian, A., Driscoll, C. T., Campbell, J. L.,** (2009) '*Hydrochemical response of forest watersheds in the Northeast to Climate Change over the 21st Century Using Dynamic Watershed Biogeochemical Model (PnET-BGC)*' Great Lakes Research Consortium (GLRC) Poster Session; Great Lakes Day in Albany, Poster Presentation, April 28, 2009, Albany, NY

- **Pourmokhtarian, A., Driscoll, C. T., Campbell, J. L.**, (2009) '*Hydrochemical Response of the Hubbard Brook Experimental Forest, NH and Huntington Wildlife Forest, NY to Climate Change and Atmospheric Deposition over the 21st Century*' Nunan Lecture and Research Day, Poster Presentation, April 17, 2009, L.C. Smith College of Engineering, Syracuse University, Syracuse, NY

- **Pourmokhtarian, A., Driscoll, C. T., Campbell, J. L.,** (2009) '*Assessment of the Response of Hydrology and Water Quality of Forest Watersheds in the Northeast to Climate Change using a Biogeochemical Model (PnET-BGC)*' 6th Annual Water Resources Research Conference (WRRC), Oral Presentation, April 7, 2009, UMass Amherst, MA

- **Pourmokhtarian, A., Driscoll, C. T., Campbell, J. L.,** (2009) '*Modeling the Response of Hydrology and Water Quality to Climate Change at the Huntington Wildlife Forest (HWF) in the Adirondack Mountains, New York using a Biogeochemical Model (PnET-BGC)*' 19th Annual Great Lakes Research Consortium (GLRC) Student/Faculty Conference, Oral Presentation, March 13-14, 2009, SUNY College of Environmental Science and Forestry, Syracuse, NY

- **Pourmokhtarian, A., Driscoll, C. T.**, (2008) '*Prediction of Soil and Surface Water Responses to Climate Change at the Hubbard Brook Using a Biogeochemical Model (PnET-BGC)*' The Northeastern Ecosystem Research Cooperative Conference, Poster Presentation, October 17, 2008, New England Center, Durham, NH

- **Pourmokhtarian, A., Driscoll, C. T.**, (2008) '*Prediction of Soil and Surface Water Responses to Climate Change at the Hubbard Brook Using a Biogeochemical Model (PnET-BGC)*' 8th Annual Syracuse Symposium on Environmental and Energy Systems, Poster Presentation, September 29-30, 2008, Oncenter, Syracuse, NY

- **Pourmokhtarian, A., Driscoll, C. T., Campbell, J. L.**, (2008) '*Predicting the consequences of climate change on soil and surface water chemistry at Hubbard Brook, NH using a biogeochemical model (PnET-BGC)*' 45th Annual Hubbard Brook Cooperators' Meeting, Oral Presentation, Hubbard Brook, NH

- **Pourmokhtarian, A., Driscoll, C. T.**, (2008) '*Application of a Biogeochemical Model (PnET-BGC) to Evaluate the Consequences of Climate Change on Soil and Surface Water Chemistry at the Hubbard Brook, NH*' 2nd. Annual Alliance for Graduate Education and the Professoriate (AGEP) Academic Excellence Symposium, Oral Presentation, June 11, 2008, Syracuse University, Syracuse, NY

- **Pourmokhtarian, A., Driscoll, C. T.**, (2008) '*Prediction of Soil and Surface Water Responses to Climate Change at the Hubbard Brook Using a Biogeochemical Model (PnET-BGC)*' Nunan Lecture and Research Day, Poster Presentation, L.C. Smith College of Engineering, Poster Presentation, April 8, 2008, Syracuse University, Syracuse, NY

- **Pourmokhtarian, A., Driscoll, C. T.**, (2008) '*Prediction of Soil and Surface Water Responses to Climate Change at the Hubbard Brook Using a Biogeochemical Model (PnET-BGC)*' 18th Annual Great Lakes Research Consortium (GLRC) Student/Faculty

Conference, Oral Presentation, March 14-15, 2008, SUNY College of Environmental Science and Forestry, Syracuse, NY

- **Pourmokhtarian, A.**, (2007) '*Biological Corrosion Control in Concrete Sewer Pipes by Adding Industrial Wastes as an Additive*' 1st Annual Alliance for Graduate Education and the Professoriate (AGEP) Academic Excellence Symposium, Oral Presentation, June 2007, Syracuse University, Syracuse, NY

- **Badkoubi, A., Pourmokhtarian, A.**, (2005) '*Biological Corrosion Control in Concrete Sewer Pipes Using Industrial Wastes as an Additive*' R'05, 7th World Congress on Integrated Resources Management (IRM), Oral Presentation and Poster, Beijing, China

- **Badkoubi, A., Pourmokhtarian, A.**, (2005) '*Recycled Plastic Usage in Polymeric Industries*' R'05, 7th World Congress on Integrated Resources Management (IRM), Oral Presentation and Poster, Beijing, China

- **Pourmokhtarian, A.**, (2003) '*Recycling Usage in Polymeric Industries*' 1st National Seminar on Recycling and Waste Management on Process Industries, Oral Presentation, Tehran, Iran

- **Pourmokhtarian, A.**, (2003) '*Affects of Air Pollution on Tehran People's Death*' 1st Air Pollution National Congress, Shahid Beheshty University, Poster Presentation, Tehran, Iran

TEACHING EXPERIENCE

- Teaching Mentor 2008-12 (Train new TAs during TA orientation)
- Teaching associate 2007-08 at Civil and Environmental Engineering Department, Syracuse University:
    - CIE 352 (Water Resources Engineering)
    - CIE 472/672 (Applied Microbiology)
    - CIE 475 (Civil and Environmental Engineering Design)
- Teaching assistant 2006-07 at Civil and Environmental Engineering Department, Syracuse University:
    - CIE 352 (Water Resources Engineering)
    - CIE 471/671 (Environmental Chemistry)
    - CIE 342 (Environmental Engineering II)
    - CIE 475 (Civil and Environmental Engineering Design)
- Instructor in PARSEH (private institute) to prepare students for nationwide competition for entering graduate school (MS) (2002-2003):
    - Fluid mechanics
    - Hydrology
    - Hydraulic structures
- Private tutor (1998-2000):
    - Professional AutoCAD in Civil Engineering and Architecture
- Private tutor (1997-1999):

- Algebra, Mathematics, Physics and Dynamic for high school students and preparing them for Iranian University Entrance Exam (Concours)

INDUSTRIAL EXPERIENCE

- Darya-Sazeh Consulting Engineers Co., Tehran, Iran
  Second top private consulting company, (1999-2004):
  - Designer of marine structures: Jetty, Berth, Breakwater, Piles
  - Structural designer and controller
  - AutoCAD supervisor
  - Computer maintenance and service
  - Supervising steel structural site

AWARDS AND HONORS

RESEARCH

- Nunan Lecture and Research Day, Syracuse University, Department Award Winner (2012)
- Nunan Lecture and Research Day, Syracuse University, Department Award Winner (2010)
- Award Winning Poster at Great Lakes Research Consortium Poster (GLRC) Session; Great Lakes Day in Albany, NY (2009)
- Nunan Lecture and Research Day, Syracuse University, Department Award Winner (2008)
- First GPA Award among Engineering Graduate Students (M.S.) class of 2005
- Top M.S. thesis award in Civil and Environmental Engineering class of 2005 (19.25/20)

TEACHING

- Teaching Mentor (2008-12)
- Outstanding Teaching Assistant Award (2007-08)
- Teaching Associate, Syracuse University (2007-08)
- Teaching Assistantship, Syracuse University (2006-2007)
- Future Professoriate Program (FPP) (2006-present)

HONOR SOCIETIES

- Phi Kappa Phi (2008-present)
- Phi Beta Delta (2007-present)
- Golden Key International (2007-present)

COMPUTER SKILLS

- Highly experienced in statistical software: MINITAB, SAS
- Highly experienced in using and teaching software for Water Resources Engineering: StormCAD, WaterGEMS, PondPack, CulvertMaster, SewerCAD, and FlowMaster
- Highly experienced in using SigmaPlot, MINEQL, SAP, ETAB, SAFE, AutoCAD, MathCAD, SDRMap, Basic, Microsoft Office (Excel, Power Point, and Word)

- Comfortable with programs such as, 3D Studio and Visual C++

CERTIFICATION / WORKSHOPS

- "*Climate Change in the Northeast, Union of Concerned Scientists*" Workshop, Worcester, MA (January 2008)
- "*Iran-POPs Enabling Activity on Stockholm Convention*" Workshop, Tehran, Iran (2004)
- "*Municipal and Hospital Wastes Treatment and Disposal*" Workshop, Tehran, Iran (2004)
- "*Clean Earth Day and Waste Management in Industries and Mines*" Workshop, Tehran, Iran (2003)

PROFESSIONAL AFFILIATIONS

- The Long Term Ecological Research (LTER) (2009-present)
- The Geological Society of America (2008-present)
- American Geophysical Union (2008-present)
- Association of Environmental Engineering and Science Professors (2008-present)
- Text and Academic Authors Association (TAA) (2008-present)
- American Society of Civil Engineering (2006-present)
- Alumni Association of Faculty of Engineering, University of Tehran, Iran (2002-present)

SERVICE TO UNIVERSITY AND ACTIVITIES

- Graduate Student Representative on Tenure and Promotions Committee (TPC) in L.C. Smith (2012-13)
- Selection Committee Member for the 2011 Excellence in Graduate Education (EGE) faculty recognition awards (2011)
- Steering Committee Member for 2010 White Eagle Conference
- Selection Committee Member for the 2010 Teaching Mentor
- Selection Committee Member for the Excellence in Graduate Education (EGE) faculty recognition awards (2009)
- Member of Doctoral Career Advisory Board (DCAB) (2008-10)
- Civil and Environmental Engineering Department senator at Graduate Student Organization (GSO) (2008-present)
- Toastmasters International, President and Charter Member of "I-Orange" (2007-08)
- Graduate Global Ambassadors, Vice President and Charter member (2006-2009)
- Peer assistant in Slutzker Center for International Students (Summer 2007)